Product emulsification in multiphase fermentations

The unspoken challenge in microbial production of sesquiterpenes

Pedraza de la Cuesta, Susana

DOI
10.4233/uuid:a48e3fc9-5e7b-4872-9984-22e0eef6686d

Publication date
2019

Document Version
Final published version

Citation (APA)
Pedraza de la Cuesta, S. (2019). *Product emulsification in multiphase fermentations: The unspoken challenge in microbial production of sesquiterpenes*. [Dissertation (TU Delft), Delft University of Technology]. https://doi.org/10.4233/uuid:a48e3fc9-5e7b-4872-9984-22e0eef6686d

Product emulsification in multiphase fermentations:

the unspoken challenge in microbial production of sesquiterpenes

Dissertation

for the purpose of obtaining the degree of doctor at Delft University of Technology by the authority of the Rector Magnificus, Prof. dr. ir. T.H.J.J. van der Hagen, chair of the Board for Doctorates to be defended publicly on Monday 11 March 2019 at 10:00 o'clock

by

Susana PEDRAZA DE LA CUESTA

Professional doctorate in Bioprocess Engineering,
Delft University of Technology, the Netherlands.

Born in Madrid, Spain.

This dissertation has been approved by the promotor.

Composition of the doctoral committee:

Rector Magnificus,	Chairperson
Prof. dr. ir. L.A.M. van der Wielen	Delft University of Technology, promotor
Dr. M.C. Cuellar Soares	Delft University of Technology, copromotor (current affiliation: DSM Biotechnology center)

Independent members:

Prof. dr. ir. J.J. Heijnen	Delft University of Technology
Prof. dr. ir. H.J. Noorman	Delft University of Technology
Prof. dr. ir. C.A. Ramirez Ramirez	Delft University of Technology
Prof. dr. A.J.A. van Maris	KTH Royal Institute of Technology, Sweden
Dr. A. Taglieber	Firmenich S.A., Switzerland
Prof. dr. ir. M.C.M. van Loosdrecht	Delft University of Technology, reserve member

The research for this thesis was performed at the Bioprocess Engineering group, Department of Biotechnology, Faculty of Applied Sciences, Delft University of Technology, the Netherlands.

This work was carried out within the BE-Basic R&D Program, which was granted a FES subsidy from the Dutch Ministry of Economic affairs, agriculture and innovation (EL&I).

Cover illustration: "*Several circles*", Wassily Kandinsky, 1926.
Printed and bound in the Netherlands by Ridderprint BV
ISBN 978-94-6375-310-4

"I am sorry to have to speak about it according to a formula which in principle excludes the dream. When will we have sleeping logicians, sleeping philosophers? I would like to sleep, in order to surrender myself to the dreamers (...)."

André Breton, Manifesto of Surrealism, 1924.

To my angels,

Arturo and Jay

Summary

Sesquiterpenes are a versatile group of 15-carbon molecules, traditionally extracted from plants for diverse applications ranging from fuels to fine chemicals and pharmaceuticals. Scarcity of natural resources and emergence of new applications have encouraged the development of sustainable solutions to produce sesquiterpenes. The recent development of engineered microbial strains able to produce and secrete sesquiterpenes reaching fermentation titres in the order of g per L, is a promising alternative to produce diesel-like biofuels from renewable biomass sources, like sugar cane bagasse. The most attractive aspect of sesquiterpene fermentations is that the extracellular product readily forms an oil phase separated from the aqueous fermentation broth in the reactor. The difference of densities between the aqueous broth and the light product phase opens the opportunity of integrating cost-efficient separation techniques (e.g. gravity separation, hydro-cyclones) with the reactor. This scenario could contribute to significantly lowering equipment and utility costs as well as reducing cost of raw materials by allowing for cell recycling. The scale-up of sesquiterpene fermentations has unveiled processing challenges that were not prominently present at laboratory scale.

Surface active components present in the fermentation medium can interact with the oil-water interface stabilizing the product in an emulsion of small droplets. In **chapter 2** of this thesis it was studied the feasibility of integrating gravity separation and microbial production of sesquiterpenes in a bubble column reactor at different reactor volumes and aspect ratios. A regime analysis was performed to identify possible windows of operation where droplet growth by coalescence and droplet creaming is promoted over emulsification and back-mixing of small droplets. Although lab scale conditions can promote droplet creaming over mixing, the integration of production and separation at large scale might only be achieved in a reactor in which two sections with different process conditions (especially superficial gas velocity) are combined.

At laboratory scale, solvents are often employed in sesquiterpene fermentations for reducing product evaporation and enhancing recovery by increasing the concentration of oil phase. The current state of the art at large scale uses surfactants to recover the emulsified product. **Chapter 3** presents a techno-economic assessment of the use of solvents at scales typical of flavor and fragrances (25 MT y^{-1}) and fuel market (25000 MT y^{-1}) compared to the

current state of the art. It also addresses the problematic of product evaporation, and how the presence of a solvent could help to reduce the loss of product in the off-gas. Based on empirical correlations, mass transfer, and process flow sheeting models, the assessment concluded that although the use of solvents did reduce sesquiterpene evaporation rate during fermentation and improved product recovery, it resulted in higher or similar cost than the base case due to the additional equipment cost for solvent-product separation. However, when selecting solvents compatible with the final product formulation (e.g. in a kerosene enrichment process), unit costs as low as 0.7 \$ kg^{-1} can be achieved while decreasing environmental impact.

In fermentations where a hydrophobic liquid is produced and/or solvent is added for *in situ* product removal, the interaction of droplets and gas bubbles can generate additional oxygen transfer routes across the oil phase. Complementing the techno-economic assessment presented in chapter 3, the mechanisms of oxygen transfer in sesquiterpene fermentations and the use of solvents as oxygen vector were studied in **chapter 4**. The enhancement of oxygen transfer coefficient $k_L a$ in fermentations with wild-type and sesquiterpene-producing *Escherichia coli* at varying oil fractions of hexadecane and dodecane was dependent on the transfer route and decreased along the fermentation age. Contrary to literature results, $k_L a$ trends were not correlated to changes in power input, oil fraction, or cell concentration, but could be explained by reduced bubble-droplet and droplet-droplet interactions due to droplet stabilization. For the first time, it was evidenced that surface active components present in the fermentation broth can limit the impact of oxygen vectors in $k_L a$ enhancement, bringing a new perspective on oxygen transfer in multiphase fermentations.

C**hapter 5** studies the integration of a fermentation with a gas enhanced oil recovery technology developed within the TU Delft Initiative Delft Integrated Column Reactor project (DIRC), and in collaboration with the start-up Delft Advanced Biorenewables (DAB, www.DelftAB.com), the BE-Basic Foundation, and the Bioprocess Pilot Facility (www.BPF.eu). Cell growth, cell viability, concentration of SACs and emulsion stability were measured in fed batch fermentations performed in a 2 L reactor and in fed batch fermentations performed in the same reactor while connected to a 500 mL aerated column. The bubble column was successfully integrated with the reactor during 24 h without affecting cell growth or cell viability. However, higher levels of surfactants and emulsion stability were measured in the integrated system compared to the base case, reducing its capacity for oil recovery. This highlights the fact that increased levels of SACs due to cellular stress must be considered when

tuning the column parameters (e.g., geometry, gas flow) for improving oil recovery. The study presented in this chapter concluded that gas induced recovery is a promising option for integrated recovery in multiphase fermentations, allowing for oil separation and cell recycling without compromising fermentation performance.

Sammenvatting

Sesquiterpenen zijn een veelzijdig groep van moleculen met15 koolstofatomen, die traditioneel uit planten worden geëxtraheerd. Deze moleculen hebben diverse toepassingen zoals brandstoffen, hoogwaardige chemicaliën en geneesmiddelen. De schaarste van natuurlijke bronnen en de opkomst van nieuwe toepassingen hebben de ontwikkeling van duurzame productiemethoden voor sesquiterpenes in gang gezet. Recent ontwikkelde genetisch gemodificeerde micro-organismen die sesquiterpenen kunnen produceren en uitscheiden, met fermentatie concentraties in de orde van grammen per liter, zijn een veelbelovend alternatief om geavanceerde biobrandstoffen te produceren uit hernieuwbare bronnen zoals suikerriet bagasse. Het belangrijkste aspect van deze sesquiterpeen fermentaties is dat het product door de micro-organismen wordt uitgescheiden en meteen een oliefase vormt bovenop de waterfase in de reactor. Het verschil in dichtheid tussen de waterfase en de oliefase maakt het mogelijk om kostenefficiënte scheidingstechnieken (e.g. *zwaartekracht scheiding*, hydrocyclonen) te integreren in de reactor zelf. Dit scenario kan zowel bijdragen aan significant lagere aanschaf- en operationele kosten van de benodigde apparatuur, als aan het verminderen van kosten voor grondstoffen door hergebruik van de microbiële cellen mogelijk te maken. Tijdens het opschalen van de sesquiterpeen fermentaties kwamen uitdagingen voor het productieproces op grote schaal aan het licht die niet nadrukkelijk aanwezig waren op laboratoriumschaal.

Oppervlakte actieve stoffen die in het fermentatiebeslag aanwezig zijn kunnen door interactie met de grenslaag tussen olie en water het product stabiliseren in een emulsie van kleine druppels. In hoofdstuk 2 van dit proefschrift is onderzocht of het haalbaar is om *de scheiding* met behulp van zwaartekracht en microbiële productie van sesquiterpenen te integreren in een bellenkolom reactor. Een regime analyse is uitgevoerd om het effect van reactor geometrie (volume, aspect ratio) en procescondities (superficiële gassnelheid) op verschillende subrocessen te bestuderen en zo een *windows of operation* te identificeren waarbij coalescentie van de oliedruppels en het rijzen van de oliedruppels wordt bevorderd ten opzichte van emulsificatie en mengen van de kleine druppels. Hoewel de condities op laboratoriumschaal gunstiger kunnen zijn voor rijzen van de druppels dan voor het doormengen, kan op grote schaal de integratie van productie en scheiding alleen worden gerealiseerd in een reactor waarin twee secties met verschillende procesomstandigheden (met name de superficiële gas snelheid) worden gecombineerd.

Op laboratoriumschaal worden vaak oplosmiddelen gebruikt om verdamping van de sesquiterpenen te verminderen en de scheiding het product te verbeteren door de concentratie van de oliefase te vergroten. De huidige technologie gebruikt op fabrieksschaal oppervlakte-actieve stoffen om het geëmulsificeerde product terug te winnen. Hoofdstuk 3 introduceert een techno-economisch analyse van het gebruik van oplosmiddelen op productieschalen die typisch zijn voor smaak- en geurstoffen (25 Mt/y) en de brandstofmarkt (25000 Mt/y), in vergelijking met de meest moderne technologie. Ook komt in deze analyse de problematiek van de verdamping van het product aan de orde en hoe de aanwezigheid van een oplosmiddel kan helpen om het verlies aan product door verdamping te verminderen. Gebaseerd op empirische correlaties, massatransport en *process flow sheeting* modellen, toonde de analyse aan dat het gebruik van oplosmiddelen de verdampingsnelheid van sesquiterpenen tijdens de fermentatie verminderd en de product recovery verbeterd. Echter, het gebruik van oplosmiddelen resulteerde in gelijke of hogere kosten in vergelijking met de standaardmethode, vanwege extra kosten voor onderdelen om het product weer van het oplosmiddel te scheiden. Wanneer oplosmiddelen worden geselecteerd die compatibel zijn met het uiteindelijke product (e.g. een kerosine verrijkingsproces), kan het gebruik van een oplosmiddel toch toegevoegde waarde hebben en kan het de productkosten omlaag brengen naar 0.7 \$ kg^{-1} terwijl de impact op het milieu daalt.

In fermentaties waar een hydrofobe vloeistof wordt geproduceerd en/of als oplosmiddel is toegevoegd om het product in-situ te verwijderen, kan de interactie tussen druppels en gasbellen extra zuurstof-overdrachtsroutes door de oliefase genereren. Ter aanvulling van de techno-economische analyse van hoofdstuk 3, zijn de mechanismen van zuurstof-overdracht in sesquiterpeen fermentaties en het gebruik van oplosmiddelen als zuurstofvector bestudeerd in hoofdstuk 4. De verbetering van de zuurstofoverdrachtscoëfficient (k_La) in fermentaties met de veldstam en de sesquiterpeen producerende *Escherichia coli* bij verschillende oliefracties van hexadecaan en dodecaan was afhankelijk van de overdrachtsroute en verminderde naarmate de fermentatietijd toenam. In tegenstelling tot de resultaten uit de literatuur zijn de k_La trends niet gecorreleerd aan veranderingen in de vermogenstoevoer, oliefractie of cel concentratie, maar kon de verbetering worden verklaard door verminderde gasbel-druppel en druppel-druppel interacties vanwege de stabilisatie van druppels. Voor de eerste keer is bewezen dat oppervlakte-actieve stoffen die in de fermentatievloeistof aanwezig zijn de impact van zuurstofvectoren in de verbetering van k_La kan limiteren, wat een nieuw perspectief biedt op zuurstofoverdracht bij meerfase-fermentaties.

Hoofdstuk 5 bestudeert de integratie van een fermentatie met een ‘gas-enhanced’ oliescheiding technologie, ontwikkeld binnen het TU Delft Initiative Delft Integrated Recovery Column (DIRC) en in samenwerking met de startup Delft Advanced Biorenewables (DAB, www.DelftAB.com), de BE-Basic Foundation, en de Bioprocess Pilot Facility (www.BPF.eu). Het effect van de integratie op verschillende procesvariabelen (celgroei, levensvatbaarheid van de cellen, concentratie van oppervlakte actieve stoffen en stabiliteit van de emulsie) is onderzocht in fed-batch fermentaties, uitgevoerd in een 2L reactor, en in een geïntegreerde opstelling, waarin dezelfde reactor verbonden was met een 500 mL bellenkolom. Het geïntegreerde system heeft met succes 24 uur lang geopereerd, zonder celgroei of levensvatbaarheid van de cellen te beïnvloeden. Echter, in het geïntegreerde systeem is een hoger niveau van oppervlakte-actieve stoffen en emulsiestabiliteit gemeten ten opzichte van de standaardopstelling, wat de capaciteit voor oliescheiding vermindert. Dit laat zien dat procesconfiguratie en -condities (e.g. geometrie, gasstroom) voor verhoogde niveaus van oppervlakte actieve stoffen kunnen zorgen, vanwege cellulaire stress, en dat er een optimalisatie stap nodig is om deze negatieve invloed te minimaliseren. De resultaten uit dit hoofdstuk laten zien dat gas-geïnduceerde scheiding een veelbelovende optie is voor geïntegreerde scheiding in fermentaties met meerdere fasen, wat het mogelijk maakt om olie te scheiden en de cellen te hergebruiken, zonder de fermentatie negatief te beïnvloeden.

Table of contents

Chapter 1. General introduction

Sesquiterpenes are a family of hydrocarbons with the formula $C_{15}H_{24}$, produced in plants and microorganisms from their precursor isoprene. With more than 300 molecular structures identified, sesquiterpenes constitute a rich source of biomaterials. Some of their applications can be traced back to folk traditions where they were extracted from plants. For example, artemisinin extracted from *Artemisia annua* was used in Chinese medicine as antimalarial drug [1]; hernandulcin obtained from *Lippia dulcis* was used as sweetener in Aztec tradition [2]; the extraction of valencene from orange peel for its use as flavour; or the use of sandalwood oil as fragrance obtained from *Santalum album* in India [3]. The portfolio of applications has largely increased the last years (e.g., cancer treatment, agriculture, flavours, fragrances, cosmetics, lubricants and drop-in biofuels [4-9]). However, traditional methods based on plant extraction are not suitable for a sustainable production. The low production yields (e.g., 0.2 hA - land kg^{-1}- artemisinin [10], 1 kton-oranges kg^{-1}-valencene [11]) have led to a shortage of natural resources [12]. Consequently, product prices have increased reaching levels of 100 to 1000 EUR kg^{-1} [13]. In cases such as the production of the antimalarial drug artemisinin, the high demand cannot be satisfied only from the oil produced by the plants and new alternatives are needed. The microbial production of sesquiterpenes via fermentation from renewable biomass sources, like sugar cane bagasse, constitutes a sustainable solution for the supply of these materials. Furthermore, it opens the opportunity for new applications, like their use as precursor for diesel-like biofuels.

1. State of the art in microbial production of sesquiterpenes

Sesquiterpenes are produced via the terpenoid pathway wherein the C5 molecule isopentenyl pyrophosphate (IPP) and its isomer dimethylallyl diphosphate (DMAPP) are used as a carbon building block to produce terpenes of different length, all of them precursors of valuable industrial products like isoprene (C5), menthol (C10), taxol (C20), and carotenes (C40) (Figure 1).

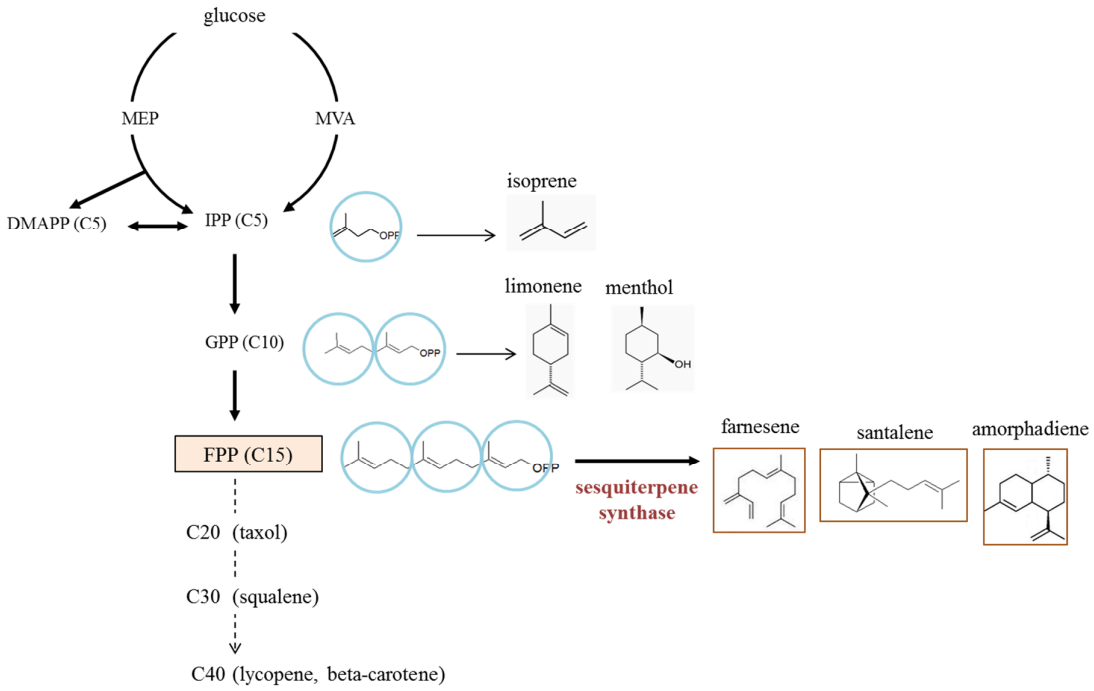

Figure 1. Overview of the terpenoid pathway whereby sesquiterpenes are produced in organisms. Blue circles indicate isopentenyl units (C5) used as carbon building blocks. Example of relevant molecules produced via this pathway are given. Eukaryotes, archaea, and a few eubacteria synthesize IPP and DMAPP from acetyl-coA via the MVA pathway. Eubacteria, cyanobacteria, green algae, apicomplexan parasites, and higher plants synthesize IPP and DMAPP from pyruvate and glyceraldehyde-3-phosphaste via the MEP pathway. MVA: mevalonic acid, MEP: methylerythritol phosphate IPP: Isopenthenyl diphosphate, GPP Geranyl diphosphate, FPP: Farnesyl diphosphate.

Following this pathway, sesquiterpene production can be divided in three sections: (i) production of C5 precursors IPP and DMAPP; (ii) addition of two units of IPP to one of DMAPP; and (iii) conversion of FPP into the target sesquiterpene by its corresponding sesquiterpene synthase.

The C5 precursors IPP and DMAPP can be synthesized by different routes depending on the considered organism. The mevalonate (MVA) pathway is present in eukaryotes, archaea, and a few eubacteria [14, 15], and synthesize IPP and DMAPP from acetyl-coA. On the other hand, the methylerythritol 4-phosphate pathway (MEP) is present in eubacteria, cyanobacteria, green algae, apicomplexan parasites, and plastids of higher plants [16, 17], and synthesize IPP and DMAPP from pyruvate and glyceraldehyde-3-phosphate.

Genetically engineered microbial strains can produce and secrete sesquiterpenes reaching titres in the order of g per L [18-20]. The target sesquiterpene can be overproduced in yeast and bacteria by (i) overproducing the precursor FPP (e.g., by improving the microorganism native pathway leading to FPP, or by inserting a heterologous one) and (ii) expressing heterologous sesquiterpene synthase genes obtained from plant cDNA. Due to the high regulation of endogenous MEP pathway in bacteria, and the low productivity achieved so far in yeast by MEP [21], the most promising options are endogenous MVA pathway in yeast (e.g. *Saccharomyces cerevisiae*) and heterologous MVA pathway in bacteria (e.g. *Escherichia coli*). Several improvements have been done in the MVA pathway by overexpression of key enzymes, and by repressing or downregulating genes involved in secondary routes (e.g., farnesol, squalene). In addition, sesquiterpene production can also be improved by regulating genes outside the MVA pathway; for example, by enhancing the supply of acetyl-CoA to the mevalonate pathway [22], or by enhancing the availability of cytosolic NADPH, required by key enzymes [23]. In addition to the results published using *S. cerevisiae* and *E. coli* as producing hosts, some alternative microorganisms able to convert lignocellulosic material are being studied [24].

The improvements in the metabolic pathway allowed to increase theoretical yields from 0.2 g g-glucose^{-1} to 0.3 g g-glucose^{-1} [20]. Also experimental yields have risen from values of < 0.1 g g-glucose^{-1} [19] to > 0.2 g g-glucose^{-1} [20], closer to the maximum theoretical yield. This is reflected in an increase in production titres in the last years (Table 1). In addition, fed-batch operation in large reactors allow for higher cell densities compared to laboratory shake flask. As a result, increasing titres up to 120 g L^{-1} have been reported. The recovery of the produced sesquiterpene from the fermentation broth should be, in principle, rather straightforward. Sesquiterpenes are extracellular hydrophobic molecules with lower density than water and thus, they form a light liquid phase (hereafter named as oil phase) in the fermentation broth. This oil phase is dispersed as droplets due to the mixing in the reactor. Ideally the droplets can collide and coalesce increasing their size. When they are large enough they rise due to buoyancy forces (mechanism called creaming) where they can further coalesce forming a clear oil layer on top of the reactor readily separated from the aqueous phase. Several companies, like Amyris, Firmenich, Evolva, Allylix, and Isobionics have seen potential in the microbial production of sesquiterpenes. Most of them are already in the stage of commercial scale production in fed-batch fermentations (Table 2).

Table 1. Examples of titres and yields for sesquiterpene and sesquiterpenoid production achieved in *E. coli* and *S. cerevisiae* in batch and fed-batch fermentations

Producing organism: *Escherichia coli*			
Product	**Titre (g L^{-1})**	**Yield (g g-cell^{-1})**	**Reference**
Amorphadiene	0.3	0.1[a]	[25]
Amorphadiene	27.4	0.3	[18]
Amorphadiene	0.5	0.4[a]	[26]
Amorphadiene	0.7	0.4[a]	[27]
Producing organism: *Saccharomyces cerevisiae*			
Product	**Titre (g L^{-1})**	**Yield (g g-cell^{-1})**	**Reference**
-	0.1	0.03[b]	[28]
Artemisinic acid	1.0	-	[29]
Amorphadiene	40	0.50 [c]	[19]
Santalene	0.1	-	[30]
Farnesene	120	-	[20]

a) assuming 0.35 g L^{-1} of cells per unit of optical density (OD); b) assuming 0.4 g L^{-1} of cells per unit of optical density (OD); c) Using ethanol as substrate; d) Using glycerol as substrate.

Table 2. Main companies involved in the microbial production of sesquiterpenes

Company	**Sesquiterpene**	**Titre (g L^{-1})** [a]	**Application**	**Reference**
Amyris	Farnesene, squalene, amorphadiene.	120	Biofuels, lubricants, pharmaceuticals	[20, 31]
Firmenich	Santalene, valencene	0.1	Flavours and fragrances	[32]
Evolva/ Allylix[b]	Valencene, nootkatone	-	Flavours and fragrances	-
Isobionics	Valencene, nootkatone, elemene, bisabolene	0.2	Flavours and fragrances	[33]

a) Highest titre reported in literature; b) Acquired by Evolva in 2014

2. Challenges in large scale production of sesquiterpenes

The scale-up of the production process of sesquiterpenes has unveiled challenges that were not prominently present at laboratory scale. Surface active components (e.g., salts, glycolipids, proteins, cells and cells debris) present in the fermentation medium can interact with the oil-water interface [34]. As a result, the product remains dispersed in a stable emulsion of small droplets (Figure 2).

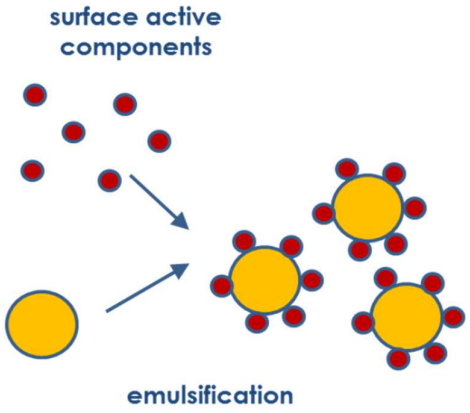

Figure 2. Schematic representation of emulsification of product droplets by the presence of surface active components.

Methods to recover sesquiterpenes from such emulsions differ by process scale. The strategy reported in laboratory scale protocols is to promote oil coalescence by adding two volumes of a solvent (e.g. methyl-tert-butyl ether, ethyl-acetate, or heptane) to one volume of sample [30, 35]. Oil phase containing solvent and product is recovered afterwards by centrifugation. At large scale, the emulsion is separated first from the aqueous medium by centrifugation. Afterwards, non-ionic surfactants are added to the emulsion and their hydrophobicity is modified by increasing and decreasing the temperature of the mixture. This switch of temperatures inverts the o/w emulsion into a emulsion of water droplets in oil [36] (Figure 3). Finally, the remaining water is eliminated by centrifugation. In the case of biofuel production, additional hydrogenation is required to saturate the double bonds of farnesene to yield the hydrocarbon farnesene. The presence of the surfactants in the product might compromise required product purity (e.g. 92% to 94% purity for cosmetics [8]), and consequently further purification steps might be required (e.g. distillation [37]).

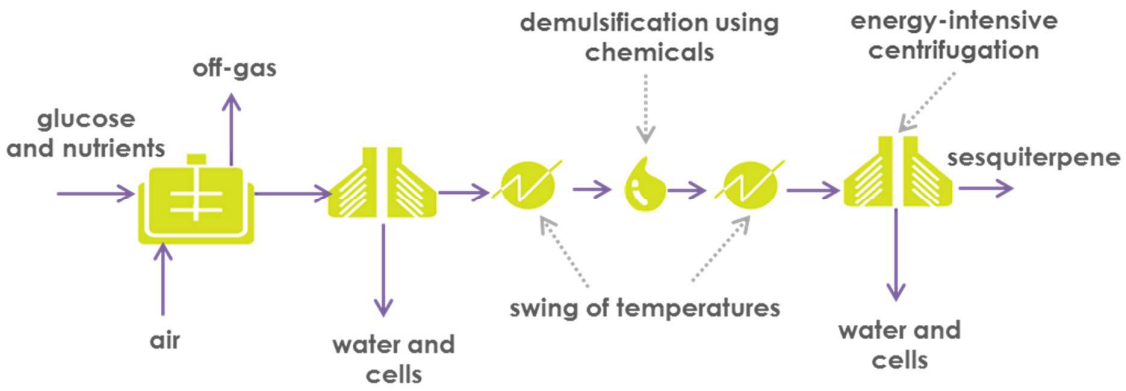

Figure 3. Block scheme of the (reported) process at large scale for the recovery of microbial sesquiterpene [36].

Another aspect that should be considered in the scale-up of the microbial production of sesquiterpenes is that they are relatively volatile molecules (vapour pressure at 25°C between 3 and 8 Pa predicted by US Environmental Protection Agency's EPISuite™). Evaporation rates in the order g L^{-1} have been reported in laboratory studies [25], which could imply product losses in the order of kg h^{-1} at large scale. A common solution is extracting sesquiterpenes with 10–20% v/v of a relatively low volatile organic solvent, like decane or dodecane (referred to as solvent overlay in laboratory protocols) [23, 25, 30, 32, 35]. Surprisingly, this practice extensively used in sesquiterpene laboratory studies, is rarely described at large scale [38]. Reported physical properties of sesquiterpenes are scarce (see for example [39] and the actual impact of evaporation and the applicability of solvents at production scale is unknown.

Finally, the transfer of oxygen from the air bubbles to the fermentation medium is typically a limiting factor in the scale-up of aerobic fermentations [40]. In multiphase systems the oil droplets can interact with the surface of gas bubbles. This alters the oxygen transfer mechanisms increasing the complexity of the scale-up problem. Although there is extensive literature on oxygen transfer in multiphasic systems, results are often contradictory [41, 42].

The issues presented above have a direct impact in the process cost, and the product price. This is of especial importance in markets, like biofuels, where tight economic margins are imposed by the low prices of the fossil-based fuels. The aim of this thesis is addressing and quantifying these challenges to improve product recovery at large scale, while reducing the

process production cost (Table 3). By identifying and characterizing the key mechanisms involved in microbial sesquiterpene process, reactor design and operational parameters can be selected to promote coalescence and creaming of the oil phase. A low-cost technology (e.g. hydrocyclon, or gravity settling) could be implemented afterwards to recover the product. In addition, the selected recovery technology should allow for cell recycling to reduce the substrate consumption to grow mass of cells in the reactor. Within the TU Delft Initiative Delft Integrated Column Reactor project (DIRC), and in collaboration with the start-up Delft Advanced Biorenewables (DAB, www.DelftAB.com), the BE-Basic Foundation, and the Bioprocess Pilot Facility (www.BPF.eu), a gas enhanced oil recovery technology has been developed. This technology consists of promoting oil droplets coalescence into a continuous oil layer by sparging gas through the emulsion. By implementing gas enhance oil recovery less separation steps might be required. Also, the use of chemicals is avoided, reducing the environmental impact and improving product quality. This thesis makes a step forward in the study of how this technology can be integrated for in-situ product recovery during the fermentation to achieve product separation while allowing for cell recycle.

In first place, a regime analysis at different scales is presented in **chapter 2** to identify possible windows of operation where droplet creaming is promoted in a bubble column. Next, **chapter 3** studies the possibility of using solvents at large scale to increase oil phase concentration and promote the coalescence of the stabilized oil droplets. In addition, it addresses the problematic of product evaporation, and how the presence of a solvent could help to reduce the loss of product in the off-gas. **Chapter 4** studies the mechanisms of oxygen transfer in sesquiterpene fermentation and the use of solvents as oxygen vector. C**hapter 5** studies the integration of gas enhanced oil recovery technology into a fermentation. Furthermore, it investigates the interaction of surface active components and emulsification and the impact of oxygen limitation in the increase of surface active components and cell stress. Finally, **chapter 6** summarizes the main conclusions and the outlook of this thesis.

Table 3. Challenges addressed in this thesis

Chapter	Challenge	Conclusion
2	Integration of production and gravity settling in reactor	There is no operational window that allows for production and recovery in the same compartment.
3	Use solvents at large scale to reduce evaporation and promote recovery	Loss of sesquiterpenes due to evaporation is aggravated at large scale. When solvents are compatible with product formulation (e.g. use of diesel in the production of farnesene for jet-fuel) it is techno-economically feasible to use them to reduce evaporation and promote product recovery at large scale.
4	Interaction of the oil phase with oxygen transfer in a multiphase fermentation.	Oxygen transfer route prevalent in a multiphase system is affected by the o/w interface properties. Enhancement of oxygen transfer due to oil droplets acting as vectors is limited by oil phase emulsification.
5	Integration of production and gas enhanced oil recovery in reactor.	It is feasible to integrate gas enhanced oil recovery to a fermentation.

3. References

1. Qinghaosu-Antimalaria-Coordinating-Research-Group, *Antimalaria studies on Qinghaosu.* Chinese Medical Journal, 1979. **92**(12): p. 811-816.

2. Attia, M., Kim, S.U., and Ro, D.K., *Molecular cloning and characterization of (+)-epi-alpha-bisabolol synthase, catalyzing the first step in the biosynthesis of the natural sweetener, hernandulcin, in Lippia dulcis.* Arch Biochem Biophys, 2012. **527**(1): p. 37-44.

3. Jones, C.G., Ghisalberti, E.L., Plummer, J.A., and Barbour, E.L., *Quantitative co-occurrence of sesquiterpenes; a tool for elucidating their biosynthesis in Indian sandalwood, Santalum album.* Phytochemistry, 2006. **67**(22): p. 2463-8.

4. Chadwick, M., Trewin, H., Gawthrop, F., and Wagstaff, C., *Sesquiterpenoids Lactones: Benefits to Plants and People.* International Journal of Molecular Sciences, 2013. **14**(6): p. 12780-12805.

5. Datta, S. and Saxena, D.B., *Pesticidal properties of parthenin (from Parthenium hysterophorus) and related compounds.* Pest Management Science, 2001. **57**(1): p. 95-101.

6. Collado, I.G., Aleu, J., Macias-Sanchez, A.J., and Hernandez-Galan, R., *Inhibition of Botrytis cinerea by new sesquiterpenoid compounds obtained from the rearrangement of isocaryophyllene.* Journal of Natural Products, 1994. **57**(6): p. 738-746.

7. Maury, J., Asadollahi, M.A., Moller, K., Clark, A., et al., *Microbial isoprenoid production: an example of green chemistry through metabolic engineering.* Adv Biochem Eng Biotechnol, 2005. **100**: p. 19-51.

8. McPhee, D.J., *Deriving Renewable Squalane from Sugarcane.* Cosmetics & Toiletries, 2014. **129**(6): p. 20-26.

9. Westfall, P.J. and Gardner, T.S., *Industrial fermentation of renewable diesel fuels.* Current Opinion in Biotechnology, 2011. **22**(3): p. 344-350.

10. Hale, V., Keasling, J.D., and Renninger, N., *Microbially Derived Artemisinin: A Biotechnology Solution to the Global Problem of Access to Affordable Antimalarial Drugs.* Am. J. Trop. Med. Hyg., 2007. **77**(Suppl 6): p. 198–202.

11. Evolva. [cited 2016 July]; Available from: http://www.evolva.com/products/valencene/.

12. Misra, U. *How India's Sandalwood Oil trade got hijacked*. 2006 [cited 2018 May]; Available from: http://www.forbesindia.com/article/on-assignment/how-indias-sandalwood-oil-trade-got-hijacked/2972/1.

13. Devi, M.P., Ghosh, S.K., Bhowmick, N., and Chakrabarty, S., *Essential oil: Its economic aspect, extraction, importance, uses, hazards and quality*, in *Value Addition of Horticultural Crops: Recent Trends and Future Directions*, A. Sharangi, Datta, S., Editor. 2015, Springer: New Delhi. p. 269-278.

14. Ajikumar, P.K., Tyo, K., Carlsen, S., Mucha, O., et al., *Terpenoids: opportunities for biosynthesis of natural product drugs using engineered microorganisms.* Mol Pharm, 2008. **5**(2): p. 167-90.

15. Goldstein, J.L. and Brown, M.S., *Regulation of the mevalonate pathway.* Nature, 1990. **343**(6257): p. 425-30.

16. Rohmer, M., *The discovery of a mevalonate-independent pathway for isoprenoid biosynthesis in bacteria, algae and higher plants.* Nat Prod Rep, 1999. **16**(5): p. 565-74.

17. Dewick, P.M., *The biosynthesis of C5-C25 terpenoid compounds.* Nat Prod Rep, 2002. **19**(2): p. 181-222.

18. Tsuruta, H., Paddon, C.J., Eng, D., Lenihan, J.R., et al., *High-level production of amorpha-4,11-diene, a precursor of the antimalarial agent artemisinin, in Escherichia coli.* PLoS One, 2009. **4**(2): p. e4489.

19. Westfall, P.J., Pitera, D.J., Lenihan, J.R., Eng, D., et al., *Production of amorphadiene in yeast, and its conversion to dihydroartemisinic acid, precursor to the antimalarial agent artemisinin.* Proc Natl Acad Sci U S A, 2012. **109**: p. e111-8.

20. Meadows, A.L., Hawkins, K.M., Tsegaye, Y., Antipov, E., et al., *Rewriting yeast central carbon metabolism for industrial isoprenoid production.* Nature, 2016. **537**(7622): p. 694-697.

21. Chang, M.C. and Keasling, J.D., *Production of isoprenoid pharmaceuticals by engineered microbes.* Nat Chem Biol, 2006. **2**(12): p. 674-81.

22. Shiba, Y., Paradise, E.M., Kirby, J., Ro, D.K., et al., *Engineering of the pyruvate dehydrogenase bypass in Saccharomyces cerevisiae for high-level production of isoprenoids.* Metab Eng, 2007. **9**(2): p. 160-8.

23. Asadollahi, M.A., Maury, J., Moller, K., Nielsen, K.F., et al., *Production of plant sesquiterpenes in Saccharomyces cerevisiae: effect of ERG9 repression on sesquiterpene biosynthesis.* Biotechnol Bioeng, 2008. **99**(3): p. 666-77.

24. Yaegashi, J., Kirby, J., Ito, M., Sun, J., et al., *Rhodosporidium toruloides: a new platform organism for conversion of lignocellulose into terpene biofuels and bioproducts.* Biotechnology for Biofuels, 2017. **10**(1): p. 241.

25. Newman, J.D., Marshall, J., Chang, M., Nowroozi, F., et al., *High-level production of amorpha-4,11-diene in a two-phase partitioning bioreactor of metabolically engineered Escherichia coli.* Biotechnol Bioeng, 2006. **95**(4): p. 684-91.

26. Redding-Johanson, A.M., Batth, T.S., Chan, R., Krupa, R., et al., *Targeted proteomics for metabolic pathway optimization: application to terpene production.* Metab Eng, 2011. **13**(2): p. 194-203.

27. Ma, S.M., Garcia, D.E., Redding-Johanson, A.M., Friedland, G.D., et al., *Optimization of a heterologous mevalonate pathway through the use of variant HMG-CoA reductases.* Metab Eng, 2011. **13**(5): p. 588-97.

28. Takahashi, S., Yeo, Y., Greenhagen, B.T., McMullin, T., et al., *Metabolic engineering of sesquiterpene metabolism in yeast.* Biotechnology and Bioengineering, 2007. **97**(1): p. 170-181.

29. Ro, D.K., Ouellet, M., Paradise, E.M., Burd, H., et al., *Induction of multiple pleiotropic drug resistance genes in yeast engineered to produce an increased level of anti-malarial drug precursor, artemisinic acid.* BMC Biotechnol, 2008. **8**: p. 83.

30. Scalcinati, G., Knuf, C., Partow, S., Chen, Y., et al., *Dynamic control of gene expression in Saccharomyces cerevisiae engineered for the production of plant sesquitepene alpha-santalene in a fed-batch mode.* Metab Eng, 2012. **14**(2): p. 91-103.

31. Paddon, C.J., Westfall, P.J., Pitera, D.J., Benjamin, K., et al., *High-level semi-synthetic production of the potent antimalarial artemisinin.* Nature, 2013. **496**(7446): p. 528-32.

32. Scalcinati, G., Partow, S., Siewers, V., Schalk, M., et al., *Combined metabolic engineering of precursor and co-factor supply to increase alpha-santalene production by Saccharomyces cerevisiae.* Microb Cell Fact, 2012. **11**: p. 117.

33. Wriessnegger, T., Augustin, P., Engleder, M., Leitner, E., et al., *Production of the sesquiterpenoid (+)-nootkatone by metabolic engineering of Pichia pastoris.* Metabolic Engineering, 2014. **24**: p. 18-29.

34. Heeres, A.S., Picone, C.S.F., van der Wielen, L.A.M., Cunha, R.L., et al., *Microbial advanced biofuels production: overcoming emulsification challenges for large-scale operation*. Trends Biotechnol. , 2014. **32**(4): p. 221-229.

35. Schalk, M.*Method for producting beta-santalene* Firmenich SA 2011. US 0281257 A1

36. Tabur, P. and Dorin, G.*Method for purifying bio-organic compounds from fermentation broth containing surfactants by temperature-induced phase inversion.* 2012. WO2012024186

37. Ohler, N.L. and Vazquez, R.*Stabilization and hydrogenation methods for microbial-derived olefins* Amyris, Inc. 2013. US 0310615 A1

38. Janssen, A.C.J.M., Kierkels, J.G.T., and Lentzen, G.F.*Two-phase fermentation process for the production of an organic compound* ISOBIONICS B.V. 2015. WO2015002528

39. Schuhfried, E., Aprea, E., Märk, T.D., and Biasioli, F., *Refined Measurements of Henry's Law Constant of Terpenes with Inert Gas Stripping Coupled with PTR-MS.* Water, Air, & Soil Pollution, 2015. **226**(4): p. 1-13.

40. Garcia-Ochoa, F. and Gomez, E., *Bioreactor scale-up and oxygen transfer rate in microbial processes: an overview.* Biotechnol Adv, 2009. **27**(2): p. 153-76.

41. Clarke, K.G. and Correia, L.D.C., *Oxygen transfer in hydrocarbon–aqueous dispersions and its applicability to alkane bioprocesses: A review.* Biochemical Engineering Journal, 2008. **39**(3): p. 405-429.

42. Dumont, E. and Delmas, H., *Mass transfer enhancement of gas absorption in oil-in-water systems: a review.* Chemical Engineering and Processing: Process Intensification, 2003. **42**(6): p. 419-438.

Chapter 2. Regime analysis for integrated product recovery in microbial advanced biofuels production

Abstract

One of the recent achievements in biofuel research is the development of microorganisms that produce advanced biofuels. These biofuels form a second liquid phase during fermentation, which creates the opportunity for low cost product separation based on the density difference with the fermentation medium. Integrating product removal and fermentation could contribute to lower equipment and utility costs and it might also enable the recycling of cells. In this paper, the feasibility of gravity separation integrated with biofuel production in a bubble column reactor is studied, using a regime analysis approach. The two crucial subprocesses are droplet coalescence and droplet creaming, but these are hindered by competing subprocesses: emulsification and mixing, respectively. The regime analysis showed that a multi-compartment reactor design is required to benefit from the advantages of integration: cell reuse, lower equipment costs, and easier separation.

This chapter has been submitted as:

Heeres*, A.S., Pedraza-de la Cuesta*, S., Heijnen, J.J., van der Wielen, L.A.M., Cuellar, M.C, Regime analysis for integrated product recovery in microbial advanced biofuels production

* Both authors contributed equally

1. Introduction

In the search for better biofuels, biotech companies such as REG Life Sciences and Amyris have developed microorganisms that are capable of converting sugars to long-chain hydrocarbon biofuels, also named advanced or drop-in biofuels, using metabolic engineering and synthetic biology [1-4]. These developments are especially relevant for jet fuels, since there are no technical renewable alternatives for airplanes. The biofuels currently produced at commercial scale, ethanol and biodiesel (transesterified lipids) produced from vegetable oils and fats, are either unsuitable as jet fuel and/or limited by feedstock availability. Target production costs for long-chain hydrocarbons of around \$0.60 L^{-1} have been mentioned to make these biofuels an alternative for conventional fuels [4], but selling prices of \$7.7 L^{-1} were recently reported [5]. In order to lower their production costs, a combination of process improvements is required: a) use of a low cost feedstock, b) enabling anaerobic fermentation to maximise product yield on substrate and to avoid aeration related investments and energy cost, c) implementing cell reuse, and d) developing low cost fermentation and product recovery technology [6].

The microbial production of advanced biofuels consists of a fermentation in which the microorganism converts substrate to biofuel and secretes it into the fermentation broth [7], resulting in a four phase mixture consisting of hydrocarbon product (oil) droplets, aqueous fermentation broth, microbial cells, and (fermentation) gas bubbles. Although not much has been reported about the secretion mechanism, the initial size of the oil droplets after secretion can be expected to be at most in the same order of magnitude as the cells (~1 µm). The recovery of the oil droplets follows then three steps: droplet growth by coalescence, phase separation – also named creaming – induced by the density difference, and further coalescence of droplets into a continuous oil phase [8].

In a fermentation process, a wide range of surface active components (SACs) can be present, originating from cells and feedstock [8]. In fact, product droplet stabilisation has been reported in the production of advanced biofuels [9]. The presence of SACs could hinder the coalescence process, preventing droplet growth and leading to product emulsification.

The droplet size that is reached after the first coalescence step, determines the options for the phase separation method. Gravity separation is the most simple and cost effective method to induce creaming, but large droplets are required because the separation is driven by only the gravitational force. Enhanced gravity methods (e.g., centrifugation and hydrocyclones)

are capable of separating smaller droplets, but these methods are more expensive. Therefore, we will focus on the application of gravity separation.

Next to applying gravity separation, the process costs could be further decreased by integration of product separation with fermentative production in a single unit, potentially decreasing equipment costs. Many large scale fermentation processes are performed in bubble column bioreactors, in which the bubbles (either sparged air in the current aerobic process or gas produced by the microorganisms in an anaerobic case) provide mixing and hence, no mechanical power input is required. This reduces the operating costs and is therefore regarded as the most suitable bioreactor type for large scale production of drop-in biofuels [10]. Integration of the production and separation may have further advantages such as enabling cell reuse and continuous process operation.

Whether product separation can be integrated in a bubble column bioreactor is dependent on the operating conditions. In this paper, the possibility of integrating gravity separation and fermentation into a single piece of equipment is studied by a regime analysis, which takes the effects of operating conditions and scale into account.

2. Regime analysis

2.1. Concept

Regime analysis is a tool that compares the rates of the different mechanisms involved in a process in order to identify the rate-limiting one. The method divides the overall process in a sequence of steps, or subprocesses, and compares their rates. The subprocess rates are represented as characteristic times, which indicate the time required by a mechanism to smooth out a change [11]. The rates are inversely proportional to their characteristic times, so a subprocess with a low rate has a large characteristic time. One subprocess is considered faster than the other when its characteristic time is at least one order of magnitude lower [11]. This comparison is done in terms of order of magnitude, since correlations used to determine characteristic times also yield an order of magnitude estimation of these. The subprocess with the largest characteristic time is the rate-limiting one, determining over-all process rate and the regime in which the process operates [12]. By assessing effect of reactor size on the characteristic times, the scale dependency of the process can be determined.

Several scale-up/scale-down studies in literature have used regime analysis as a tool for assessing scale effects, applying it for a variety of processes: gluconic acid production [13], microbial desulfurisation [14], butanol production [15], baker's yeast production [11] and, more recently, Baeyer–Villiger bioconversion of ketones [16, 17] and production of biopharmaceutical proteins [18]. To achieve similar process performance when moving from lab to large scale, the regime should be the same on both scales [12]. Regime analysis can be used to determine if a regime change will take place when the scale of the process is increased.

2.2. Subprocess sequence definition

The first step in a regime analysis is to list the subprocesses in the production system, which leads to the simplified sequence of subprocesses shown in Figure 1. The microbial production of advanced biofuel starts with the substrate, which is fed to the reactor and mixed in the fermentation broth (1). Microorganisms take the substrate (2), convert the substrate to biofuel (3) and secrete it (4). The recovery of the biofuel begins with small product droplets that grow by coalescence (5). When they reach a critical size, the droplets cream (6) and finally they can form a continuous oil phase on top of the reactor (7).

For conventional fermentation processes, mixing, heat removal, and oxygen transfer are generally considered the rate-limiting subprocesses [19]. In this paper, we will focus the regime analysis on the integration of product separation with its microbial production, which will result in additional subprocesses that have to be evaluated. SACs produced by the microorganisms (e.g., proteins) can stabilise the oil droplets hindering coalescence and leading to product emulsification. In addition, mixing in the reactor (1) competes with the creaming of the droplets (6) preventing the formation of a continuous oil phase. Because we focus on the integration of the separation process, we take the subprocesses related to the microorganisms not to be limiting.

In this study, different process parameters influencing droplet coalescence, droplet creaming, mixing, and adsorption of SACSs are assessed by a regime analysis. Integration is considered feasible at operating conditions in which characteristic times of coalescence (τ_{coa}) and creaming (τ_{crm}) are one order of magnitude lower than the characteristic times of adsorption of SACs (τ_{ads}) and mixing (τ_{mix}), respectively:

$$\tau_{coa} < 10 \cdot \tau_{ads} \quad (1)$$

$$\tau_{crm} < 10 \cdot \tau_{mix} \tag{2}$$

Next step is expressing these characteristic times as a function of different process parameters. A single process parameter can influence multiple characteristic times. For example, the volumetric power input in the reactor influences the characteristic times of mixing, coalescence, and SAC adsorption, as will be shown in the following paragraphs.

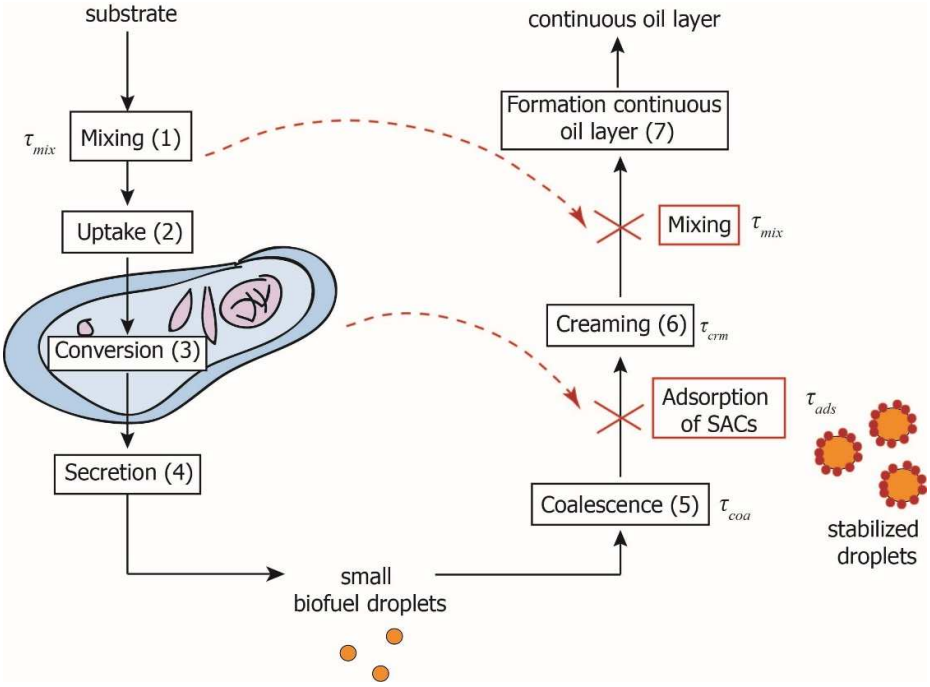

Figure 1. Schematic presentation of the subprocesses involved in the microbial production (left) and separation (right) of biofuel. Interactions resulting from the integration are represented with dashed lines.

2.3. Characteristic times derivation

2.3.1. Droplet coalescence

Coalescence is a three stage subprocess (Fig. 2): the droplets first collide, then the liquid film between the droplets drains, and finally the film ruptures and the droplets merge [20].

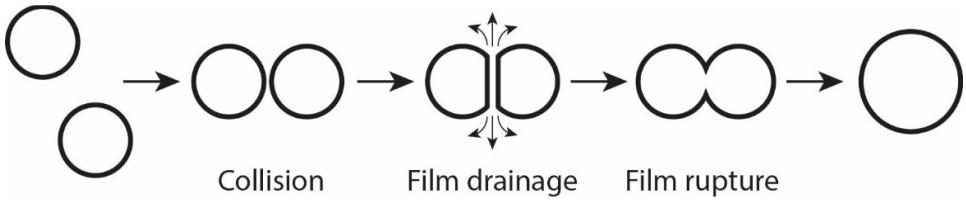

Figure 2. Illustration of the three steps in the coalescence subprocess.

When the droplet interface is not stabilized by SACs, film drainage and rupture occur rapidly. Hence, droplet collision is the (slowest) rate determining step in coalescence of unstabilized droplets [21]. The characteristic time for the coalescence process can be described by the collision time of equally sized droplets is shown in Equation (3) [22]:

$$\tau_{coa} = \frac{d_d^{2/3} \rho_l^{1/3}}{15 \phi_{oil} e_v^{1/3}}. \quad (3)$$

The droplet collision rate depends on the volumetric oil fraction (ϕ_{oil}), the droplet diameter (d_d), the overall liquid density (ρ_l), taking into account the volume fractions of oil and water, and the volumetric power input (e_v). The power input in a bubble column is determined by the gas flow rate and the reactor geometry, combining the two in the superficial gas velocity. Equation (4) approximates the volumetric power input by the gas displacement, using the gravitational acceleration constant (g), overall liquid density and superficial gas velocity (v_{gs}, volumetric gas flow over cross sectional area of the column) [23]:

$$e_v = g \rho_l v_{gs}. \quad (4)$$

Ionic strength and pH influence the effective droplet charge, creating or neutralizing repulsive electrostatic forces and thereby influencing coalescence. However, at the ion concentrations present in fermentations, the droplet charge is shielded, and any electrostatic repulsive forces are eliminated, therefore these do not have to be taken into account [24, 25].

2.3.2. Droplet stabilization

SACs can adsorb at the oil/water interface of the droplets, lowering the interfacial tension, or causing steric or charge stabilization of the interface, preventing coalescence and droplet growth. The characteristic time for the adsorption of these SACs at a droplet surface is given by Equation (5) [22],

$$\tau_{ads} = \frac{10\Gamma\eta_w^{\frac{1}{2}}}{d_d\, c_{SAC}\, e_v^{\frac{1}{2}}}. \tag{5}$$

This equation includes the surface excess concentration (Γ), which is the amount of SACs adsorbing at the oil/water interface, droplet diameter (d_d), the concentration of SACs in the bulk (c_{SAC}), and the volumetric power input as a measure for the mixing in the reactor.

2.3.3. Droplet creaming

The density difference between the oil droplets and the continuous phase results in a buoyancy force that induces the rising of the droplets, also called droplet creaming. The characteristic time for droplet creaming was defined as the time required for an oil droplet within a swarm of droplets to rise with a certain creaming velocity ($v_{d,swarm}$) over the height of the column (H), as in Equation (6).

$$\tau_{crm} = \frac{H}{v_{d,swarm}}. \tag{6}$$

To obtain the velocity of droplets in a swarm, we first need to calculate the creaming velocity of a single droplet (v_d), which depends on the density difference between oil and aqueous phase (ρ_{aq}), droplet diameter, drag coefficient (C_D) and gravitational acceleration constant as given by Equation (7) [26].

$$v_d = \sqrt{\frac{4g\left(\rho_{aq} - \rho_{oil}\right)d_d}{3C_D\rho_w}}\,. \tag{7}$$

An initial guess for the creaming velocity can be used to calculate the Reynolds number (Re):

$$Re = \frac{v_d \rho_{aq} d_d}{\eta}\,. \tag{8}$$

An estimate of the drag coefficient can be determined, using Equation (9) [26].

$$C_D = \frac{24}{Re} + 3Re^{-1/2} + 0.34 \tag{9}$$

By an iterative approach, Equations (7) to (9) determine the creaming velocity of a single droplet. Since high oil fractions are considered, hindered creaming of the oil droplets will occur and droplets should be considered to rise as a swarm instead of single droplets. The Richardson-Zaki equation can be used to correct the droplet creaming velocity for this effect [27]:

$$v_{d,swarm} = v_d(1-\phi_{oil})^n\,. \tag{10}$$

In this equation, n is a parameter that is dependent on the Reynolds number, droplet diameter, and vessel diameter [28].

2.3.4. Mixing

Mixing is the subprocess considered to compete with the droplet creaming. When mixing is too strong, the droplets will move with the bulk liquid instead of creaming to the top of the reactor. The mixing time in a bubble column can be determined by making an estimation of the circulation time of the liquid in such a column. Groen developed the following correlations for describing the characteristic time of mixing (τ_{mix}) in different flow regimes in a bubble column as function of volumetric power input, bubble diameter, column diameter (D) and the column height (H) [29]. For superficial gas velocities lower than 4 cm s^{-1}, the bubble flow is steady and well distributed over the whole reactor, resulting in a homogeneous regime [29]. In this flow regime, the mixing time can be estimated as:

$$\tau_{mix,\mathrm{hom}} = 0.008\left(\frac{D^6}{{d_b}^4 e_v/\rho_l}\right)^{1/3}\left(\frac{H}{D}\right)^2 \tag{11}$$

For superficial gas velocities higher than 4 cm s^{-1}, the heterogeneous mixing regime is obtained, in which the mixing caused by the bubbles has a more irregular, turbulent pattern [29]. In this case, a distinction must be made for low and high aspect ratio bubble columns. For a bubble column with an aspect ratio between 1 and 3 can be described by

$$\tau_{mix,het} = 16\left(\frac{D^2}{e_v/\rho_l}\right)^{1/3} \tag{12}$$

When the aspect ratio of the column is higher than three, Equation (13) gives the characteristic mixing time:

$$\tau_{mix} = 1.496\left(\frac{D^2}{e_v/\rho_l}\right)^{1/3}\left(\frac{H}{D}\right)^2 \tag{13}$$

3. Base case definition

The base case for the regime analysis is a continuous fermentation in a bubble column, in which the mixing is provided by gas bubbles. Bubble column bioreactors are often chosen for large scale processes, since they do not require mechanical power input for mixing. The performed regime analysis aims at exploring the possibility of the integration of oil recovery in a fermentation process. Therefore, the analysis is focused on the effects of process conditions on the droplet coalescence and creaming steps, aiming at achieving conditions in which these steps are enabled. This results in process conditions requirements for the integration of the separation, which are in the end compared to conditions required for fermentations (i.e., mixing requirements), without going into detail in specific fermentation related subprocesses (e.g., substrate uptake, oxygen uptake).

Both bacteria and yeast have been genetically modified to produce advanced biofuels, but yeast cells are generally considered as the most robust microorganisms for industrial fermentation [4]. Therefore, the yeast *S. cerevisiae* has been chosen as microorganism for this base case. Current advanced biofuel producing microorganisms operate in aerobic conditions, as metabolic pathways require cofactors regeneration by respiration [30]. However, research

for microbial production of bulk chemicals is directed at developing anaerobic metabolic pathways to increase metabolic yields, and potentially decreasing production costs [31]. The regime analysis presented in this study can be applied for both aerobic and anaerobic cases, since gas composition has no effect on mixing. The required gas flow can be controlled by the gas inflow (e.g., by a gas recycle).

For the regime analysis, the effect of process parameters and process scale on the characteristic times were evaluated over the specified range, while keeping all other parameters at their default values. Table 1 summarises the complete set of model parameters values used in the regime analysis, unless specified differently (e.g., when a parameter is varied over a range).

Table 1. Base case parameter values and ranges.

Parameter	Base case	Range
V_r (m^3)	1	$10^{-2} - 10^3$
H / D (-)	4	1 – 15
σ_{oil} (mN m^{-1})	52	
ρ_{oil} (kg m^{-3})	776	
ϕ_{oil} (-)	0.1	0 – 0.4
v_{gs} (cm s^{-1})	5	1 – 10
d_b (mm)	5	
η_w (mPa·s)	1	
c_{SAC} (mg L^{-1})	0.4	0.1 – 0.4
Γ (mg m^{-2})	3	1 – 3
d_d	d_{max}	$d_{min} - d_{max}$

The reactor scale, geometry and superficial gas velocity are the main parameters that determine the reactor design and influence the characteristic times of the subprocesses. The column geometry is determined by the reactor volume (V_r) and aspect ratio (H / D). The reactor volume is varied over the complete range from 10 L to 1000 m^3, with a default value of 1000 L. The aspect ratio is varied from 1 to 15, with a default value of 4.

Mixing is provided by the flow of gas bubbles through the column. The parameter describing the gas flow in a bubble column is the superficial gas velocity. The default value used in the analysis is 5 cm s^{-1} and it is varied within a range up to 10 cm s^{-1} [32]. Bubbles are

assumed to have a diameter (d_b) of 5 mm, which is a typical bubble diameter in bubble columns [33].

The physical properties of the drop-in biofuel (interfacial tension, σ_{oil}, and density, ρ_{oil}) are taken similar to those of hexadecane, which is the most abundant component in diesel fuels [34]. The highest applicable oil fraction in biotechnological processes is considered to be 40%, at higher values severe mass transfer limitations can occur locally [35]. The default volumetric oil fraction was 10% and a range up to 40% is evaluated.

The physical properties of the bulk phase, this is the fermentation broth, are taken similar to those of water. Fermentations at large scale are typically performed at high cell density (50 - 100 g-cell L^{-1}). The presence of cells increases the viscosity of the bulk phase. However, for that range of cell concentration viscosity remains in the same order of magnitude of water [36].

Considering the stabilisation of the droplets, the assumption is made that the product is secreted without any stabilising components present at the oil/water interface of the initial droplets. The droplets can be stabilised against coalescence by the adsorption of surface active components. One of the best-known SACs released by *Saccharomyces cerevisiae* are mannoproteins. These components are potent emulsifiers, being readily released by the microorganisms [37, 38]. In a batch experiment, 0.2 mg of mannoproteins per gram of cell dry weight per hour were released [39]. A continuous process would result in lower concentrations of the surface active component and a default value of 0.4 mg L^{-1} was used, the evaluated range was between 0.1 to 4 mg L^{-1}. The amount of protein adsorbing at the oil/water interface is given by the surface excess concentration. For different oil/water/protein combinations, the surface excess concentration ranges between 1.5 and 3 mg m^{-2} [40, 41], the default value was 3 mg m^{-2} and the range of 1 to 3 mg m^{-2} was evaluated.

The parameter that comes forward in three of the four subprocesses is the droplet size, which is determined by a combination of process conditions and oil phase properties. This study considers two scenarios with different droplet sizes: $d_{\min}$ and $d_{\max}$.

The calculation of minimum and maximum stable droplet size was based on the turbulence in the reactor. Walstra et al. developed Equation (14) for the maximum droplet size

($d_{\max}$) stable to breakup, defined by the interfacial tension (σ_{oil}), the overall liquid density (ρ_l) and volumetric power input (e_v).

$$d_{max} = \left(\frac{\sigma_{oil}^{\ 3}}{\rho_l e_v^{\ 2}} \right)^{1/5} \tag{14}$$

This is the maximum size of the droplets that do not breakup anymore due to the shear forces caused by turbulence. This approach takes the effects of hydrodynamic interactions on droplet collisions into account, which are directly related to the mixing of the droplet (by the power input). This relation, based on the degree of turbulence in the system, was developed for dispersions under isentropic conditions, but also appeared to be valid for lower Reynolds numbers [42, 43].

An expression for the minimum droplet diameter ($d_{\min}$) was developed by Thomas [44], by relating the forces in a turbulent mixture to the force and contact time of two droplets. When the contact time exceeds the time required for film drainage, dependent on the critical film thickness, coalescence takes place. From this condition, Equation (15) was derived, relating $d_{\min}$ to the continuous phase viscosity (η_w), the critical film thickness for coalescence (h), interfacial tension (σ_{oil}), and volumetric power input (e_v):

$$d_{min} \sim \frac{\sigma_{oil}^{\ 2} h^2}{\eta_w e_v}. \tag{15}$$

Droplets below this minimum droplet size will have a high chance of coalescence and therefore exist for only a short time. By experimental work of Liu and Li, Equation (15) could be further developed to

$$d_{min} = \left(\frac{\sigma_{oil}^{\ 1.38} B^{0.46} \rho_l^{\ 0.05}}{0.072 \eta_w e_v^{\ 0.89}} \right)^{\frac{1}{3.11}}, \tag{16}$$

eliminating any empirical parameters specifically dependent on the system. It includes the continuous phase density and the van der Waals constant ($B = 10^{-28}$ Jm) as a measure for the intermolecular forces [21].

4. Results and discussion

The starting points for all characteristic time calculations were the minimum and maximum droplet diameters, which are determined by the power input provided by the gas bubbles. Figure 3 shows the minimum and maximum stable droplet diameters as a function of the superficial gas velocity, calculated using Equations (14) and (16). The largest stable droplets are in the order of millimetres, the minimum droplet diameter was about an order of magnitude lower and both decrease with increasing superficial gas velocity.

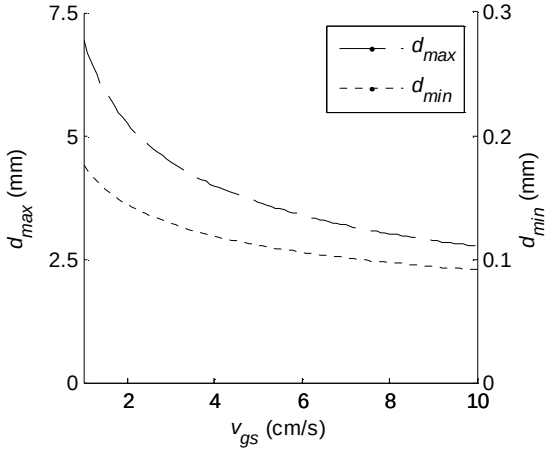

Figure 3. The minimum and maximum droplet diameters at varying superficial gas velocities (V_r = 1m^3, H / D = 4, c_{SAC} = 0.4 mg L^{-1}, ϕ_{oil} = 0.1).

4.1. Coalescence vs SAC adsorption

The first step in the recovery process is droplet growth by coalescence. Figure 4 compares the characteristic times for coalescence and stabilization by SAC adsorption for the minimum sized droplets, showing that coalescence is three orders of magnitude faster than stabilization of those droplets. This indicates that no emulsification problems are expected for the very small droplets. Since droplet coalescence is slower for larger droplets, coalescence of droplets smaller than $d_{\max}$ will be faster than for droplets of size $d_{\max}$, so when coalescence of the maximum sized droplets is not limiting, the smaller droplets can also coalesce. However, for the largest stable droplets the characteristic times of SAC adsorption and coalescence are in the same order of magnitude (Fig. 5). At a superficial gas velocity higher than 2 cm s^{-1}, coalescence is calculated to be faster than adsorption but since there is no order of magnitude

difference between the characteristic times, this only indicates that coalescence might be promoted over emulsification with increasing superficial gas velocity. Since the model shows that droplet stabilization of the smallest droplets is of no concern, from here on we will focus on coalescence of the large droplets.

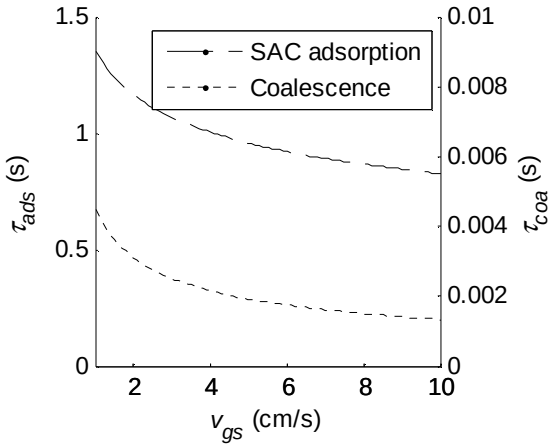

Figure 4. Characteristic times of SAC adsorption and coalescence for $d_{\min}$ as a function of superficial gas velocity (V_r = 1 m^3, H/D = 4, c_{SAC} = 0.4 mg/L, ϕ_{oil} = 0.1).

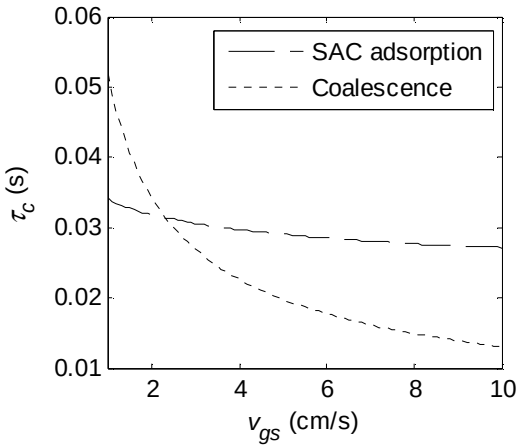

Figure 5. Characteristic times (τ_c) of SAC adsorption and coalescence for $d_{\max}$ as a function of superficial gas velocity (V_r = 1 m^3, H/D = 4, c_{SAC} = 0.4 mg/L, ϕ_{oil} = 0.1).

As Equations (3) and (5) show, SAC concentration, oil fraction, and surface excess concentration also influence the characteristic times. The former two are in turn influenced by the process conditions, while the latter is a physicochemical property of the emulsifier for the dispersion and hence, is scale independent When the process operates at high oil fraction, coalescence is promoted (Fig. 6). Increasing the oil fraction should preferably be achieved by improved microorganism productivity instead of by operating at higher cell concentrations, since increased cell concentrations will likely lead to higher concentrations of SACs, which in turn enhance droplet stabilization (Fig. 7).

The surface excess concentration of the emulsifier describes the minimum amount of emulsifier required to cover the droplet surface. The exact value is dependent on the type of emulsifier and composition of the aqueous and organic phase. The influence of the surface excess concentration on the stabilization characteristic time is limited. For the considered surface excess range, 1.5-3 mg m^{-2}, the order of magnitude of stabilization remains the same.

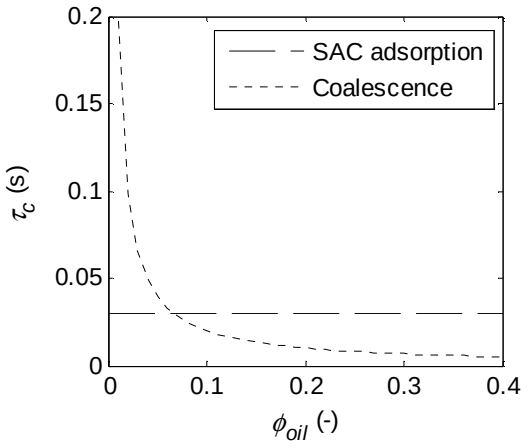

Figure 6. Characteristic times (τ_c) of SAC adsorption and coalescence for $d_{\max}$ as a function of volumetric oil fraction (V_r = 1 m^3, H/D = 4, v_{gs} = 5 cm s^{-1}, c_{SAC} = 0.4 mg L^{-1}).

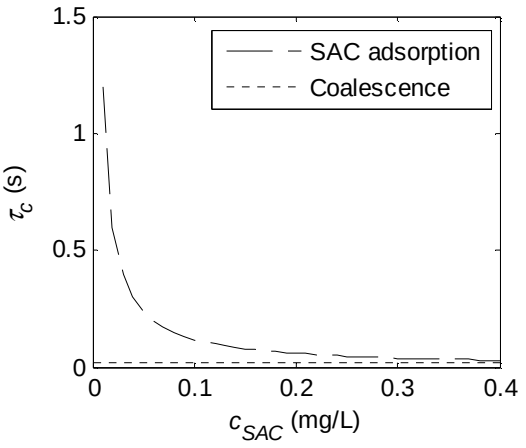

Figure 7. Characteristic times (τ_c) of SAC adsorption and coalescence for *dmax* as a function of SAC concentration (V_r = 1 m^3, H/D = 4, v_{gs} = 5 cm s^{-1}, ϕ_{oil} = 0.1).

In all previous comparisons of the characteristic times for coalescence and emulsification, none of the parameter variations results in one process being conclusively faster than the other. However, when the process is operated at the upper boundary of the oil fraction (0.4) and a low SAC concentration is achieved (0.1 mg L^{-1}), an order of magnitude difference between the characteristic times for coalescence and SAC adsorption can be reached, as shown by the ratio of characteristic times in Figure 8. In such conditions, droplet growth by coalescence readily occurs and the droplets might be recovered by gravity separation.

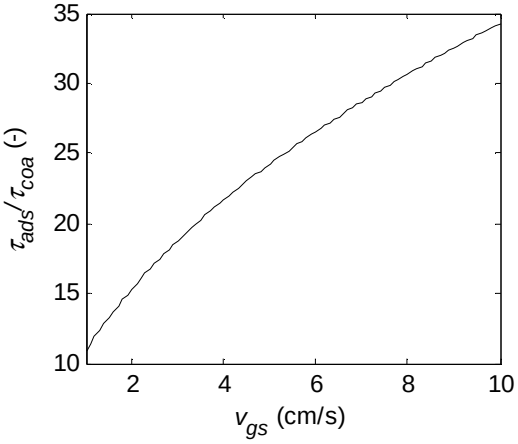

Figure 8. Coalescence is an order of magnitude faster than droplet stabilization (V_r = 1m^3, H / D = 4, c_{SAC} = 0.1 mg L^{-1}, ϕ_{oil} = 0.4).

4.2. Droplet creaming vs mixing

To facilitate droplet creaming, the characteristic time for creaming must be lower than that for mixing. The superficial gas velocity, determining the power input, influences both creaming and mixing (Fig. 9).

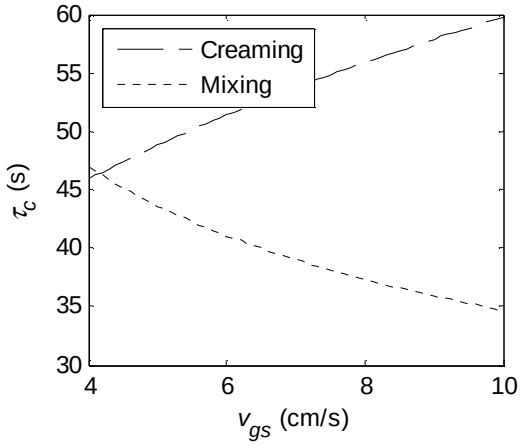

Figure 9. Characteristic times (τ_c) of creaming and mixing for $d_{\max}$ as function of superficial gas velocity in the heterogeneous regime (V_r = 1 m^3, H / D = 4, ϕ_{oil} = 0.1).

As mentioned before, two mixing regimes are distinguished: the homogeneous and heterogeneous regime. In the homogeneous flow regime, mixing is gentle, and the droplet creaming will occur (results not shown). However, the limited mixing in that case is likely to be insufficient for the fermentation process and is therefore we only consider superficial gas velocities in the heterogeneous regime (v_{gs} > 4 cm s^{-1}). When the superficial gas velocity is increased, and the heterogeneous regime is reached, τ_{mix} decreases below τ_{crm}. However, there is no order of magnitude difference between them, so none of the subprocesses is conclusively faster than the other.

Furthermore, τ_{mix} is strongly influenced by the reactor geometry of the bubble column (both aspect ratio and volume). Only at extreme aspect ratios, an effect on the mixing time can be expected (Fig. 10). The influence of the aspect ratio is limited in the lower range and only when it exceeds a value of 3, the τ_{mix} increases. This sudden change is explained by the regimes existing below and above an aspect ratio of 3, as shown in the section describing the mixing time. The mixing and creaming characteristic times are influenced similarly when the reactor

volume is increased. Both subprocesses slow down with increasing scale, but droplet creaming is slightly stronger affected than mixing (Fig. 11). This clearly suggests that integrated gravity separation will become more difficult at large scale.

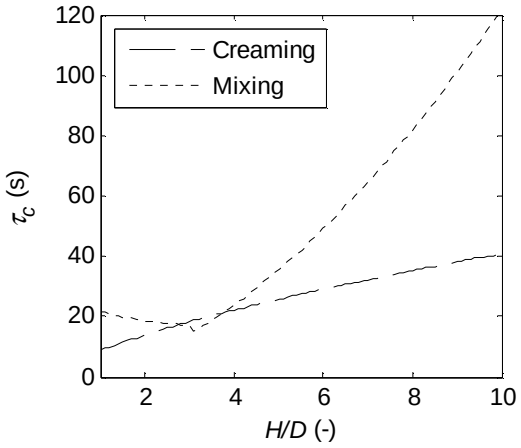

Figure 10. Characteristic times (τ_c) of creaming and mixing for d_{max} as function of aspect ratio (V_r = 1m³, v_{gs} = 5 cm s⁻¹).

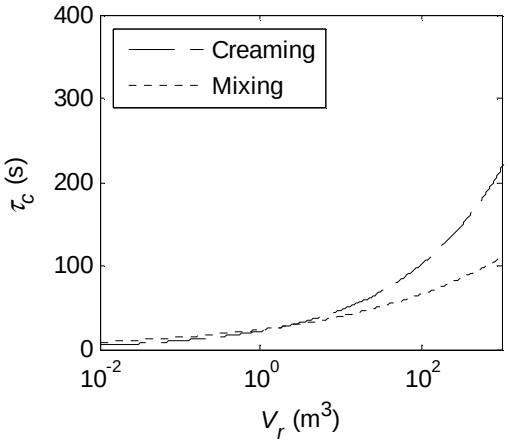

Figure 11. Characteristic times (τ_c) of creaming and mixing for d_{max} as function of reactor volume (H / D = 4, v_{gs} = 5 cm s⁻¹).

This also shows from the ratio of characteristic times at the optimal conditions (Fig. 12). When operating at the low end of the heterogeneous regime (5 cm s^{-1}) and at extreme aspect ratio (15), the τ_{crm} is close to an order of magnitude lower than the τ_{mix} at lab scale volumes (1 L). But when the reactor volume is increased, this difference is rapidly lost, showing that scale up will cause recovery difficulties. Furthermore, the mixing time at large scale reactors under these conditions is likely to be insufficient for facilitating the fermentation. For example, in lab scale stirred vessel and bubble column the mixing times will be similar [45]. When the reactor size is increased, mixing times will start to differ. In a 20 m^3 reactor, mixing times of approximately 50 s can be achieved for stirred vessels [46] and 150 s for high aspect ratio bubble columns (Equation (13)).

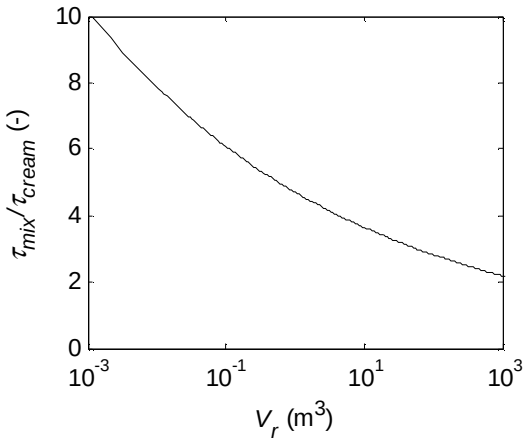

Figure 12. Ratio characteristic times of mixing and creaming for $d_{\max}$ (v_{gs} = 5 cm s^{-1}, H / D = 15).

5. Conclusions

Process integration can contribute to lowering the production costs of advanced biofuels. The most straightforward case of integration is combining production and gravity separation in a single bubble column. The possibility of this integration was studied by regime analysis. This tool is conventionally used to determine the rate limiting step in scale up, but here it was used to identify whether adverse subprocesses (such as mixing and droplet stabilization by SAC adsorption) would hinder the integration of advanced biofuel production and separation. Parameter variation was used to determine whether operating conditions and reactor geometry can be chosen in a way that the separation can take place, and those conditions were compared to conditions required for fermentation from laboratory to production scale.

The first step in the oil recovery, droplet growth by coalescence, is not directly scale dependent. The regime analysis showed the importance of limiting the SAC concentration and obtaining a high oil concentration for coalescence, which both can be related to the microorganism performance. From the perspective of the integrated process, improving the microbial productivity is preferred over increasing the overall productivity by operating at high cell concentrations, because the latter will likely result in increased SAC concentrations. Furthermore, taking the release of SACs by the microorganism into account during strain development could also contribute to enhanced droplet growth. When a high oil fraction is

reached, and the SAC concentration is limited, droplet growth by coalescence takes place and droplet stabilization by SACs will not be a problem. This is valid under the earlier made assumption that the secreted product is not initially stabilised. When this is the case, the coalescence subprocess should be described in a different way. In this chapter, the collision frequency is used to obtain an expression for the characteristic time of coalescence, but when the droplets are formed already stabilised, a characteristic time based on the rupture of the stabilising film would be required.

For the next step in the oil recovery, droplet creaming, gravity separation is the cheapest process option. The regime analysis compares the characteristic times for creaming with mixing. When mixing is too strong, the droplets will be back-mixed instead of separated. The analysis showed that it is possible to achieve conditions at lab scale in which droplet creaming is faster than mixing, with a comparable mixing time in the bubble column as in a lab scale stirred vessel. However, at increased production scale, the limited superficial gas velocities and extreme aspect ratios required to promote droplet creaming over mixing, cause that droplet creaming cannot be promoted while maintaining suitable fermentation conditions. So for large scale integration, the integration of production and separation might only be achieved in a reactor in which two sections with different process conditions (especially superficial gas velocity) are combined, one section for fermentation and one for separation.

Challenges in such a design are to control the hydrodynamics in the different sections and to couple them, while maintaining the microbial cell performance. The design of such an reactor and experimental testing of the scale-up effects are the next steps to be taken in developing low-cost process technology, which in the end is one of the aspects required for economically feasible production of advanced biofuels.

Acknowledgements

This work was partly carried out within the BE-Basic R&D Program, which was granted a FES subsidy from the Dutch Ministry of Economic affairs, agriculture and innovation (EL&I).

Nomenclature

Roman

B	Van Der Waals parameter
C_D	Drag coefficient
D	Diameter
H	Height
Re	Reynolds number
V	Volume
c	Concentration
e	Power input
d	Particle diameter
g	Gravitational constant
h	Critical film thickness
n	Richardson-Zaki parameter
v	Velocity

Greek

Γ	Surface excess concentration
η	Viscosity
ρ	Density
σ	Interfacial tension
τ	Characteristic time
ϕ	Volume fraction

Subscripts

v	Volume specific

b	Bubble
d	Droplet
l	Liquid
r	Reactor
aq	Aqueous
oil	Oil
ads	Adsorption
coa	Coalescence
crm	Creaming
mix	Mixing
max	Maximum
min	Minumum
SAC	Surface active component

References

1. Rude, M.A. and Schirmer, A., *New microbial fuels: a biotech perspective.* Curr. Opin. Microbiol., 2009. **12**(3): p. 274-281.

2. Schirmer, A., Rude, M.A., Li, X., Popova, E., et al., *Microbial biosynthesis of alkanes* Science, 2010. **329**: p. 559-562.

3. Renniger, N.S. and McPhee, D.J.*Fuel compositions comprising farnesane and farnesane derivatives and method of making and using same.* Amyris Biotechnologies, Inc. 2008. US 7399323 B2

4. Westfall, P.J. and Gardner, T.S., *Industrial fermentation of renewable diesel fuels.* Curr. Opin. Biotech., 2011. **22**(3): p. 344-350.

5. Bullis, K. *Why Amyris is focusing on moisturizers, not fuel, for now.* MIT Technology Review, 2012.

6. Cuellar, M.C., Heijnen, J.J., and van der Wielen, L.A.M., *Large-scale production of diesel-like biofuels - process design as an inherent part of microorganism development.* Biotechnol. J., 2013. **8**(6): p. 682-689.

7. Dunlop, M.J., Dossani, Z.Y., Szmidt, H.L., Chu, H.C., et al., *Engineering microbial biofuel tolerance and export using efflux pumps.* Mol. Syst. Biol., 2011. **7**.

8. Heeres, A.S., Picone, C.S.F., van der Wielen, L.A.M., Cunha, R.L., et al., *Microbial advanced biofuels production: overcoming emulsification challenges for large-scale operation*. Trends Biotechnol. , 2014. **32**(4): p. 221-229.

9. Tabur, P. and Dorin, G.*Method for purifying bio-organic compounds from fermentation broth containing surfactants by temperature-induced phase inversion.* 2012. WO2012024186

10. Keasling, J.D., Hu, Z., Somerville, C., Church, G., et al.*Production of fatty acids and derivatives thereof.* Ls9 Inc. 2011. WO2007136762A3

11. Sweere, A.P.J., Luyben, K.C.A.M., and Kossen, N.W.F., *Regime analysis and scale-down: Tools to investigate the performance of bioreactors.* Enzyme Microb. Tech., 1987. **9**(7): p. 386-398.

12. Johnstone, R.E. and Thring, M.W., *Pilot plants, models, and scale-up methods in chemical engineering*. 1957: McGraw-Hill.

13. Oosterhuis, N.M.G., *Scale-up of bioreactors: A scale-down approach*, in *Biotechnology*. 1984, Technical University Delft: Delft.

14. Huber, T., Kossen, N., Bos, P., and Kuenen, J., *Design and scale up of a reactor for microbial desulphurization of coal: A regime analysis.* Innov. Biotechnol. , 1984. **20**: p. 179-189.

15. Schoutens, G.H., *Modelling and design of animmobilized cell process for solvent production*, in *Applied Sciences*. 1986, Technical University Delft: Delft.

16. Law, H.E.M., Baldwin, C.V.F., Chen, B.H., and Woodley, J.M., *Process limitations in a whole-cell catalysed oxidation: Sensitivity analysis.* Chem. Eng. Sci., 2006. **61**(20): p. 6646-6652.

17. Melgarejo-Torres, R., Torres-Martínez, D., Gutiérrez-Rojas, M., Gómez de Jesús, A., et al., *Regime analysis of a Baeyer–Villiger bioconversion in a three-phase (air–water–ionic liquid) stirred tank bioreactor*. Biochem. Eng. J., 2011. **58**: p. 87-95.

18. Titchener-Hooker, N.J., Dunnill, P., and Hoare, M., *Micro biochemical engineering to accelerate the design of industrial-scale downstream processes for biopharmaceutical proteins.* Biotechnol. Bioeng., 2008. **100**(3): p. 473-487.

19. Garcia-Ochoa, F. and Gomez, E., *Bioreactor scale-up and oxygen transfer rate in microbial processes: An overview.* Biotech. Adv., 2009. **27**(2): p. 153-176.

20. Frising, T., Noïk, C., and Dalmazzone, C., *The liquid/liquid sedimentation process: from droplet coalescence to technologically enhanced water/oil emulsion gravity separators: a review.* J. Dispers. Sci. Technol. , 2006. **27**: p. 1035-1057.

21. Liu, S. and Li, D., *Drop coalescence in turbulent dispersions.* Chem. Eng. Sci., 1999. **54**: p. 5667-5675.

22. Walstra, P., *Principles of emulsion formation.* Chem. Eng. Sci., 1993. **48**(2): p. 333-349.

23. Sánchez Pérez, J.A., Rodríguez Porcel, E.M., Casas López, J.L., Fernández Sevilla, J.M., et al., *Shear rate in stirred tank and bubble column bioreactors.* Chem. Eng. J., 2006. **124**(1–3): p. 1-5.

24. Deshiikan, S.R. and Papadopoulos, K.D., *London-van der Waals and EDL effects in the coalescence of oil drops: II. ionic strength and pH effects.* J. Colloid Interface Sci., 1995. **174**(2): p. 313-318.

25. Tobin, T. and Ramkrishna, D., *Coalescence of charged droplets in agitated liquid-liquid dispersions.* AIChE J., 1992. **38**(8): p. 1199-1205.

26. Reynolds, T.D. and Richards, P.A., *Sedimentation*, in *Unit operations and processes in environmental engineering*. 1996, CL Engineering. p. 219-283.

27. Walstra, P., *Emulson Stability*, in *Encyclopedia of Emulsion Technology. Vol. 4*, P. Dekker, Editor. 1996, Marcel Dekker, Inc.: New York.

28. Janssen, L.P.B.M. and Warmoeskerken, M.M.C.G., *Transport phenomena data companion*. 2001, Delft: VSSD.

29. Groen, D.J., *Macromixing in bioreactors*. 1994, Delft University of Technology: Delft.

30. Ladygina, N., Dedyukhina, E.G., and Vainshtein, M.B., *A review on microbial synthesis of hydrocarbons.* Process Biochem., 2006. **41**(5): p. 1001-1014.

31. Weusthuis, R.A., Lamot, I., van der Oost, J., and Sanders, J.P.M., *Microbial production of bulk chemicals: development of anaerobic processes.* Trends Biotechnol., 2011. **29**(4): p. 153-158.

32. Almeida, J.R.M., Modig, T., Petersson, A., Hähn-Hägerdal, B., et al., *Increased tolerance and conversion of inhibitors in lignocellulosic hydrolysates by Saccharomyces cerevisiae.* J. Chem. Technol. Biotechnol., 2007. **82**(4): p. 340-349.

33. Heijnen, J.J. and Van't Riet, K., *Mass transfer, mixing and heat transfer phenomena in low viscosity bubble column reactors.* Chem. Eng. J., 1984. **28**(2): p. B21-B42.

34. Bacha, J., Freel, J., and Gibbs, A., *Diesel Fuels Technical Review*. 2007, Chevron Products Company.

35. Cabral, J.M.S., Mota, M., and Tramper, J., *Multiphase Bioreactor Design*. 2001: CRC press.

36. Reuß, M., Josić, D., Popović, M., and Bronn, W.K., *Viscosity of yeast suspensions.* Eur. J. Appl. Microbiol. Biotechnol., 1979. **8**(3): p. 167-175.

37. Cameron, D.R., Cooper, D.G., and Neufeld, R.J., *The mannoprotein of Saccharomyces cerevisiae is an effective bioemulsifier.* Appl. Environ. Microbiol., 1988. **54**: p. 1420-1425.

38. Cameron, D.R., *Identification and characterisation of mannoprotein emulsifier from Bakers yeast*, in *Department of Biotechnology*. 1992, McGill University: Montreal, Quebec, Canada.

39. Dupin, I.V.S., McKinnon, B.M., Ryan, C., Boulay, M., et al., *Saccharomyces cerevisiae mannoproteins that protect wine from protein haze: their release during fermentation and lees contact and a proposal for their mechanism of action.* J. Agric. Food Chem. , 2000. **48**(8): p. 3098-3105.

40. Bos, M.A. and van Vliet, T., *Interfacial rheological properties of adsorbed protein layers and surfactants: a review.* Adv. Colloid Interface Sci., 2001. **91**(3): p. 437-471.

41. Tcholakova, S., Denkov, N.D., Ivanov, I.B., and Campbell, B., *Coalescence in β-Lactoglobulin-Stabilized Emulsions: Effects of Protein Adsorption and Drop Size*. Langmuir, 2002. **18**(23): p. 8960-8971.

42. Levich, V.G., *Physicochemical Hydrodynamics*. 1962. ISBN: 978-0136744405, Englewood Cliffs: Prentice-Hall. 395-471.

43. Walstra, P. and Smulders, P.E.A., *Emulsion formation*, in *Modern aspects of emulsion science*, B.P. Binks, Editor. 1998, The Royal Socielety of Chemistry: Cambridge. p. 58-74.

44. Thomas, R.M., *Bubble coalescence in turbulent flows.* Int. J. Multiph. Flow, 1981. **7**: p. 719-717.

45. Amanullah, A., Buckland, B.C., and Nienow, A.W., *Mixing in the fermentation and cell culture industries*, in *Handbook of industrial mixing: science and practice*, E.L. Paul, V. Atiemo-Obeng, and S.M. Kresta, Editors. 2004, John Wiley & Sons: New Jersey. p. 1071-1110.

46. Hewitt, C.J. and Nienow, A.W., *The scale-up of microbial batch and fed-batch fermentation processes.* Adv. Appl. Microbiol., 2007. **62**: p. 105-35.

Chapter 3. Techno-economic assessment of the use of solvents in the scale-up of microbial sesquiterpene production for fuels and fine chemicals

Abstract

Sesquiterpenes are a group of versatile, 15-carbon molecules with applications ranging from fuels to fine chemicals and pharmaceuticals. When produced by microbial fermentation at laboratory scale, solvents are often employed for reducing product evaporation and enhancing recovery. However, it is not clear whether such approach constitutes a favorable techno-economic alternative at production scale. In this study empirical correlations, mass transfer and process flow sheeting models were used to perform a techno-economic assessment of solvent-based processes at scales typical of flavor and fragrances (25 MT y^{-1}) and fuel market (25000 MT y^{-1}). Different solvent-based process options were compared to the current state of the art which employs surfactants for product recovery. Although the use of solvents did reduce sesquiterpene evaporation rate during fermentation and improved product recovery, it resulted in higher or similar cost than the base case due to the additional equipment cost for solvent-product separation. However, when selecting solvents compatible with the final product formulation (e.g. in a kerosene enrichment process), unit costs as low as 0.7 \$ kg^{-1} can be achieved while decreasing environmental impact.

This chapter has been published as:

Pedraza-de la Cuesta Cuesta, S., Knopper, L. , van der Wielen, L. A. and Cuellar, M. C. (2019), Techno-economic assessment of the use of solvents in the scale-up of microbial sesquiterpene production for fuels and fine chemicals. Biofuels, Bioprod. Bioref., 2019. 13: 140-152.

1. Introduction

Sesquiterpenes are 15-carbon isoprenoids with applications in different markets like flavors, fragrances, cosmetics, pharmaceuticals, foams, lubricants, and biofuels [1, 2]. Normally sesquiterpenes are extracted from plants, in which they naturally occur. However, this method is costly, presents low yields and raw materials are usually scarce, resulting in high product prices ranging from ~100 to ~1000 EUR kg^{-1} [3]. The use of genetically modified microorganisms to produce sesquiterpenes via fermentation is a promising alternative to overcome these problems. Recently developed strains can secrete sesquiterpenes to the extracellular medium reaching titers in the order of grams per liter [4, 5]. Sesquiterpene forms a separate oil phase with lower density than water, which is very attractive from the point of view of product recovery. Several companies like Amyris, Firmenich, Isobionics, Allylix and Evolva are currently developing processes at commercial scale. For example, Amyris already produces farnesene (a precursor for farnesane, commercialized under the name of Biofene®). Moreover, they have successfully developed a microorganism for the production of amorpha-1,4-diene, a precursor for the malaria medicine artemisinin, while Sanofi Aventis is currently working in the process scale up and commercialization.

In spite of these industrial developments, literature on process technology and quantitative data is limited to a few patents [6-10]. Scientific publications are mainly focused on metabolic improvements and fermentation yields [4, 5, 11-16]. Those laboratory scale studies briefly describe the processing of sesquiterpenes for analytic purposes (Figure 1A), and typically employ solvents during fermentation and sample handling [8, 13]. However, the reason for applying this method, the impact of the solvent in the process, or its applicability at industrial scale is not explicitly stated. In the following section the mechanisms in which solvents play a role in the laboratory scale protocols and their potential application at large scale are discussed.

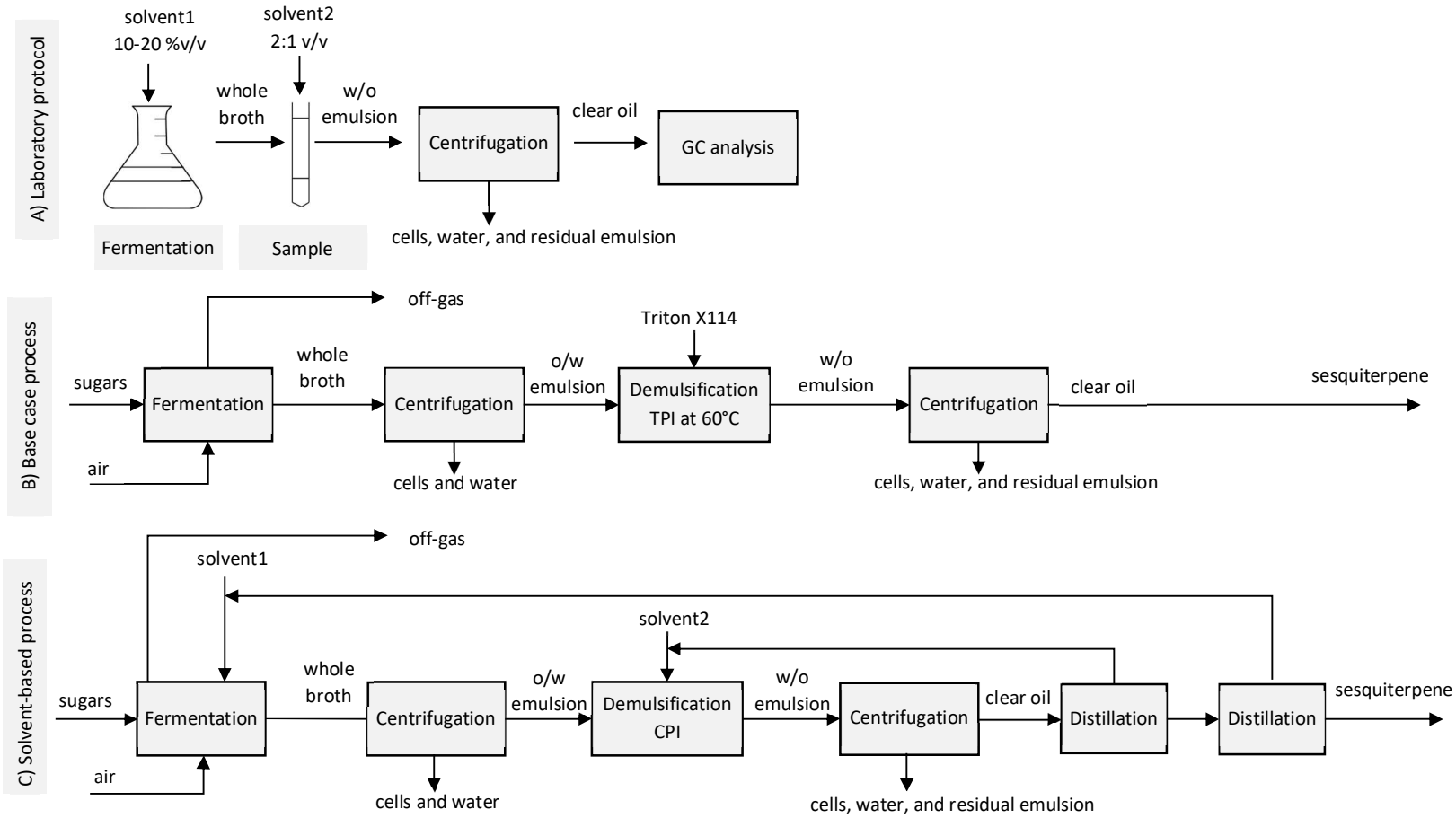

Figure 1: Process options for the production of sesquiterpenes. A) Lab scale protocol [8]; B) Base case [9]; C) Solvent-based process evaluated in this work.

Table 1: Predicted physical properties sesquiterpenes and solvents typically used in sesquiterpene production. Unless indicated otherwise, source: ChemSpider database (Data generated using the US Environmental Protection Agency's EPISuite™) at 25°C.

	Example	ρ (g mL^{-1})	T_b (°C)	p^{vap} (Pa)	k_H (atm m^3 mol^{-1})	$LogP_{ow}$ -	C^w (mg L^{-1})	σ_{oa} (mN m^{-1})	σ_{ow} (mN m^{-1})
Santalene		0.89[h]	238	7.6	0.39	6.4	0.039	36[a]	-
Caryophyllene		0.89[h]	257	4.2	0.69	6.3	0.050	31[f]	51[g]
Farnesene		0.86[h]	261	3.3	0.10	7.1	0.011	26[a]	-
Amorphadiene		0.90[a]	258	4.0	0.69	6.3	0.054	26[a]	-
Dodecane	[13]	0.75[h]	206	18	9.35	6.1	0.110	25[f]	50[g]
Decane	[8]	0.74[h]	165	191	5.30	5.0	1.252	24[b]	52[b]
Ethyl acetate	[8]	0.90[h]	78	1243	2.3 10^{-4}	0.7	2.99 10^4	24[c]	7[c]
MTBE	[46]	0.74[h]	47	33331	2.0 10^{-3}	0.9	1.98 10^4	19[d]	11[e]
Triton x-114	[9]	1.06[i]	-	-	-	-	Soluble	31[i]	-

a ACD/Labs Percepta Platform - PhysChem Module; b Dataphysics [47] @20 °C and Demond and Lindner [38] (Temperature not reported); c CAMEOdatabase [48]@20 °C; d Montaño *et al.*[49] @20 °C; e Hickel *et al.* [50] (Temperature not reported); f Experimentally determined in this work at room temperature; g estimated from experimental results using [37]; h Chem Src Safety Data sheets; i Dow Safety Data Sheets

1.1. Roles of solvent in the production of sesquiterpenes

1.1.1. Lowering evaporation rate of sesquiterpene

Sesquiterpenes are relatively volatile molecules (Table **1**), and thus, part of the product can be transferred to the gas phase during the fermentation. Evaporation rates in the order of mg h^{-1} have been reported to occur at laboratory scale fermentations reaching product titers in the order of mg per L [16]. In addition, 3% of product loss has been reported in a 2L scale bioreactor reaching product titers in the order of g per L [6]. A typical solution is adding an overlay of 10%–20% v/v of a relatively low volatile organic solvent (e.g. decane or dodecane) to the fermentation medium (Figure 1A), capturing the hydrophobic sesquiterpene molecules in the organic phase [8, 11, 13, 16, 17]. Although this is a common practice at laboratory scale, the actual impact of the solvent on the product evaporation rate is unknown, and studies on sesquiterpene evaporation, and VLE physical properties of sesquiterpenes are scarce; see for example Schuhfried *et al.* [18].

Solvent selection criteria for sesquiterpene fermentations are, among others, low volatility, low tendency to form emulsions, and a partition coefficient octanol/water higher than 10^5 (log P_{ow}>5) which, in principle, excludes toxicity problems in microorganisms like *S. cerevisiae* [19]. When using solvents at production scale, additional solvent selection criteria like high relative volatility should be considered for a cost-effective solvent-product separation. Alternatively, this separation step could be bypassed by choosing solvents compatible with the final product formulation. Examples include the use of methyl oleate or isopropyl myristate in the production of amorphadiene [5], canola oil in the production of the sesquiterpene alcohol bisabolol [20], and farnesene as solvent in the production of the monoterpene limonene [21].

1.1.2. Enhancing oxygen transfer during fermentation

In aerobic fermentations oxygen is generally supplied by sparging air bubbles into the bioreactor. The oxygen is transferred from the bubbles into the aqueous phase, and once there, it is available to be consumed by the microorganisms. The oxygen transfer rate (OTR) depends on the overall mass transfer coefficient ($k_L a$), and the difference in oxygen concentration between the gas/liquid interface and the bulk liquid phase (ΔC_{O_2}):

$$OTR = k_L a \cdot \Delta C_{O_2} \cdot V \quad (1)$$

The $k_L a$ is dependent on physical properties of the system, bioreactor geometry, and hydrodynamic conditions [22]. OTR is typically one of the limiting factors in scale-up of aerobic fermentations [22]. Due to the low solubility of oxygen in water, oxygen limitation may occur affecting the fermentation performance. Oxygen limitation can be avoided by increasing the power input of the system, but this is highly energy demanding (e.g. due to aeration and agitation), especially at large scale. Since oxygen presents 10-times higher solubility in hydrocarbons than in water [23], a possible alternative is using solvents as oxygen vector to enhance OTR. This concept has been claimed in a patent application by Isobionics for the production of the sesquiterpene valencene [24]; However, the net effect of the solvent on the OTR is controversial since it depends among other factors on the oil fraction used [23].

1.1.3. Product recovery: enhancing coalescence and creaming of the oil phase

Sesquiterpenes are hydrophobic liquids, with lower density than water (Table 1). During the fermentation, microorganisms synthesize and secrete sesquiterpene to the extracellular medium, where it forms a separated phase (addressed in this work as oil phase) dispersed as droplets due to the mixing in the reactor. Dispersed oil droplets can and coalesce into larger ones. These large droplets can rise due to their lower density than the aqueous medium. This mechanism is called creaming, and its velocity (v_d) depends on the size (d_{oil}) and the density of the oil droplets (ρ_{oil}):

$$v_d = \sqrt{4 \cdot g \cdot (\rho_l - \rho_{oil}) \cdot d_{oil} / (3 \cdot C_D \cdot \rho_{aq})} \qquad (2)$$

Coalescence and creaming contribute to product phase separation and therefore are desirable mechanisms for reducing product recovery costs. When fermentations are performed in the presence of solvent, there is a larger total oil fraction in the bioreactor. For example, a 15% v/v oil phase was described in an amorphadiene fermentation, of which 10% v/v accounted for solvent [5]. Higher oil fractions increase the droplet collision leading to larger averaged droplet size [25, 26]. Moreover, depending on the density of the selected solvent (Table 1) the overall density of the oil phase can be reduced, contributing to its creaming. Therefore, implementing solvents for reducing product evaporation, could also contribute to improve product recovery.

1.1.4. Demulsification of the oil phase by phase inversion

Several components of the fermentation broth (e.g., salts, glycolipids, proteins, cells and cells debris) can hinder coalescence by lowering the oil/water (o/w) interfacial tension and/or stabilizing the o/w interface [27]. As a result, the product is not a homogeneous continuous phase, but a stable emulsion. Although the formation of sesquiterpene emulsions are usually not mentioned in laboratory scale studies [20, 28], this problem has been reported at larger scales [9]. Reported recovery methods consist on inducing phase inversion, obtaining an emulsion of water in a continuous oil phase (w/o) which is separated afterwards by centrifugation. Phase inversion can be (i) transitional (TPI), (ii) catastrophic (CPI) or (iii) induced by partial crystallization of the solvent.

TPI consists in adding a nonionic-surfactant and increasing the emulsion temperature until the surfactant becomes more soluble in the oil phase [29]. Tabur and Dorin [9] report the use of Triton-X114 and temperatures of 60 °C for TPI of sesquiterpene emulsions at large scale (300 L fermentation). CPI is induced by adding oil phase until a critical concentration is reached [29-31]. Applicability of CPI as a recovery step in a production process involving microbial emulsions has been reported by Glonke *et al*. [32]. There is no experimental data on critical o/w ratios for inversion of sesquiterpene emulsions, however laboratory scale protocols report the addition of 2 volumes of solvent per volume of broth [8,13] (Figure 1A). Finally, phase inversion by partial crystallization of the solvent can be induced by first lowering the temperature in order to form a crystal network of solvent across the droplets walls, and then heating the emulsion above the solvent melting temperature. To our knowledge, there is no data regarding the applicability of this method to sesquiterpene emulsions.

Using CPI instead of TPI has the advantage of avoiding the use of costly surfactants and changes of temperature. The main disadvantage of CPI is that it requires an extra step for solvent-product separation; However, TPI might also require additional purification steps like distillation [10] for meeting the purity specifications of some applications (e.g. 92%-94% w/w purity for cosmetics [2]). Furthermore, solvent-product separation costs can be reduced by selecting solvents with high vapor pressure; for example, methyl-tert-butylether (MTBE), ethyl-acetate or heptane are typically used at laboratory scale [8, 13]. On the other hand, these solvents can be toxic for cells due to their higher solubility in water, compromising the possibility of cell recycling. Hence, interesting alternatives for reducing solvent-product separation steps include using the same solvent as in the bioreactor for reducing evaporation,

using a solvent compatible with the final product formulation (e.g., diesel for sesquiterpene-based biofuels), or increasing the oil fraction by recycling sesquiterpene.

1.2. Aim of this work

This work studies the effect of solvent in the evaporation rate, droplet size and oil phase recovery in sesquiterpene fermentations by using empirical correlations and transfer models based on predicted VLE properties. In addition, it evaluates the techno-economic impact of using solvents in a microbial sesquiterpene production process by means of flow sheeting at two scales, namely 25 MT y^{-1} (flavors and fragrances market) and 25000 MT y^{-1} (aviation fuel market).

2. Materials and methods

2.1. Experiments

2.1.1. Preparation of o/w dispersions

Oil in water dispersions were prepared in a 2-L jacketed vessel (Applikon, The Netherlands) containing 1.275 L of demineralized water, and 0% to 10% v/v of sesquiterpene and dodecane (Sigma Aldrich, >99% purity). Experiments were performed using the sesquiterpene caryophyllene (kindly provided by Firmenich, >95% purity), since it presented higher stability than commercially available synthetic farnesene, and their physical properties are expected to be similar (Table 1). The vessel was aerated using pressurized air at a flow rate of 1.5 nL min^{-1}, controlled by a mass flow controller (Brooks Instrument, Hatfield, United States); the temperature was maintained at 35°C; and the stirring speed of a 6-blade Rushton impeller of 45 mm diameter was kept at 1000 rpm. Aeration, temperature and stirring speed were chosen in order to mimic typical fermentation conditions. To eliminate effects of any residual surfactants the vessel was cleaned with a regular dish soap, rinsed two times with demi-water, cleaned two times with 70% ethanol and rinsed again with demi-water.

2.1.2. Droplet size analysis

Droplet images were recorded in situ by a SOPAT probe (SOPAT Gmbh), and analysed using the image analysis software provided by SOPAT Gmbh [33] as described by Heeres *et al.* [34]. A set of 100 pictures was taken 30 minutes after every oil addition, ensuring a stable droplet size and more than 1000 droplets per data point.

2.1.3. Surface tension

Surface tension of water (σ_{wa}), caryophyllene (σ_{oa}), and dodecane (σ_{oa}) (Table 1) were measured using a Krüss ring tensiometer (model 01260).

2.2. Modeling

2.2.1. Droplet size and required separation area

In this work, the model proposed by Alopaeus *et al.* [35] which applies for turbulent conditions, was chosen to estimate the droplet size (d_{oil}) in the bioreactor, using the volume fraction of the dispersed phase (ϕ_{oil}), the power input per unit mass (e_G), the o/w interfacial tension (σ_{ow}), the viscosity of the continuous phase (η_w), the densities of the dispersed (ρ_{oil}) and continuous phase (ρ_l), and a set of universal constants, which are independent of the operating conditions and design parameters (C_1=4.87 10^{-3}; C_2=5.52 10^{-2}; C_3= 2.17 10^{-4}; C_4=2.28 10^{13} m^2) [36]:

$$\ln\left(10.8038\cdot\phi\frac{C_3}{C_1}\right)=C_4\frac{\eta_w\cdot\rho_l\cdot e_G}{{\sigma_{ow}}^2\left(1+\phi\right)^3}\left(\frac{d_{oil}}{2}\right)^4-C_2\frac{\sigma_{ow}\left(1+\phi\right)^2}{\rho_{oil}\cdot {e_G}^{2/3}\cdot {d_{oil}}^{5/3}} \quad (3)$$

The required separation area for recovering the dispersed oil droplets of size (d_{oil}) and density (ρ_{oil}) in a disk-stack centrifuge was estimated based on the sigma factor (Σ). This factor is the equivalent cross-sectional area of a gravity settler and depends on the efficiency of the centrifuge (ξ), the viscosity of the aqueous phase (η_w), and the maximum capacity throughput (Q):

$$\Sigma=\frac{Q}{\xi}\frac{18\cdot\eta_w}{{d_{oil}}^2\cdot\left(\rho_l-\rho_{oil}\right)\cdot g} \quad (4)$$

2.2.2. Evaporation rate: L-V and L-L-V transfer models

The evaporation rate of sesquiterpene (R_{evap}) can be estimated from its molar fraction in the gas phase (y), and the total flow of gas leaving the bioreactor (F_G):

$$R_{evap}=y\cdot F_G \quad (5)$$

In this work, the maximum evaporation rate of sesquiterpenes at different aeration rates, fermentor volumes, and solvent volumetric fractions was evaluated by phase equilibrium models based on predicted physical properties (Table 1), and experimental data from Schuhfried *et al.* [18]. Two possible transfer routes were considered:

- Transfer from oil droplets to gas bubbles via aqueous phase (L-L-V): This model determines the molar fraction of the sesquiterpene in the gas phase (y) in equilibrium with the aqueous phase as a function of the Henry's constant (k_H), the total pressure (P_{tot}), and the concentration of sesquiterpene in the aqueous phase (C^w).

$$y = \frac{k_H}{P_{tot}} C^w \tag{6}$$

Assuming equilibrium conditions between the oil and the aqueous phase, the concentration of sesquiterpene in the aqueous phase was estimated as the ratio between the concentration of sesquiterpene in the oil (C^{oil}), and the predicted values of the sesquiterpene distribution coefficient between 1-octanol and water (P_{ow}):

$$C^w = \frac{C^{org}}{P_{ow}} \tag{7}$$

- Direct transfer from oil to gas phase (L-V): This model assumes that oil droplets collide with gas bubbles allowing direct transfer of sesquiterpene from oil to the gas phase. Assuming ideal behaviour, the gas phase composition (y) in equilibrium with an oil phase of composition (x) can be estimated by the Raoult's Law:

$$y = x \cdot (p^{vap} / P_{tot}) \tag{8}$$

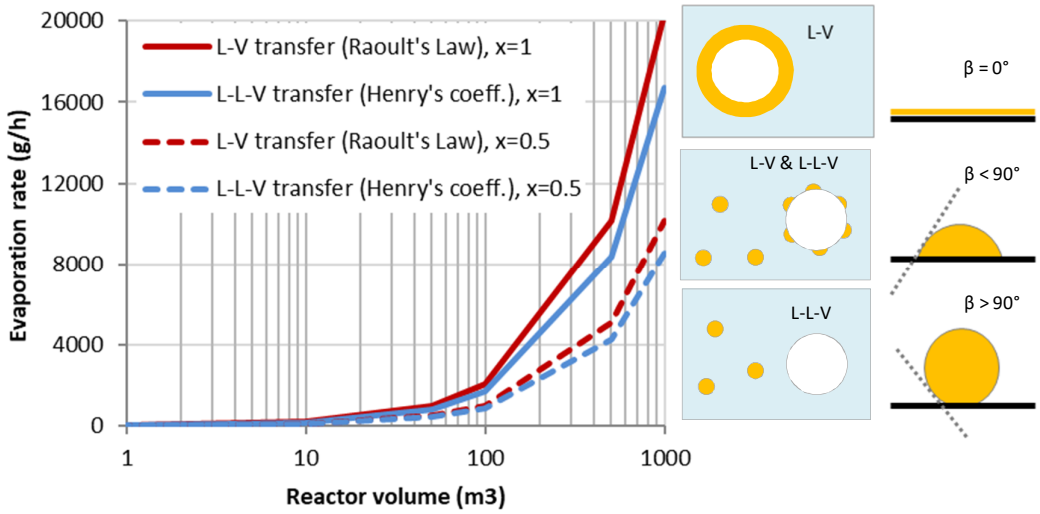

Figure 2: Maximum estimated evaporation rate at 1vvm gas flow and 35°C, as function of the fermentor working volume for two different routes: L-V modelled by Raoult's law, and L-L-V modelled by Henry's law. x=1 is the composition of an oil phase purely composed of sesquiterpene and x=0.5 represents a situation where 10%v/v of sesquiterpene is produced in a bioreactor containing 10% v/v of solvent. Distribution of oil phase on gas-water interface depends on the contact angle β: (i) When β=0° oil phase is fully spread onto gas surface (ii) β<90° oil beads with large contact area oil-gas are formed, and (iii) if β>90° oil beads with low oil-gas contact area are formed.

Using the properties of farnesene as reference, the maximum evaporation rate of sesquiterpene in a bioreactor working at 35°C, 1 atm and aerated at 1 vvm were estimated for both routes at different working scales (Figure 2). A preliminary analysis considering interfacial tensions was performed to elucidate which route is more probable. The prevalence of one the other depends on the interfacial properties of the three phases. Upon droplet-bubble collision, oil can remain on the bubble surface as beads, or it can spread forming a layer (Figure 2). The first situation would favour L-L-V transfer of sesquiterpene via aqueous phase, whereas the formation of an oil layer on the bubble would promote direct L-V transfer of sesquiterpene. The values of interfacial tension (σ_{ow}) for caryophyllene and dodecane (Table 1) were estimated following the method developed by Girifalco and Good [37] Eq. (9) using Φ=0.5595 as indicated by Demond and Lindner [38] for aliphatic hydrocarbons.

$$\sigma_{ow} = \sigma_{oa} + \sigma_{wa} - 2 \cdot \Phi \cdot (\sigma_{oa} \cdot \sigma_{wa})^{1/2} \quad (9)$$

The spreading coefficient (*S*), indicating the wetting of a gas bubble by the oil phase in presence of water, and the contact angle (β) between the three phases were calculated from the interfacial tension values as described by Rowlinson and Widom [39]:

$$S = \sigma_{wa} - (\sigma_{oa} + \sigma_{ow}) \tag{10}$$

$$\cos(\beta) = \left((\sigma_{wa})^2 - (\sigma_{ow})^2 - (\sigma_{oa})^2\right) / (2 \cdot \sigma_{ow} \cdot \sigma_{oa}) \tag{11}$$

2.2.3. Process simulation: Basic assumptions

The techno-economic performance of a reference case (Figure 1B) based on Tabur and Dorin [9] has been compared to a solvent-based process (Figure 1C) by using the flowsheet simulation software SuperPro Designer™ (v 9.5 build 3). Farnesene has been selected as reference sesquiterpene due to its wide range of applications at different production scales (e.g., flavors, fragrances and fuels), and due to the availability of some experimental data for product recovery. Several cases have been considered for the solvent-based process in order to account for the different roles that solvents can play (Table 2). In addition, a scenario in which produced sesquiterpene is used to enrich kerosene has been considered to represent an alternative in which solvents are compatible with the final product formulation. All cases included fermentation, primary recovery by centrifugation, demulsification and, when indicated, product/solvent separation. The basic assumptions per step are described below.

- **Fermentation: Stoichiometric model based on metabolic pathway**

In this work, 100 g L^{-1} of sesquiterpene are produced in a continuous bioreactor by a recombinant strain of *S. cerevisiae* via glycolysis and mevalonate pathways according to the following process reaction:

$$-5.3C_6H_{12}O_6 - 6.0O_2 - 0.9NH_4OH + 1.0C_{15}H_{24} + 4.4CH_{1.8}O_{0.5}N_{0.2} + 12.2CO_2 + 17.8H_2O \tag{12}$$

The previous equation assumes a production of 12 mol ATP per mol of sesquiterpene (based on metabolic pathway), a yield of 16.5 g cells per mol of generated ATP [40], a maintenance coefficient of 0.05 mol ATP C-mol$X^{-1}\cdot h^{-1}$ [41], and a specific growth rate of 0.04 h^{-1}.

The evaporation rate of sesquiterpene in the bioreactor was estimated by the L-V model presented in Eq.(5), considering fermenters without off-gas condenser. In order to evaluate the

use of solvent for reducing product evaporation, case 1 using 10% v/v of dodecane in the fermentation, is compared to case 2 and case 2B. Case 2 implements an off-gas condenser at 15 °C to recover the evaporated sesquiterpene, followed by a settler to separate the sesquiterpene from condensation water. Case 2B does not incorporate product recovery from the off-gas.

No effects in fermentation performance have been reported in sesquiterpene literature for oil fractions of 0.1 v/v to 0.2 v/v. At these oil fractions it is expected that it only affects the stirring and aeration requirements for maintaining enough dissolved oxygen in the fermentation broth. In consequence, the current work does not consider any impact of the solvent in the fermentation model. Potential improvements in oxygen transfer would be reflected in utilities requirements (i.e. power consumption for stirring and aeration). However, our results show that in all cases the utilities contribution to the operating costs is less than 7.5% (see Table S8 in Supplementary Material). Hence, no significant economic impact is expected.

- **Recovery of dispersed oil phase from aqueous broth: Disk stack centrifuge**

The dispersed organic phase is separated from the aqueous phase and the cells using a disk stack centrifuge. Based on data reported by Tabur and Dorin [9], it is assumed that 90% w/w of the oil phase is recovered in the form of an emulsion containing: 75% w/w oil, 5% w/w cells, and 20% w/w water. The droplet size of the dispersion entering the centrifuge was calculated using the model presented in Eq. (3).

In order to evaluate the impact of solvent in oil recovery by promoting coalescence and creaming in the reactor, case 1 using 10% v/v of dodecane in the fermentation is compared to case 2 which does not incorporate any solvent in the fermentation.

- **Demulsification and recovery of clear oil phase: Disk stack centrifuge**

In the base case the o/w emulsion is inverted by TPI by adding 0.5% w/w of Triton x- 114 as reported by Tabur and Dorin [9]. In cases 1 and 2 the o/w emulsion is inverted by CPI by adding to the emulsion 2 volumes of MTBE per volume of fermentation broth leaving the reactor as reported in laboratory scale protocols [8].

For evaluating alternative solvents to MTBE for CIP, cases 3 to 5 were developed using 2:1 v/v of dodecane, recycled farnesene and kerosene respectively. In all cases, the continuous oil phase is separated from the water phase by centrifugation in a disk-stack centrifuge assuming

98% of clear oil recovery, a cell diameter of 5 μm [42] and a cell density of 1050 g L^{-1} (SuperPro Designer™ database).

- **Solvent-product separation: Distillation**

Solvent-product separation is simulated in SuperPro Designer™ using a distillation column. In case of using more than one type of solvent an additional column was considered. Due to the large number of separation stages required, the use of a continuous distillation column at small scale would lead to an unfeasible high aspect ratio, and therefore distillation is simulated in a batch column.

Vapour pressure of the light key (p_i^{vap}) and heavy key (p_j^{vap}) components were evaluated at the molar averaged temperature of the bottoms Eq. (13) and used to calculate their relative volatility (α_{ij}) Eq. (14). The Antoine coefficients for the components mentioned in this work are obtained from the SuperPro Designer™ database and Tochigi *et al.* [43].

$$\log_{10}(p^{vap}) = A - B/(T + C) \tag{13}$$

$$\alpha_{ij} = p_i^{vap} / p_j^{vap} \tag{14}$$

2.2.4. Economic model and environmental impact

Cases were compared on economic performance and environmental impact. Economic performance was assessed on the basis of the unit cost (\$ kg^{-1}), calculated according to the SuperPro Designer™ built-in model for a new plant, considering materials cost (e.g. glucose, nutrients, and solvents), utilities cost (e.g. heating, cooling, and power), and facility-dependent cost (e.g., depreciation and maintenance); and excluding labour-dependent and waste treatment costs. These economic estimates are expected to have an accuracy of 25%-40%, as usual in conceptual design stages. To evaluate the environmental impact of the process, the E factor (kg waste kg^{-1} product) has been estimated [44]. This E factor accounts for the fermentation off-gas emissions, and the bottom streams of the centrifuges containing cells, residual sesquiterpene and residual solvent. As indicated by Sheldon [44] water was excluded from the calculations of the aqueous waste streams. More details on the economic model can be found in the Supplementary Material.

Table 2: Overview of process simulation parameters. Base case: TPI demulsification, Case 1: Dodecane in bioreactor and CPI demulsification, Case 2: condenser in bioreactor and CPI emulsification, Case 3: Dodecane in bioreactor and dodecane for CPI, Case 4: Farnesene for CPI, Case 5: Kerosene for CPI.

Scale: 25 MT y^{-1} (Flavors and fragrances, pharma, fine chemicals)								
		Base case	Case 1	Case 2	Case 2B	Case 3	Case 4	Case 5
Fermentation	V(m^3)	1.16	1.27	1.16	1.17	1.21	1.17	0.06
	Evaporation Farnesene (g h^{-1})	24	15	24	24	15	24	1
	Evaporation dodecane (g h^{-1})	Na	75	Na	Na	72	Na	Na
	Condenser T(°C)	Na	Na	15	Na	Na	Na	Na
Centrifugation 1	o/w separation area (m^2)	0.02	0.01	0.02	0.02	0.01	0.02	0.001
Demulsification	Demulsifier	Triton 0.5% w/w	MTBE 2:1 (v/v)	MTBE 2:1 (v/v)	MTBE 2:1 (v/v)	Dodecane 2:1 (v/v)	Farnesene 2:1 (v/v)	Kerosene 2:1 (v/v)
Distillation 1	V (m^3)	Na	2.20	1.97	1.97	2.11	Na	Na
Distillation 2	V (m^3)	Na	0.19	Na	Na	Na	Na	Na
Scale: 25000 MT y^{-1} (Biofuels and bulk chemicals)								
Fermentation	Vreactor (m^3)	579(x2)	604(x2)	581(x2)	584(x2)	601(x2)	985(x2)	64
	Evaporation Farnesene (kg h^{-1})	12	7	12	12	7	12	1
	Evaporation dodecane (kg h^{-1})	Na	36	Na	Na	36	Na	Na
	Condenser T(°C)	Na	Na	15	Na	Na	Na	Na
Centrifugation 1	o/w separation area (m^2)	21	12	21	21	12	21	1
Demulsification	Demulsifier	Triton 0.5% w/w	MTBE 2:1 (v/v)	MTBE 2:1 (v/v)	MTBE 2:1 (v/v)	Dodecane 2:1 (v/v)	Farnesene 2:1 (v/v)	Kerosene 2:1 (v/v)
Distillation 1	Number of distillation stages	Na	25	20	20	47	Na	Na
Distillation 2	Number of distillation stages	Na	34	Na	Na	Na	Na	Na

Table 3: Overview of techno-economic evaluation. Base case: TPI demulsification, Case 1: Dodecane in bioreactor and CPI demulsification, Case 2: condenser in bioreactor and CPI emulsification, Case 3: Dodecane in bioreactor and dodecane for CPI, Case 4: Farnesene for CPI, Case 5: Kerosene for CPI.

Scale: 25 MT y^{-1} (Flavors and fragrances, pharma, fine chemicals)							
	Base case	Case 1	Case 2	Case 2B	Case 3	Case 4	Case 5
E factor (kg waste kg^{-1} product)	5	5	4	5	5	5	0.3
purity (% w/w)	99	96	100	100	95	100	5
Unit cost ($ kg^{-1}) total stream	49.0	106.0	82.4	80.3	84.0	79.7	37.7
Glucose (%)	5	2	3	3	3	3	0
Other raw materials (%)	0	1	1	1	3	40	1
Utilities (%)	0	0	0	1	0	0	0
Depreciation and facility costs (%)	94	97	96	96	94	57	98
Scale: 25000 MT y^{-1} (Biofuels and bulk chemicals)							
E factor	5	5	4	5	5	5	0.3
purity (% w/w)	99	95	100	100	96	100	5
Unit cost ($ kg^{-1}) total stream	3.2	4.1	3.8	3.7	5.6	5.3	0.7
Glucose (%)	78	59	67	68	43	48	19
Other raw materials (%)	5	24	15	15	42	42	69
Utilities (%)	4	5	7	6	8	2	1
Depreciation and facility costs (%)	13	11	12	12	8	8	11

3. Results and discussion

The base cases corresponding to the current state of the art at 25 MT y^{-1} and 25000 MT y^{-1}, resulted in unit costs of 49.0 \$ kg^{-1} and 3.2 \$ kg^{-1}, respectively (Table 3). The unit cost obtained at 25000 MT y^{-1} is within the range publicly reported (www.amyris.com) in 2012 and 2015 (9.6 \$ kg^{-1} and 2.15 \$ kg^{-1}, respectively). Note that at both scales, unit cost is dominated by the fermentation section. At 25 MT y^{-1} fermentation costs represent 74% of the unit cost, already accounting for 36.3 \$ kg^{-1}. At 25000 MT y^{-1} this increases to 99%, or 3.17 \$ kg^{-1} (see supplementary material).

3.1. Lowering evaporation rate of sesquiterpene

The sesquiterpene caryophyllene has a negative spread coefficient S<0, and an oil - gas - water contact angle of $\beta = 56°$. In this situation, both L-L-V and L-V transfer routes seem feasible (Figure 2). Similar results are expected for other sesquiterpenes based on their comparable properties (Table 1). The lower contact angle for dodecane $\beta = 34°$ suggests that some solvents could promote the spreading of the oil phase onto the gas bubble and consequently direct transfer of sesquiterpene from oil to gas phase. Evaporation rates estimated at 35 °C, 1 atm, and 1vvm were similar for both routes (Figure 2), ranging from ~g h^{-1} in 1 m^3 reactors to ~kg h^{-1} in 1000 m^3 reactors. In the simulation of a continuous fermentation these rates represented about 1% of the total product (Table 2). However, the current state of the art in microbial sesquiterpene fermentations is fed-batch operation. In this case lower productivities are achieved (e.g., 0.2 to 0.4 g $L^{-1}h^{-1}$ [4, 5]) and evaporation could result in 5 to 10% of product loss. This estimation agrees with reported loss of 3% farnesene in a 2 L scale bioreactor operating in fed-batch at 30°C and 1 vvm [6].

The addition of 10% v/v of solvent in the bioreactor can reduce the evaporation rate by 50% (Figure 2; Table 2) but it increases process complexity by requiring more unit operations (Figure 1C). The need of an additional distillation column led to higher unit costs (Case 1, 106.0 \$ kg^{-1} at 25 MT y^{-1} or 4.1 \$ kg^{-1} at 25000 MT y^{-1}) than recovering the sesquiterpene from the off-gas using a condenser (Case 2, 82.4 \$ kg^{-1} /3.8 \$ kg^{-1}), or even higher than not recovering the sesquiterpene from the off-gas at all (Case 2B, 80.3 \$ kg^{-1} /3.7 \$ kg^{-1}) (Table 3).

3.2. Enhancing coalescence and creaming of the oil phase

Sesquiterpenes and dodecane have similar interfacial tension (Table 1), and thus, estimated droplet sizes for dispersions of sesquiterpene in water and dodecane in water were comparable (Figure 3). In spite of this, adding solvent in the bioreactor results in higher oil fraction and lower oil phase density, leading to larger droplet size and lower required centrifugation area (Figure 3) for a given recovery percentage. Experimental droplet size values were ~50 µm lower than predicted ones and Eq. (3) could only predict experimental data when interfacial tension was lowered to about 15 mN m^{-1}. This interfacial tension values are similar to data reported for biosurfactants [45], which suggests that residual surfactants were present despite the thorough cleaning procedure of the mixing vessel (Figure 3). Although the required o/w separation area has probably been underestimated, the required o/w separation areas are very small (Table 2). Using the cost-model available in SuperPro Designer™ the economic results are not affected unless areas above 10000 m^2 are needed, what would correspond to droplet sizes smaller than 10 µm. In addition, the disk stack centrifuge accounts for less than 15% of the total equipment cost, and therefore this underestimation does not have a remarkable effect in the overall techno-economic performance.

3.3. Demulsification of the oil phase by phase inversion

At 25 MT y^{-1} commercial demulsifiers like Triton-X114 yielded significant lower unit cost (49.0 \$ kg^{-1}) than using low-boiling point solvents, like MTBE, as demulsifiers (82.4 \$ kg^{-1}) (Table 3). At large scale both alternatives presented similar costs (3.2 \$ kg^{-1} in the base case and 3.8 \$ kg^{-1} in case 2), and similar environmental impact in terms of E factor (5 kg waste kg^{-1} product in both cases). The E-factors of all the analyzed cases are in the order of values expected for bulk chemicals [44].

Some alternatives to MTBE were proposed. Using dodecane for reducing evaporation and for demulsification (Case 3, 84.0 \$ kg^{-1} / 5.6 \$ kg^{-1}) could not compete with the base case (49.0 \$ kg^{-1} / 3.2 \$ kg^{-1}). Although recycling farnesene as solvent in CPI presented lower cost (Case 4, 79.7 \$ kg^{-1}/ 5.3 \$ kg^{-1}) than MTBE or dodecane, it was still less competitive than the base case. The main reason is the partial loss of farnesene in the second centrifugation step, which requires a considerably amount of farnesene as make-up of the recycle stream. On the other hand, enrichment of kerosene with 5% of farnesene (37.7 \$ kg^{-1} / 0.7 \$ kg^{-1}) is a promising option with lower unit costs than the base case at any scale.

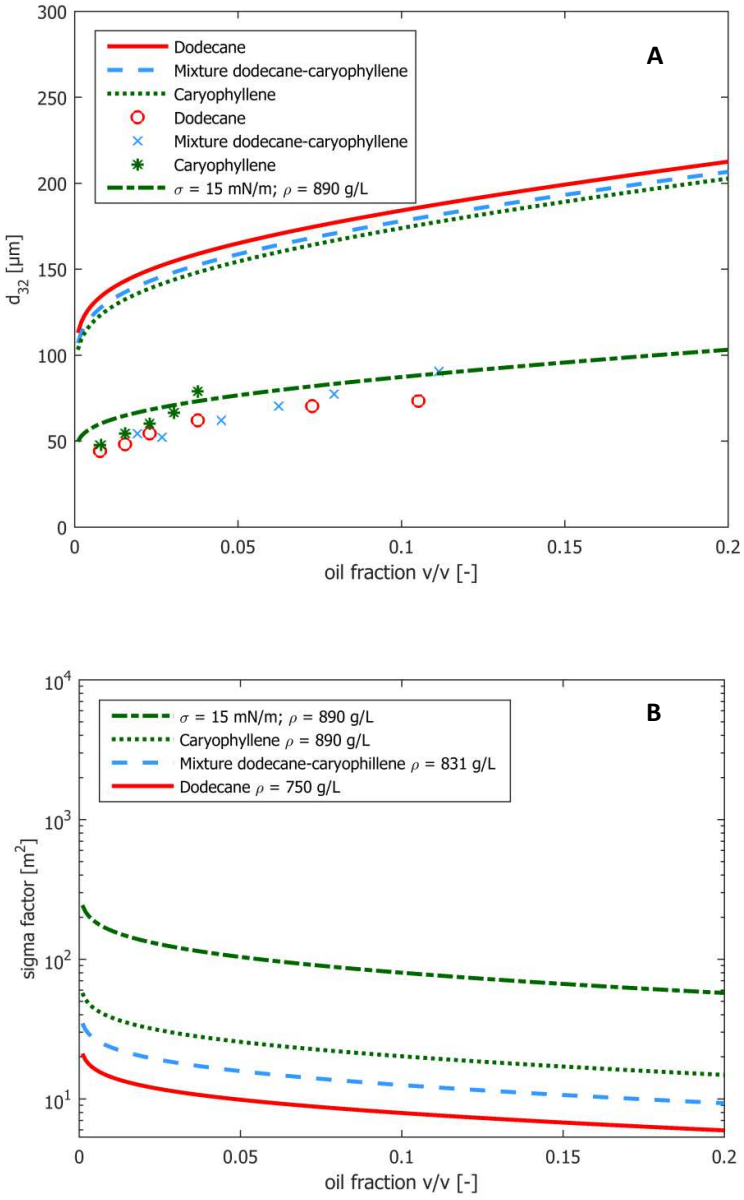

Figure 3: Theoretical values of droplet size (A) and required sigma factor (B) for recovering oil droplets in a disk stack centrifuge of 30% efficiency and 11 L s^{-1} capacity as function of oil fraction estimated at a constant power input of 2.4 W kg^{-1} (corresponding to 1.5 kg fermentor, stirring rate of 1000 rpm, and 1 vvm of gas flow) compared to experimental droplet size values (indicated as markers) at power input ranging from 2.2-2.7 W kg^{-1} (corresponding to 1.275 L of water and different amounts of caryophyllene and dodecane). Potential effect of lowering interfacial tension to 15 mN m^{-1} by surface active components in a caryophyllene/water dispersion is also shown.

Finally, it is important to remark that this work employed 2 volumes of solvent per volume of generated broth, as reported in literature. However, in the studied processes aqueous broth and cells are partially removed prior to the CPI. Therefore the actual volume ratios of solvent:emulsion are about 10:1, and a possible reduction in solvent cost seems feasible. As an example, reducing the amount of solvent by 50% in case 2, leads to 7% of unit cost savings at 25 MT y^{-1} and 3% savings at 25000 MT y^{-1}.

3.4. Impact of scale in techno-economic performance

The main advantages of using solvent at process scale are: a) reducing product evaporation, and consequently glucose consumption; b) avoiding the presence of surfactants in the final product; c) enhancing product recovery by reducing o/w separation area in the disk stack centrifuge; and eventually d) reducing the power input requirements in the fermentation. On the other hand, extra investment in solvent-product separation is needed.

When a new plant is considered, as in this work, at the small scale typical of the flavors and fragrances market equipment cost dominate over operating cost (see Table 3 and Supplementary Material). As a result, savings in raw material when reducing product evaporation cannot overcome the extra investment in equipment required for solvent-product separation (case 1). A solvent-based process can only compete with the current state of the art when considering options that do not require extra separation units, like product recycle (case 4) or using solvents compatible with final product formulation (case 5). These options did not bring any remarkable economic advantage compared to the base case, however they yielded higher product purity and resulted in lower environmental impact, respectively (Table 3).

At larger scales typical of bulk chemicals and fuels, however, unit operating cost are significantly reduced. Furthermore, raw materials have a much higher contribution to the costs than the equipment (e.g. about 80% in the base case), and consequently, the advantages of using solvents in the fermentation become more relevant. In addition, some equipment like distillation columns can be operated in continuous mode allowing for a more efficient solvent-product separation. As a result, unit costs of solvent-based processes (3.7-5.6 \$ kg^{-1}) are comparable with the current state of the art (3.2 \$ kg^{-1}), or even lower in the context of a kerosene enrichment process (0.7 \$ kg^{-1}). Larger savings in solvent-based sesquiterpene process would require improving the CPI demulsification efficiency, by reducing the required amount of solvent and reducing the loss of solvent and product in the aqueous streams of the centrifuges.

4. Conclusions

In this work a solvent-based process for microbial sesquiterpene production was evaluated at different scales. Although several simplifications were made, and absolute values should be taken with care, trends and comparison among cases are expected to be correct. Solvents reduce sesquiterpene evaporation in fermentation and enhance product recovery. However, solvent selection should consider compatibility with final product formulations to avoid extra separation costs. Further reduction in product recovery costs and environmental impact can be achieved in sesquiterpene production by lowering the amount of demulsifiers (e.g., solvent, surfactants), or by implementing alternative recovery methods with higher yields and less unit operations.

Acknowledgements

This work was carried out within the BE-Basic R&D Program, which was granted a FES subsidy from the Dutch Ministry of Economic affairs.

Nomenclature

A	Antoine coefficient
α_{LH}	relative volatility
B	Antoine coefficient
β	L-L-V contact angle
C_D	drag coefficient
C	Antoine coefficient
C^{oil}	concentration of sesquiterpene in the oil
d_{oil}	droplet size
ΔC_{O_2}	difference in oxygen concentration
e_G	power input per unit mass
F_G	Gas flow leaving the bioreactor
ϕ	volume fraction of oil
Φ	molecular interaction parameter
g	gravitational constant
η_w	viscosity of the continuous phase
k_H	Henry's constant
$k_L a$	overall mass transfer coefficient
L	liquid phase
OTR	oxygen transfer rate
p^{vap}	vapour pressure
p_i^{vap}	vapour pressure of the light key
p_j^{vap}	vapour pressure of the heavy key
P_{tot}	total pressure
P_{ow}	distribution coefficient between 1-octanol and water
Q	maximum capacity throughput
ρ_l	aqueous phase density
ρ_{oil}	oil density
R_{evap}	evaporation rate
σ_{wa}	surface tension of water
σ_{oa}	surface tension of oil
σ_{ow}	oil/water interfacial tension
σ_{oa}	oil/air interfacial tension
S	spreading coefficient
Σ	sigma factor
T	Temperature
v_d	creaming velocity
V	Volume
V	Vapour phase
x	molar composition of oil phase
ξ	efficiency of the centrifuge
y	molar fraction in the gas phase

References

1. Maury, J., Asadollahi, M.A., Moller, K., Clark, A., Nielsen, J. *Microbial isoprenoid production: an example of green chemistry through metabolic engineering.* Advances in biochemical engineering/biotechnology. 2005;**100**: p. 19-51.

2. McPhee, D.J. *Deriving Renewable Squalane from Sugarcane.* Cosmetics & Toiletries. 2014;**129**(6): p. 20-26.

3. Devi, M.P., Ghosh, S.K., Bhowmick, N., and Chakrabarty, S., *Essential oil: Its economic aspect, extraction, importance, uses, hazards and quality*, in *Value Addition of Horticultural Crops: Recent Trends and Future Directions*, A. Sharangi, Datta, S., Editor. 2015, Springer: New Delhi. p. 269-278.

4. Tsuruta, H., Paddon, C.J., Eng, D., Lenihan, J.R., Horning, T., Anthony, L.C., et al. *High-level production of amorpha-4,11-diene, a precursor of the antimalarial agent artemisinin, in Escherichia coli*. PLoS One. 2009;**4**(2):e4489.

5. Westfall, P.J., Pitera, D.J., Lenihan, J.R., Eng, D., Woolard, F.X., Regentin, R., et al. *Production of amorphadiene in yeast, and its conversion to dihydroartemisinic acid, precursor to the antimalarial agent artemisinin*. PNAS. 2012;**109**(3):e111-e118.

6. Renninger, N.S., McPhee, D.J., *Fuel compositions comprising farnesane and farnesene and method of making the same.* Amyris Inc. 2010, US 7846222 B2.

7. Renninger, N.S., Newman, J., Reiling, K.K., Regentin, R., Paddon, C.J., *Production of isoprenoids.* Amyris Inc. 2011, US 0287476 A1.

8. Schalk, M., *Method for producting beta-santalene*. Firmenich S.A. 2011, US 0281257 A1.

9. Tabur, P., Dorin, G., *Method for purifying bio-organic compounds from fermentation broth containing surfactants by temperature-induced phase inversion*. Amyris Inc. 2012, US 0040396.

10. Ohler, N.L., Vazquez, R., *Stabilization and hydrogenation methods for microbial-derived olefins.* Amyris, Inc. 2013, US 0310615 A1.

11. Scalcinati, G., Partow, S., Siewers, V., Schalk, M., Daviet, L., Nielsen, J. *Combined metabolic engineering of precursor and co-factor supply to increase alpha-santalene production by Saccharomyces cerevisiae.* Microbial cell factories. 2012;**11**:p. 117.

12. Tippmann, S., Scalcinati, G., Siewers, V., Nielsen, J. *Production of farnesene and santalene by Saccharomyces cerevisiae using fed-batch cultivations with RQ-controlled feed*. Biotechnol Bioeng. 2016;**113**(1):p. 72-81.

13. Scalcinati, G., Knuf, C., Partow, S., Chen, Y., Maury, J., Schalk, M., et al. *Dynamic control of gene expression in Saccharomyces cerevisiae engineered for the production of plant sesquitepene alpha-santalene in a fed-batch mode.* Metab Eng. 2012;**14**(2):p. 91-103.

14. Wang, C., Yoon, S.-H., Jang, H.J., Chung, Y.-R., Kim, J.Y., Choi, E.S., et al. *Metabolic engineering of Escherichia coli for α-farnesene production*. Metabolic Engineering. 2011;**13**(6):p. 648-655.

15. Lindahl, A.L., Olsson, M., Mercke, P., Tollbom, Ö., Schelin, J., Brodelius, M., et al. *Production of the Artemisinin Precursor Amorpha-4,11-diene by Engineered Saccharomyces cerevisiae.* Biotechnology Letters. 2006;**28**(8):p. 571-580.

16. Newman, J.D., Marshall, J., Chang, M., Nowroozi, F., Paradise, E., Pitera, D., et al. *High-level production of amorpha-4,11-diene in a two-phase partitioning bioreactor of metabolically engineered Escherichia coli.* Biotechnology and Bioengineering. 2006;**95**(4):p. 684-691.

17. Asadollahi, M.A., Maury, J., Moller, K., Nielsen, K.F., Schalk, M., Clark, A., et al. *Production of plant sesquiterpenes in Saccharomyces cerevisiae: effect of ERG9 repression on sesquiterpene biosynthesis.* Biotechnol Bioeng. 2008;**99**(3):p. 666-77.

18. Schuhfried, E., Aprea, E., Märk, T.D., Biasioli, F. *Refined Measurements of Henry's Law Constant of Terpenes with Inert Gas Stripping Coupled with PTR-MS*. Water, Air, & Soil Pollution. 2015;**226**(4):p. 1-13.

19. Bruce, L.J., Daugulis, A.J. *Solvent Selection Strategies for Extractive Biocatalysis*. Biotechnology progress. 1991;**7**(2):p. 116-124.

20. Han, G.H., Kim, S.K., Yoon, P.K.S., Kang, Y., Kim, B.S., Fu, Y., et al. *Fermentative production and direct extraction of (−)-α-bisabolol in metabolically engineered Escherichia coli.* Microbial cell factories. 2016;**15**(1):p. 185.

21. Brennan, T.C.R., Turner, C.D., Krömer, J.O., Nielsen, L.K. *Alleviating monoterpene toxicity using a two-phase extractive fermentation for the bioproduction of jet fuel mixtures in Saccharomyces cerevisiae*. Biotechnology and Bioengineering. 2012;**109**(10):p. 2513-2522.

22. Garcia-Ochoa, F., Gomez, E. *Bioreactor scale-up and oxygen transfer rate in microbial processes: An overview*. Biotech Adv. 2009;**27**(2):p. 153-176.

23. Clarke, K.G., Correia, L.D.C. *Oxygen transfer in hydrocarbon–aqueous dispersions and its applicability to alkane bioprocesses: a review*. Biochemical Engineering Journal. 2008;**39**(3):p. 405-429.

24. Janssen, A.C.J.M., Kierkels, J.G.T., Lentzen, G.F., *Two-phase fermentation process for the production of an organic compound*. Isobionics B.V. 2015, WO 002528 A1.

25. Coulaloglou, C.A., Tavlarides, L.L. *Description of interaction processes in agitated liquid-liquid dispersions*. Chemical Engineering Science. 1977;**32**(11):p. 1289-1297.

26. Walstra, P. *Principles of emulsion formation*. Chem Eng Sci. 1993;**48**(2):p. 333-349.

27. Heeres, A.S., Picone, C.S.F., van der Wielen, L.A.M., Cunha, R.L., Cuellar, M.C. *Microbial advanced biofuels production: overcoming emulsification challenges for large-scale operation*. Trends Biotechnol. 2014;**32**(4):p. 221-229.

28. Tippmann, S., Nielsen, J., Khoomrung, S. *Improved quantification of farnesene during microbial production from Saccharomyces cerevisiae in two-liquid-phase fermentations.* Talanta. 2016;**146**:p. 100-106.

29. Perazzo, A., Preziosi, V., Guido, S. *Phase inversion emulsification: Current understanding and applications.* Advances in Colloid and Interface Science. 2015;**222**:p. 581-599.

30. Salager, J.L., Morgan, J.C., Schechter, R.S., Wade, W.H., Vasquez, E. *Optimum Formulation of Surfactant/Water/Oil Systems for Minimum Interfacial Tension or Phase Behavior.* SPE-7054-PA. 1979;**17**(2):p. 107-115.

31. Yeo, L.Y., Matar, O.K., de Ortiz, E.S.P., Hewitt, G.F. *Phase Inversion and Associated Phenomena.* Multiphase Science and Technology. 2000;**12**(1):p. 66.

32. Glonke, S., Sadowski, G., Brandenbusch, C. *Applied catastrophic phase inversion: a continuous non-centrifugal phase separation step in biphasic whole-cell biocatalysis.* Journal of industrial microbiology & biotechnology. 2016;**43**(11):p. 1527-1535.

33. Maaß, S., Rojahn, J., Hänsch, R., Kraume, M. *Automated drop detection using image analysis for online particle size monitoring in multiphase systems.* Comput Chem Eng. 2012;**45**:p. 27-37.

34. Heeres, A.S., Schroen, K., Heijnen, J.J., van der Wielen, L.A.M., Cuellar, M.C. *Fermentation broth components influence droplet coalescence and hinder advanced biofuel recovery during fermentation.* Biotechnology journal. 2015;**10**(8):p. 1206-15.

35. Alopaeus, V., Koskinen, J., Keskinen, K.I. *Simulation of the population balances for liquid-liquid systems in a nonideal stirred tank. Part 1 Description and qualitative validation of the model.* Chemical Engineering Science. 1999;**54**(24):p. 5887-5899.

36. Coulaloglou, C.A. *Dispersed phase interactions in an agitated flow vessel.* PhD Thesis, Illinois Institute of Technology, Chicago. 1975.

37. Girifalco, L.A., Good, R.J. *A Theory for the Estimation of Surface and Interfacial Energies. I. Derivation and Application to Interfacial Tension.* The Journal of Physical Chemistry. 1957;**61**(7):p. 904-909.

38. Demond, A.H., Lindner, A.S.. *Estimation of interfacial tension between organic liquids and water. Environmental science & technology*. 1993;**27**(12):p. 2318-2331.

39. Rowlinson, J.S., Widom, B. *Three-phase equilibrium. Molecular Theory of capillarity.* Dover ed. ed: Dover Publications; 2002. p. 207-248.

40. Verduyn, C., Stouthamer, A., Scheffers, W.A., van Dijken, J. A *theoretical evaluation of growth yields of yeasts.* A Van Leeuw J Microb. 1991;**59**(1):p. 49-63.

41. Gustafsson, L., Ölz, R., Larsson, K., Larssson, C., Adler, L. *Energy balance calculations as a tool to determine maintenance energy requirements under stress conditions*. Pure and Applied Chemistry. 1993;**65**(9):p. 1893-1898.

42. Ahmad, M.R., Nakajima, M., Kojima, S., Homma, M., Fukuda, T. *The effects of cell sizes, environmental conditions, and growth phases on the strength of individual W303 yeast cells inside ESEM*. IEEE transactions on nanobioscience. 2008;**7**(3):p. 185-93.

43. Tochigi, K., Yamagishi, M., Ando, S., Matsuda, H., Kurihara, K. *Prediction of Antoine constants using a group contribution method*. Fluid Phase Equilibria. 2010;**297**(2):p. 200-204.

44. Sheldon, R.A. *The E Factor: fifteen years on*. *Green Chemistry*. 2007;9(12):p. 1273-1283.

45. Rodrigues, L.R., Banat, I.M., van der Mei, H.C., Teixeira, J.A., Oliveira, R. *Interference in adhesion of bacteria and yeasts isolated from explanted voice prostheses to silicone rubber by rhamnolipid biosurfactants*. Journal of Applied Microbiology. 2006;**100**(3):p. 470-480.

46. Gonzales-Vigil, E., Hufnagel, D.E., Kim, J., Last, R.L., Barry, C.S. *Evolution of TPS20-related terpene synthases influences chemical diversity in the glandular trichomes of the wild tomato relative Solanum habrochaites*. The Plant journal : for cell and molecular biology. 2012;**71**(6):p. 921-35.

47. Dataphysics. *Surface tension datasheet.* Retrieved January 2017 from: http://www.surface-tension.de/. Dataphysics Instruments GmbH. 2015.

48. CAMEOdatabase. *Ethyl-acetate* datasheet. CAMEO database of hazardous materials National Oceanic and Atmospheric Administration USA gov. 2015.

49. Montaño, D., Bandrés, I., Ballesteros, L., Lafuente, C., Royo, F. *Study of the Surface Tensions of Binary Mixtures of Isomeric Chlorobutanes with Methyl tert-Butyl Ether*. J Solution Chem. 2011;**40**(7):p. 1173-1186.

50. Hickel, A., Radke, C.J., Blanch, H.W. *Role of organic solvents on Pa-hydroxynitrile lyase interfacial activity and stability*. Biotechnology and Bioengineering. 2001;**74**(1):p. 18-28

.

Supplementary material: Flow-sheet model parameters

Unless specified otherwise, default values suggested by SuperPro Designer (v 9.5) have been used for the simulation.

Table S1: Prices for raw materials, solvents, demulsifiers and main product. Unless specified otherwise, used values are calculated as average of available range values. When more than one source is available, used values are calculated as an average.

	Price ($ MT^{-1})	
Component	References	Simulation
Glucose	350-500 [(a)]	475
Ammonium hydroxide	425-851 [(b)]	774
Water	-	1.20
Dodecane	2000-4000 [(c)]	3000
MTBE	887-1319 [(b)]	1206
Non-ionic surfactant Triton x-114 (Octyl phenol ethoxylate)	1500-3000 [(d)] 900 - 3100 [(e)]	2125
Sesquiterpene	1475000 [(f)] 279000 [(g)]	279000
Kerosene	517 [(h)]	517

(a) Index Mundi, commodity prices http://www.indexmundi.com/commodities/?commodity=sugar
(b) ICIS
(c) AliBaba
(d) AliBaba price for Nonyl phenol Ethoxylate (Triton N-57)
(e) AliBaba price for Nonionic surfactant TX-10
(f) ICIS Price for Sandalwood oil
(g) value reported by Sigma-Aldrich for mixture of isomers of farnesene (99.9%purity) (March 2015)
(h) http://ycharts.com/indicators/jet_fuel_spot_price(March, 2015) 1.554 USD gal^{-1} (0.795 kg L^{-1})

Table S2: Fermentation overview

Fermentation: Stoichiometric continuous reactor						
Scale: 25 MT y^{-1} (Flavors and fragrances, pharma, fine chemicals)						
	Base case	Case 1	Case 2	Case 3	Case 4	Case 5
V(m^3)	1.16	1.27	1.16	1.21	1.94	0.06
Number of units	1	1	1	1	1	1
T(°C)	35	35	35	35	35	35
Residence time (h)	25	25	25	25	25	25
Power input (kW m^{-3})	2.4	2.4	2.4	2.4	2.4	2.4
$x_{C15,org}$ (w/w)	1	0.6	1	0.6	1	1
o/w (v/v)	0.1	0.2	0.1	0.2	0.1	0.1
Product (g L^{-1}) [(a)]	100	118	99	100	99	99
Cells (g L^{-1}) [(a)]	53	51	53	53	53	53
Evaporation rate farnesene (g h^{-1})	24	15	24	15	39	1
Solvent	Na	dodecane	Na	dodecane	Na	Na
Evaporation rate solvent (g h^{-1})	Na	75	Na	72	Na	Na
Condenser T(°C)	Na	Na	15	Na	Na	Na
Scale: 25000 MT y^{-1} (Biofuels and bulk chemicals)						
	Base case	Case 1	Case 2	Case 3	Case 4	Case 5
V(m^3)	579	604	581	601	963	64
Number of units	2	2	2	2	2	1
T(°C)	35	35	35	35	35	35
Residence time (h)	25	25	25	25	25	25
Power input (kW m^{-3})	2.4	2.4	2.4	2.4	2.4	2.4
$x_{C15,org}$ (w/w)	1	0.6	1	0.6	1	1
o/w (v/v)	0.1	0.2	0.1	0.2	0.1	0.1
Product (g L^{-1})[(a)]	100	100	100	100	100	99
Cells (g L^{-1}) [(a)]	53	53	53	53	53	53
Evaporation rate farnesene (kg h^{-1})	11.8	7.4	11.8	7.3	19.6	1.3
Solvent	Na	dodecane	Na	dodecane	Na	Na
Evaporation rate solvent (kg h^{-1})	Na	35.7	Na	35.5	Na	Na
Condenser T(°C)	Na	Na	15	Na	Na	Na

(a) Product concentration aims for 100 g per L of aqueous broth (water, glucose, NH_4OH and cells) excluding solvent.

Table S3: Centrifugation 1 overview

Centrifugation 1						
Scale: 25 MT y^{-1} (Flavors and fragrances, pharma, fine chemicals)						
	Base case	Case 1	Case 2	Case 3	Case 4	Case 5
Limiting oil diameter (µm)	175	207	175	207	175	175
Oil density (g L^{-1})	860	817	860	810	860	860
Exit T(°C)	35	35	35	35	35	35
Farnesene removal (%)	90	90	90	90	90	90
ISPR solvent removal (%)	Na	90	Na	90	Na	Na
Cells removal (%)	11	19	11	19	11	11
Aq. removal (%)	3	5	3	5	3	3
Farnesene top stream (% w/w)	74.5	49.5	74.4	43.7	74.4	74.4
ISPR solvent top stream (%)	Na	27.5	Na	31.3	Na	Na
Biomass top stream (%w/w)	4.8	4.5	4.8	4.9	4.8	4.8
Aq. Top stream (%w/w)	20.6	18.7	20.6	20.1	20.6	20.6
Inlet droplet diameter (µm)	175	207	175	175	207	175
Separation area (m^2)	0.02	0.01	0.02	0.01	0.04	0.001
Scale: 25000 MT y^{-1} (Biofuels and bulk chemicals)						
	Base case	Case 1	Case 2	Case 3	Case 4	Case 5
Limiting oil diameter (µm)	175	207	175	207	175	175
Oil density (g L^{-1})	860	812	860	812	860	860
Exit T(°C)	35	35	35	35	35	35
Farnesene removal (%)	90	90	90	90	90	90
ISPR solvent removal (%)	Na	90	Na	90	Na	Na
Cells removal (%)	11	19	11	19	11	11
Aq. removal (%)	3	5	3	5	3	3
Farnesene top stream (% w/w)	74.5	44.5	74.5	44.5	74.5	74.4
ISPR solvent top stream (%)	Na	30	Na	30	Na	Na
Biomass top stream (%w/w)	4.8	4.9	4.8	4.9	4.8	4.8
Aq. Top stream (%w/w)	20.5	20.4	20.6	20.4	20.6	20.6
Inlet droplet diameter (µm)	175	207	175	175	207	175
Separation area (m^2)	21	12	21	12	35	1

Table S4: Demulsification overview

Demulsification						
Scale: 25 MT y^{-1} (Flavors and fragrances, pharma, fine chemicals)						
	Base case	Case 1	Case 2	Case 3	Case 4	Case 5
Demulsifier	Triton-X114	MTBE	MTBE	Dodecane	Farnesene	Kerosene
T(°C)	60	35	35	35	35	35
Target concentration[(b)]	0.5% w/w	2:1 (v/v)	2:1 (v/v)	2:1 (v/v)	2:1 (v/v)	2:1 (v/v)
Actual conc. [(b)]	0.5% w/w	1.96:1 (v/v)	2:1 (v/v)	1.99:1 (v/v)	2:1 (v/v)	2:1 (v/v)
Scale: 25000 MT y^{-1} (Biofuels and bulk chemicals)						
	Base case	Case 1	Case 2	Case 3	Case 4	Case 5
Demulsifier	Triton-X114	MTBE	MTBE	Dodecane	Farnesene	Kerosene
T(°C)	60	35	35	35	35	35
Target concentration[(b)]	0.5% w/w	2:1 (v/v)	2:1 (v/v)	2:1 (v/v)	2:1 (v/v)	2:1 (v/v)
Actual concentration [(b)]	0.5% w/w	2:1 (v/v)	2:1 (v/v)	2:1 (v/v)	2:1 (v/v)	2:1 (v/v)

(b) Triton concentration calculated using exit top stream of the centrifuge as reference, based on protocol from[1]. Solvent concentration for demulsification calculated using exit stream of fermentation as reference, based on lab protocols

Table S5: Centrifugation 2 overview

Centrifugation 2						
Scale: 25 MT y^{-1} (Flavors and fragrances, pharma, fine chemicals)						
	Base case	Case 1	Case 2	Case 3	Case 4	Case 5
Limiting solid diameter (µm)	5	5	5	5	5	5
Solid density (g L^{-1})	1050	1050	1050	1050	1050	1050
Exit T(°C)	35	35	35	35	35	35
Farnesene removal top (%)	98	98	98	98	98	98
Demulsifier removal top (%)	98	98	98	98	98	98
ISPR solvent removal top (%)	Na	98	Na	98	Na	Na
Cells removal bottom (%)	100	100	100	100	100	100
Aq. removal bottom (%)	100	100	100	100	100	100
Separation area (m^2)	9.87	176	156	168	260	8.61
Scale: 25000 MT y^{-1} (Biofuels and bulk chemicals)						
	Base case	Case 1	Case 2	Case 3	Case 4	Case 5
Limiting solid diameter (µm)	5	5	5	5	5	5
Solid density (g L^{-1})	1050	1050	1050	1050	1050	1050
Exit T(°C)	35	35	35	35	35	35
Farnesene removal top (%)	98	98	98	98	98	98
Demulsifier removal top (%)	98	98	98	98	98	98
ISPR solvent removal top (%)	Na	98	Na	98	98	98
Cells removal bottom (%)	100	100	100	100	100	100
Aq. removal bottom (%)	100	100	100	100	100	100
Separation area (m^2)	9865	168683	155963	165345	258215	8609

Table S6: Distillation 1 overview

Distillation 1						
Scale: 25 MT y^{-1} (Flavors and fragrances, pharma, fine chemicals)						
	Base case	Case 1	Case 2	Case 3	Case 4	Case 5
Hold up time (h)	Na	24	24	24	Na	Na
$X_{L,D}$ [(d)]	Na	100	100	98	Na	Na
$X_{H,B}$ [(e)]	Na	64.5	100	95	Na	Na
V (m^3)	Na	2.21	1.97	2.11	Na	Na
Scale: 25000 MT y^{-1} (Biofuels and bulk chemicals)						
	Base case	Case 1	Case 2	Case 3	Case 4	Case 5
T condens (°C) [(c)]	Na	47	47	206	Na	Na
T reboiler (°C) [(c)]	Na	236	259	258	Na	Na
Volatility Farnesene	Na	0.3611	1.0000	1.0000	Na	Na
Volatility Dodecane	Na	1.0000	Na	2.6300	Na	Na
Volatility MTBE	Na	23.4400	49.7108	Na	Na	Na
X L,D(d)	Na	99.99	100	100	Na	Na
X H,B(e)	Na	40.26	99.83	95.51	Na	Na
N (f)	Na	25	20	47	Na	Na

(c) T reboiler (averaged boiling point) is used by SPD to calculate relative volatility, T condens is used to determine outlet temperature, not for mass or energy balances.

(d) %w/w of the light component on top

(e) %w/w of the heavy component on bottom

(f) Number of distillation stages

Table S7:Distillation 2 overview

Distillation 2						
Scale: 25 MT y^{-1} (Flavors and fragrances, pharma, fine chemicals)						
	Base case	Case 1	Case 2	Case 3	Case 4	Case 5
Hold up time (h)	Na	24	Na	Na	Na	Na
$X_{L,D}$ (d)	Na	72	Na	Na	Na	Na
$X_{H,B}$ (e)	Na	96	Na	Na	Na	Na
V (m^3)	Na	0.19	Na	Na	Na	Na
Scale: 25000 MT y^{-1} (Biofuels and bulk chemicals)						
	Base case	Case 1	Case 2	Case 3	Case 4	Case 5
T condens(°C) (c)	Na	205	Na	Na	Na	Na
T reboiler(°C) (c)	Na	258	Na	Na	Na	Na
Volatility Farnesene	Na	1.0000	Na	Na	Na	Na
Volatility Dodecane	Na	2.6180	Na	Na	Na	Na
Volatility MTBE	Na	50.2328	Na	Na	Na	Na
$X_{L,D}$ (d)	Na	99.70	Na	Na	Na	Na
$X_{H,B}$ (e)	Na	95.49	Na	Na	Na	Na
N (f)	Na	34	Na	Na	Na	Na

(c) T reboiler (averaged boiling point) is used by SPD to calculate relative volatility, T condens is used to determine outlet temperature, not for mass or energy balances.

(d) %w/w of the light component on top

(e) %w/w of the heavy component on bottom

(f) Number of distillation stages

Table S8: Economic parameters

Economic parameters							
Scale: 25 MT y^{-1} (Flavors and fragrances, pharma, fine chemicals)							
	Base case	Case 1	Case 2	Case 2B	Case 3	Case 4	Case 5
purity % w/w	99.3	95.55	100.00	100.00	95.05	100.00	5.47
unit cost ($ per total kg)	49.01	105.98	82.41	80.29	84.00	52.61	37.67
unit cost ($ per kg farnesene)	49.33	110.90	82.41	80.29	88.37	52.61	688.66
Raw materials ($ y^{-1})	67000	88000	77000	77000	123000	111000	16000
Of which Glucose ($ y^{-1})	63034	62316	62983	63463	59986	104699	3472
Of which solvent ($ y^{-1})	0	10898	10145	10222	0	0	12467
Depreciation ($ y^{-1})	582000	1288000	997000	967000	994000	604000	466000
Other facility cost ($ y^{-1})	572000	1267000	980000	950000	977000	593000	458000
Utilities ($ y^{-1})	4000	6000	7000	13000	6000	8000	1000
Total operating costs ($ y^{-1})	1225000	2649000	2060000	2007000	2100000	1315000	942000
Scale: 25000 MT y^{-1} (Biofuels and bulk chemicals)							
	Base case	Case 1	Case 2	Case 2B	Case 3	Case 4	Case 5
purity % w/w	99.33	95.49	99.83	100.00	95.51	100.00	5.47
unit cost ($ per total kg)	3.20	4.07	3.76	3.72	5.64	5.18	0.74
unit cost ($ per kg farnesene)	3.22	4.26	3.77	3.72	5.91	5.18	13.52
Raw materials ($ y^{-1})	66745000	84927000	76647000	76935000	119126000	110038000	16135000
Of which Glucose ($ y^{-1})	62825623	60335029	62906880	63143211	60178828	104147246	3471864
Of which solvent ($ y^{-1})	0	10597850	10181991	10220243	0	0	12467119
Depreciation ($ y^{-1})	5214000	5653000	5530000	5503000	5654000	7291000	1065000
Other facility cost ($ y^{-1})	5131000	5562000	5441000	5414000	5563000	7173000	1047000
Utilities ($ y^{-1})	2951000	5563000	6407000	5142000	10627000	4880000	171000
Total operating costs ($ y^{-1})	80041000	101705000	94025000	92994000	140969000	129381000	18417000

Table S9: Cost breakdown per section in $ per kg

Cost breakdown per section							
Scale: 25 MT y^{-1} (Flavors and fragrances, pharma, fine chemicals)							
	Base case	Case 1	Case 2	Case 2B	Case 3	Case 4	Case 5
Fermentation	36.342 (74.15%)	37.237 (35.14%)	38.833 (47.12%)	36.417 (45.36%)	38.761 (46.15%)	36.417 (45.68%)	25.337 (67.27%)
Centrifugation	5.903 (12.04%)	5.902 (5.57%)	5.903 (7.16%)	6.202 (7.72%)	5.902 (7.03%)	5.902 (7.40%)	5.901 (15.67%)
Demulsification	6.764 (13.80%)	6.432 (6.07%)	6.398 (7.76%)	6.401 (7.97%)	5.994 (7.14%)	37.396 (46.91%)	6.427 (17.06%)
Distillation	Na	56.404 (53.22%)	31.273 (37.95%)	31.271 (38.95%)	33.340 (39.69%)	Na	Na
Scale: 25000 MT y^{-1} (Biofuels and bulk chemicals)							
	Base case	Case 1	Case 2	Case 2B	Case 3	Case 4	Case 5
Fermentation	3.173 (99.10%)	3.506 (86.18%)	3.232 (85.93%)	3.189 (85.73%)	5.296 (93.91%)	3.194 (60.18%)	0.226 (30.65%)
Centrifugation	0.006 (0.19%)	0.006 (0.15%)	0.006 (0.16%)	0.006 (0.16%)	0.006 (0.11%)	0.006 (0.11%)	0.006 (0.80%)
Demulsification	0.023 (0.71%)	0.459 (11.29%)	0.441 (11.73%)	0.443 (11.91%)	0.132 (2.34%)	2.107 (39.71%)	0.505 (68.54%)
Distillation	Na	0.097 (2.38%)	0.082 (2.18%)	0.082 (2.21%)	0.205 (3.64%)	Na	Na

Table S10: Main equipment cost breakdown

Main equipment cost breakdown							
Scale: 25 MT y^{-1} (Flavors and fragrances, pharma, fine chemicals)							
	Base case	Case 1	Case 2	Case 2B	Case 3	Case 4	Case 5
Fermenter ($)	601000	609000	602000	602000	604000	646000	451000
Centrifuge 1 ($)	101000	101000	101000	101000	101000	101000	101000
Centrifuge 2 ($)	101000	101000	101000	101000	101000	101000	101000
Distillation 1 ($)	0	568000	560000	560000	597000	0	0
Distillation 2 ($)	0	442000	0	0	0	0	0
Condenser ($)	0	0	31000	0	0	0	0
Oil separator ($)	0	0	10000	0	0	0	0
Total equipment cost ($)	1021000	2276000	1756000	1705000	1754000	1060000	816000
Scale: 25000 MT y^{-1} (Biofuels and bulk chemicals)							
	Base case	Case 1	Case 2	Case 2B	Case 3	Case 4	Case 5
Fermenter ($)	7184000	7360000	7200000	7216000	7338000	9676000	1301000
Centrifuge 1 ($)	101000	101000	101000	101000	101000	101000	101000
Centrifuge 2 ($)	101000	439000	421000	422000	434000	553000	101000
Distillation 1 ($)	0	41000	60000	61000	147000	0	0
Distillation 2 ($)	0	76000	0	0	0	0	0
Condenser ($)	0	0	44000	0	0	0	0
Oil separator ($)	0	0	10000	0	0	0	0
Total equipment cost ($)	9250000	10021000	9794000	9750000	10025000	12913000	1879000

Table S11: Liquid waste stream composition

Liquid waste stream composition							
Scale: 25 MT y^{-1} (Flavors and fragrances, pharma, fine chemicals)							
	Base case	Case 1	Case 2	Case 2B	Case 3	Case 4	Case 5
From Centrifugation 1							
Farnesene (%)	1.2	1.4	1.2	1.2	1.2	1.2	1.2
Biomass (%)	1.7	5.0	5.4	5.4	5.0	5.4	5.4
Solvent (%)	0	0.8	0	0	0.8	0	0
Water (%)	92.9	92.2	92.9	92.9	92.4	92.9	92.9
Total mass flow (kg h^{-1})	30.8	30.0	31.1	31.3	28.8	51.3	1.7
From Centrifugation 2							
Farnesene (%)	5.5	2.5	2.9	2.9	2.7	54.2	2.8
Biomass (%)	17.8	11.5	9.3	9.3	11.4	8.6	9.1
Solvent (%)	0	37.1	47.8	47.8	38.4	0	48.7
Water (%)	76.2	47.3	39.8	39.8	47.2	37.0	39.1
Total mass flow (kg h^{-1})	1.6	3.1	2.2	2.6	3.0	4.0	0.1
Scale: 25000 MT y^{-1} (Biofuels and bulk chemicals)							
	Base case	Case 1	Case 2	Case 2B	Case 3	Case 4	Case 5
From Centrifugation 1							
Farnesene (%)	1.2	1.2	1.2	1.2	1.2	1.2	1.2
Biomass (%)	5.4	5.0	5.4	5.4	5.0	5.4	5.4
Solvent (%)	0	0.8	0	0	0.8	0	0
Water (%)	92.9	92.4	92.8	92.9	92.4	92.9	92.9
Total mass flow (kg h^{-1})	30677	28983	30818	30934	28906	51022	1700
From Centrifugation 2							
Farnesene (%)	5.5	2.1	2.9	2.9	2.1	54.2	2.8
Biomass (%)	17.8	11.5	9.3	9.3	11.4	8.6	9.1
Solvent (%)	0	38.5	47.8	47.7	38.9	0	48.7
Water (%)	76.2	47.5	39.8	39.8	47.3	37.0	39.1
Total mass flow (kg h^{-1})	1156	2967	2221	2230	2975	3963	124

Table S12: Experimental and reported values of surface tension (σ_{oa}) and interfacial tension interfacial tension (σ_{ow}) for sesquiterpenes, common solvents and surfactants used in laboratory protocols for microbial sesquiterpene production.

	σ_{oa} (mN m^{-1})	σ_{ow} (mN m^{-1})	Example in literature
Santalene	36 [(a)]		
Caryophyllene	30[(a)] 31[(b)]	50.5[(e)]	
Farnesene	26 [(a)]		
Amorphadiene	26 [(a)]		
Dodecane	25.5[(b)] 25.35 [(d)]	49.9[(c)] 52.8 [(e)]	[2]
MTBE	18.70 [(f)]	10.5 [(g)]	[3]
Triton x-114	31 [(h)]	-	[1]

(a) ACD/Labs Percepta Platform - PhysChem Module
(b) Experimentally determined in this work at room temperature
(c) Estimated from experimental results using [4]
(d) Data_Physics_Instruments_GmbH (2015) @20 °C
(e) Demond and Lindner [5] (Temperature not reported)
(f) Montaño, Bandrés [6] @20 °C
(g) Hickel, Radke [7] (Temperature not reported)
(h) Triton X-114 Technical Data Sheet. DOW

Table S13: Antoine coefficients for different solvents and sesquiterpenes to determine their vapour pressure in the distillation. Log Base 10, pressure in mmHg and T (bottom temperature of the distillation column) in K.

Component	A	B	C	Source
Dodecane	6.9979	1639.2700	-91.3600	SuperPro Designer database (v. 9.5)
MTBE	6.8500	1103.7300	-50.5000	SuperPro Designer database (v. 9.5)
Farnesene	6.9898	1798.9000	-96.3500	[8]

References

1. Tabur, P. and Dorin, G.*Method for purifying bio-organic compounds from fermentation broth containing surfactants by temperature-induced phase inversion.* 2012. WO2012024186

2. Scalcinati, G., Knuf, C., Partow, S., Chen, Y., et al., *Dynamic control of gene expression in Saccharomyces cerevisiae engineered for the production of plant sesquitepene alpha-santalene in a fed-batch mode.* Metab Eng, 2012. **14**(2): p. 91-103.

3. Gonzales-Vigil, E., Hufnagel, D.E., Kim, J., Last, R.L., et al., *Evolution of TPS20-related terpene synthases influences chemical diversity in the glandular trichomes of the wild tomato relative Solanum habrochaites.* Plant J, 2012. **71**(6): p. 921-35.

4. Girifalco, L.A. and Good, R.J., *A Theory for the Estimation of Surface and Interfacial Energies. I. Derivation and Application to Interfacial Tension.* The Journal of Physical Chemistry, 1957. **61**(7): p. 904-909.

5. Demond, A.H. and Lindner, A.S., *Estimation of interfacial tension between organic liquids and water.* Environmental Science & Technology, 1993. **27**(12): p. 2318-2331.

6. Montaño, D., Bandrés, I., Ballesteros, L., Lafuente, C., et al., *Study of the Surface Tensions of Binary Mixtures of Isomeric Chlorobutanes with Methyl tert-Butyl Ether.* Journal of Solution Chemistry, 2011. **40**(7): p. 1173-1186.

7. Hickel, A., Radke, C.J., and Blanch, H.W., *Role of organic solvents on Pa-hydroxynitrile lyase interfacial activity and stability.* Biotechnology and Bioengineering, 2001. **74**(1): p. 18-28.

8. Tochigi, K., Yamagishi, M., Ando, S., Matsuda, H., et al., *Prediction of Antoine constants using a group contribution method*. Fluid Phase Equilibria, 2010. **297**(2): p. 200-204.

Chapter 4. Organic phase emulsification limits oxygen transfer enhancement in multiphase fermentations for the production of advanced biofuels and chemicals

Abstract

In fermentations where a hydrophobic liquid is produced and/or solvent is added for in-situ product removal, droplets are dispersed in the broth due to the mixing in the reactor. In aerobic fermentations, these droplets can interact with the gas bubbles generating additional oxygen transfer routes across the oil phase. However, there is no agreement yet in literature about the role of oil phase in oxygen transfer enhancement.

In this work, oxygen transfer was studied in fermentations with wild-type and sesquiterpene-producing *Escherichia coli* at varying oil fractions of hexadecane and dodecane. Experimental $k_L a$ was compared to a mathematical model based on growth kinetics and a mixed transfer route across dispersed droplets and droplets covering bubble surface. The degree of $k_L a$ enhancement upon oil addition was dependent on the transfer route and decreased along the fermentation age. Contrary to literature results, $k_L a$ trends were not correlated to changes in power input, oil fraction, or cell concentration, but could be explained by reduced bubble-droplet and droplet-droplet interactions due to droplet stabilization. These results present evidence, for the first time, that surface active components present in the broth can limit the impact of oxygen vectors in $k_L a$ enhancement, bringing a new perspective on oxygen transfer in multiphase fermentations.

This chapter has been submitted as:

Pedraza-de la Cuesta, S., van Houten, C., Feskens-Snoeck, F., van der Wielen, L.A.M., Cuellar, M.C. Organic phase emulsification limits oxygen transfer enhancement in multiphase fermentations for the production of advanced biofuels and chemicals

1. Introduction

In multiphase fermentations a product secreted by the microbial cells forms a second phase in the aqueous broth and/or a solvent is added to recover the product. Multiphase fermentations are very common in the production of long-chain hydrocarbons for biofuels and chemicals, e.g. microbial production of alkanes [1]; microbial production and bioconversion of sesquiterpenes [2, 3]. Sesquiterpenes are C15 isoprenoids which traditionally have been extracted from plants because of their medical, flavor and fragrance properties. Production of sesquiterpenes using modified microorganisms is a promising alternative to overcome the scarcity of raw material for plant extraction, while reducing process cost. Genetically engineered strains of *Escherichia coli* and *Saccharomyces cerevisiae* can produce extracellular sesquiterpenes in aerobic fermentations, reaching titers in the order of g L^{-1} [2, 3]. Several companies are currently working on the process scale-up and commercialization of microbial sesquiterpenes for diverse applications such as advanced biofuels, antimalarial drugs, or flavors and fragrances.

The current sesquiterpene productivities between 0.2 and 0.4 g L^{-1} h^{-1} achieved in fed-batch operation [2, 3] require high cell density fermentations to meet up product titers. This implies a large concentration of cells, cell debris and extracellular proteins, all with surface active properties [4]. Due to the turbulent conditions required for fermentation, the hydrophobic, light organic phase is dispersed in small droplets and stabilized by such surface active components (SACs). Surfactants are normally added after the fermentation to break the emulsion and enhance the product recovery [5]. Alternatively, solvents like dodecane can be added in the reactor reducing product evaporation [6-9], while enhancing recovery [10]. Some authors claim that increasing the oil fraction in the system by adding solvents can enhance oxygen transfer in sesquiterpene fermentations [11]. Oxygen supply is typically one of the main limiting factors in the scale-up of aerobic fermentations [12]. This is particularly relevant in sesquiterpene fermentations which have a high oxygen demand [13]. Oxygen limitation in the reactor broth can lead to lower productivity and to a higher degree of emulsification, by increasing the level of SACs due to cellular stress [14]. Although oxygen transfer in multiphase systems has been extensively studied in literature (e.g.,[15-20]), several results are contradictory and do not allow to predict what the net effect of the oil phase would be [16, 21].

In aerobic fermentations, air bubbles are sparged into the aqueous medium to provide oxygen for the microorganisms. The oxygen transfer rate (OTR) depends on the liquid mass transfer coefficient (k_L), the volumetric transfer area (a), the difference between the oxygen concentration and its equilibrium value $\left(C_{w,eq} - C_w\right)$, and the system volume (V).

$$OTR = k_L \cdot a \cdot \left(C_{w,eq} - C_w\right) \cdot V \qquad (1)$$

The presence of a second liquid phase in the reactor can affect the OTR in different manners. In first place, droplets can coalesce with bubbles and spread on their surface. This can reduce the overall transfer coefficient k_L by creating an additional transfer barrier (Figure 1). On the other hand, solubility of oxygen in hydrocarbons is higher than in water. The solubility of oxygen in the broth could be increased by about 2 times in the presence of a hydrocarbon phase (e.g. sesquiterpenes and/or a solvent) (Table 1). In addition, droplets can act as oxygen vectors increasing the available transfer area a. All these mechanisms are greatly affected by the interfacial tension between gas, oil and aqueous medium. Consequently, the net effect of the oil phase in the oxygen transfer could be affected by the presence of SACs in the medium.

The aim of this work is to elucidate the impact of an oil phase in the oxygen transfer in microbial sesquiterpene fermentations. In addition, this research studies the applicability of solvents like dodecane and hexadecane as oxygen vectors. For these purposes, $k_L a$ was experimentally determined in four fermentations under different conditions of oil concentration, type of oil, cell concentration and volumetric power input (Table 2). In addition, $k_L a$ was modelled using cell growth kinetics and assuming parallel oxygen transfer across gas/oil/water (g/o/w) and gas/water (g/w) interfaces. Model and experimental results were compared to literature data on dispersions (hexadecane in water [18], and dodecane in water containing quiescent cells [15]), and the most probable transfer routes along the fermentation were identified.

Table 1 Partition coefficient, mass transfer coefficient and oxygen solubility for gas-oil-water (g/o/w) systems. (a)hexadecane, (b)dodecane, (c)sesquiterpenes, and (d) heptane.

Parameter	Value	Unit	Remark
Partition coefficient			
$m_{o/w}$	6.2[(a)]	mol/mol	Calculated from log P [22]
$m_{g/w}$	36.5[(a)]	mol/mol	Calculated from Henry coefficient at 35°C, 1atm, and 21% oxygen in air [23]
$m_{g/o}$	3.8[(a)] 2.8[(b)]	mol/mol	Calculated from Henry coefficient for hexadecane at 25°C, 1atm, and 21% oxygen in air [24] corrected for dodecane [25].
Mass transfer coefficient			
k_o	0.060[(d)] 0.03-0.10[(c)]	m/h	[26][(a)] [27][(c)]
k_w	0.108	m/h	[26]
$k_{o/w}$	0.084[(a)]	m/h	Calculated from Eq. 3
Oxygen solubility			
$C_{o,eq\_g/o}$	2.23[(a)] 3.06[(b)]	mol-O_2/m^3-oil	Calculated from $m_{g/o}$
$C_{w,eq\_g/w}$	0.23[(a)]	mol-O_2/m^3-water	Calculated from $m_{g/w}$
$C_{w,eq\_g/o/w}$	0.36[(a)] 0.50[(b)]	mol-O_2/m^3-water	Calculated from $m_{g/o}$ *and* $m_{g/w}$

Table 2 Summary of the experiments indicating fermentation periods selected for this study, their range in cell concentration, volumetric power input, and their averaged oil concentration.

ID	Solvent	Microorganism	period	Time (h)	Cell concentration ($g \cdot L^{-1}$)	$P \cdot V^{-1}$ ($W \cdot m^{-3}$)	Oil fraction (%v/v)
F01	-	*E. coli K12*	1	29-49	17→39	4000→3500	0
F02	Hexadecane	*E. coli K12*	1	29-49	14→47	4000→3500	7.5±0.2
F03	Dodecane	rec-*E. coli*	1	45-64	30→39	8500→6500	6.3±0.5
			2	65-92	39→45	8000→5500	4.7±0.4
			3	95-107	45→33	7000→6000	3.6±0.1
F04	Dodecane	rec-*E. coli*	1	24-59	20→36	9000→6500	8.5±1.2
			2	65-85	37→30	8500→6500	5.5±0.5

2. Theoretical Background

2.1. Transfer mechanisms in multiphase fermentations

In multiphase fermentations droplets of immiscible product and/or solvent can interact with gas bubbles affecting the oxygen transfer mechanisms (Figure 1). Droplet-bubble interactions are influenced by operational parameters (e.g. agitation, aeration rate, and oil concentration) and physical properties like the interfacial tension (σ) between the gas, oil, and water phases. Interfacial tension is responsible for the spreadability of the oil on the bubble surface and determines the oil-gas contact angle (θ) [28]:

$$\cos(\theta) = \left((\sigma_{wa})^2 - (\sigma_{ow})^2 - (\sigma_{oa})^2\right) / (2 \cdot \sigma_{ow} \cdot \sigma_{oa}) \quad (2)$$

Droplets can fully spread on the bubble surface forming a thin oil layer (θ=0°). Rols and Goma [20] proposed that the liquid mass transfer coefficient across the gas-oil-water (g/o/w) interface (k_{ow}) is lower than the one across gas-water (k_w) due to the additional oil resistance transfer layer (Figure 1B). The resulting k_{ow} depends on the transfer coefficients of the aqueous (k_w) and oil phase (k_o) and the oxygen partition coefficient between oil and water phase ($m_{o/w}$).

$$\frac{1}{k_{o/w}} = \frac{1}{k_w} + \frac{1}{m_{o/w} \cdot k_o} \quad (3)$$

Droplets can also partially cover the bubble forming beads on its surface (θ <90°). Some authors [29] consider a degree of oil coverage (β) to account for the ration between gas surface covered by oil beads ($a_{g/o}$) and the total gas area available (a_g).

$$\beta = \frac{a_{g/o}}{a_g} \quad (4)$$

The gas surface in contact with water ($a_{g/w}$) is therefore:

$$a_{g/w} = (1 - \beta) \cdot a_g \quad (5)$$

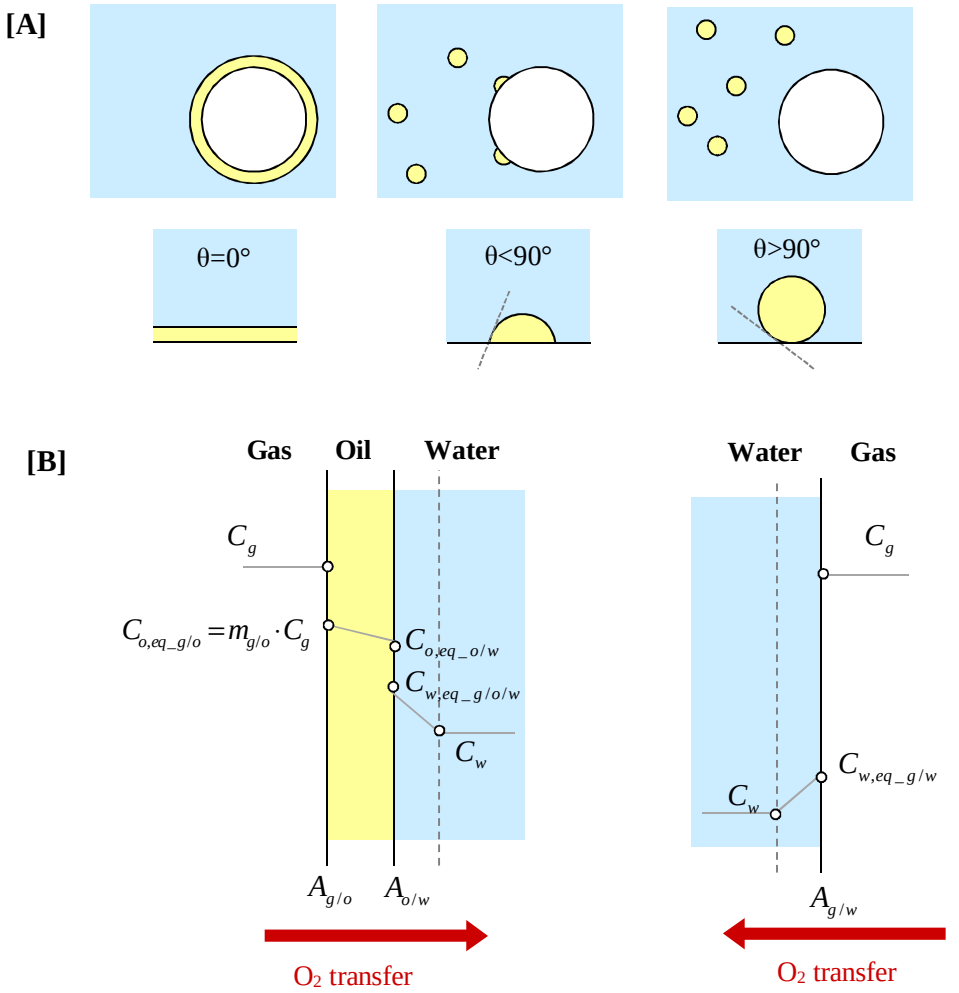

Figure 1 [A] three different scenarios for interactions between gas-oil-water (g/o/w) phases. Depending on the g/o contact angle (θ), oil droplets can spread on the bubble surface forming a thin layer θ=0°, partially spread on the bubble surface forming beads θ<90°; mostly remain dispersed in the aqueous medium θ>90°. [B] Depending on the interaction, oxygen can be transferred from the bubble to the aqueous medium via oil phase (left) or directly across the bubble surface (right). Due to the higher solubility of oxygen in hydrocarbons, the solubility of oxygen in water can be increased in the presence of oil.

Oil droplets rich in oxygen can be sheared from the bubble and dispersed again in the aqueous phase becoming an additional source of oxygen transfer area ($\alpha \cdot a_{o/w}$). This is the case if a gas bubble leaves the liquid system [20], or if the oil layer covering the bubble becomes too thick and is sheared-off due to the mixing [30]. Even if droplets remain mostly dispersed in the aqueous medium (θ >90°) (Figure 1A), they can still play a role in the oxygen transfer. Droplets are typically 100 times smaller than the bubbles [31]. They can enter the stagnant aqueous layer around the bubble which is rich in oxygen and carry it to a region poor in dissolved oxygen. This mechanism is known as shuttle effect [30, 32-34]. Some authors account for the effect of the dispersed oil droplets rich in oxygen by multiplying the available oil volumetric area ($a_{o/w}$) by an enhancement factor (α) related to the degree of mixing in the dispersed oil phase and the renewal of g/o surface [30].

$$OTR_{g/o/w} = k_{o/w} \cdot (\alpha \cdot a_{o/w}) \cdot \left(C_{w,eq} - C_w\right) \cdot V_w \tag{6}$$

This enhancement is influenced by operational parameters such as power input (usually provided via agitation and/or aeration), and oil concentration.

2.2. Characterization of oxygen transfer via $k_L a$ measurements

Due to experimental limitations to determine them separately, the parameters k_L and a are usually lumped as the volumetric mass transfer coefficient $k_L a$. When using this parameter to compare results from different studies, the following aspects must be considered:

- **Measurement method:** $k_L a$ can be measured by stationary or dynamic methods [35]. In steady-state fermentations (e.g. continuous fermentations) $k_L a$ can be determined by monitoring the concentration of oxygen dissolved in the aqueous medium (C_w) and in the gas out-flow stream ($y_{O_2}^{out}$). This method, known as stationary, can also be applied to fed-batch fermentations, if the oxygen concentration is in a pseudo-steady state ($dC_w/dt \sim 0$), which typically happens at low growth rates.

$$k_L a\left(C_{w,eq} - C_w\right)V = F_G^{in} \cdot y_{O_2}^{in} - F_G^{out} \cdot y_{O_2}^{out} \tag{7}$$

$$k_L a = \frac{F_G^{in} \cdot y_{O_2}^{in} - F_G^{out} \cdot y_{O_2}^{out}}{\left(C_{w,eq} - C_w\right)V} \tag{8}$$

When (pseudo)steady-state condition does not apply, or the concentration of oxygen in the gas-outlet cannot be determined, an alternative dynamic method can be used instead. In this method, the medium is first depleted from oxygen by sparging nitrogen. Afterwards the gas inflow is changed to air. $k_L a$ can be calculated by integrating the oxygen balance in the aqueous phase:

$$k_L a\left(C_{w,eq} - C_w\right) = \frac{dC_w}{dt} \tag{9}$$

$$k_L a = \frac{\ln \frac{C_{w,eq} - C_{w,0}}{C_{w,eq} - C_w}}{t - t_0} \tag{10}$$

As pointed out by [36], results obtained from one or other method might be contradictory, since the dynamic method does not account for interaction of cells with bubbles.

- **Calibration of dissolved oxygen probe:** The output of the dissolved oxygen probe measurement is typically given as a percentage of the oxygen saturation values in the medium.

$$C_w = DOT(\%) \cdot C_{w,eq} \tag{11}$$

Solubility of oxygen in alkanes is 10 times higher than in water (Table 2). The presence of a hydrocarbon phase can increase the oxygen concentration in the medium, and therefore it should be reported whether the calibration of the oxygen probe is performed before or after oil addition.

- **Saturation value of oxygen:** There are different definitions for the value of equilibrium concentration of oxygen in water ($C_{w,eq}$) required for calculating C_w and $k_L a$. Besides using the saturation values based on g/w equilibrium (Eq. 12), or g/o/w equilibrium (Eq. 13), some authors propose estimating a volumetric average aiming to represent an oil-water mixture [19] (Eq. 14).

$$C_{w,eq} = C_{w,eq\_g/w} = m_{g/w} \cdot C_g \tag{12}$$

$$C_{w,eq} = C_{w,eq\_g/o/w} = m_{g/o} \cdot m_{o/w} \cdot C_g \tag{13}$$

$$C_{w,eq} = C_{w,eq\_averaged} = \left(\Phi_o \cdot m_{g/o} + \left(1 - \Phi_o\right) \cdot m_{g/w}\right) \cdot C_g \tag{14}$$

3. Materials and methods

3.1. Strains and pre-culture

Pre-cultures of the wild type strain *Escherichia coli* K12 (MG1655) were prepared as indicated in [14]. Pre-cultures of the sesquiterpene-producing strain *Escherichia coli Bl21(DE3)* were cultivated in two steps. The first pre-culture was incubated for 15 hours at 34°C and 200 rpm in a 250 mL shake flask containing 50 mL of LB-medium, 0.050 g L^{-1} carbenicillin, and 0.034 g L^{-1} of chloramphenicol. The second pre-culture was inoculated with first pre-culture reaching an initial optical density of 0.2 and incubated for 8 hours at 34°C and 200 rpm in a 500 mL shake flask containing 200 mL of LB-medium, 0.050 g L^{-1} carbenicillin, 0.034 g L^{-1} of chloramphenicol, and 0.0045 g L^{-1} of Thiamine·HCl.

3.2. Fermentation medium

100 g of *E. coli* K12 pre-culture was inoculated in 900 g of sterile fermentation medium prepared as indicated in [14].

100 g of recombinant *E. coli* Bl21(DE3) was inoculated in 2000 g of medium sterilized by filtration (0.2 μm). The composition of this medium was: 4.2 g kg^{-1} KH_2PO_4, 1.68 g kg^{-1} K_2HPO_4, 2 g kg^{-1} $(NH_4)_2SO_4$, 1.7 g kg^{-1} citric acid, 0.0084 EDTA, 5 g kg^{-1} yeast extract, 30 g kg^{-1} glycerol, 0.30 g kg^{-1} trace metal solution (of composition: 10 g kg^{-1} Fe(III)citrate, 0.25 g kg^{-1} $CoCl_2 \cdot 6H_2O$, 1.5 g kg^{-1} $MnCl_2 \cdot 4H_2O$, 0.118 g kg^{-1} $CuCl_2 \cdot 2H_2O$, 0.3 g kg^{-1} H_3BO_3, 0.25 g kg^{-1} $Na_2MoO_4 \cdot 2H_2O$, and 1.3 g kg^{-1} $Zn(CHCOO)_2 \cdot 2H_2O$), 1.23 g kg^{-1} $MgSO4 \cdot 7H_2O$ (1M aqueous solution), 0.1 g kg^{-1} carbenicillin, 0.017 g kg^{-1} Chloramphenicol, and 0.0045 g kg^{-1} Thiamine·HCl. Prior to inoculation and addition of antibiotics and vitamine, pH was adjusted to 7.0 with NaOH 4M.

3.3. Equipment set up

The experimental set up for the experiments F01 and F02 with wild type *E. coli* K12 (Table 2) consisted of a 2 L jacketed reactor (Applikon, The Netherlands), working in fed-batch mode under glucose limitation. Fermentations were performed at an aeration rate of 1.5 nL min^{-1} controlled by a mass flow controller (Brooks, United states), and stirred with a 6-

blade Rushton impeller of 45 mm diameter at speed of 1000 rpm. The temperature was set to 35°C and the pH was maintained at 6.5 by adding acid (2M H_2SO_4) and base (NH_4OH 25%v/v). Fermentation settings were controlled by a ADI-1030 controller (Applikon, The Netherlands). Foam was controlled by manual addition of an aqueous solution of 10% v/v antifoam Erol - DF7911K (PMC Ouvrie, France) up to a maximum of 30 g. After approximately 9 h of fermentation, glucose was consumed, and the DOT increased indicating the end of the batch phase. At that point, a glucose solution containing 700 g L^{-1} $C_6H_{12}O_6 \cdot 1H_2O$, 20 g L^{-1} $MgSO_4 \cdot 7H_2O$, 0.045 g L^{-1} Thiamine·HCl, and the same trace metal concentration as in the batch medium, was fed into the bioreactor using a Masterflex peristaltic pump (Cole Parmer, United States). During the analyzed period (29-49 h) the feed rate was kept constant at a rate of 6.5 ± 0.4 g h^{-1}.

The experimental set up for the experiments F03 and F04 with recombinant *E. coli* Bl21(DE3) consisted of a 7 L jacketed reactor (Applikon, The Netherlands), working in fed-batch mode under glycerol limitation. Fermentations were performed at an aeration rate of 2.0 nL min^{-1} controlled by a mass flow controller (Brooks, United states), and stirred with a 6 - blade Rushton impeller of 84 mm diameter at speed of 500 rpm during the batch phase (0 - 19h), 750 rpm before induction (19 - 22 h), and 600 rpm afterwards. The temperature was set to 30°C at the beginning of the fermentation and lowered to 25°C after 22 hours, just before induction; the pH was maintained at 7.0 by adding acid (3M H_3PO_4) and base (5M NH_4OH). Fermentation data acquisition and control were carried out by a DCU system and a computer system running Multi Fermentor Control System /Windows.

Foam was controlled by manual addition of an aqueous solution of 10% v/v antifoam Erol-DF7911K (PMC Ouvrie, France). After approximately 19 h of fermentation, glycerol was consumed, and the DOT increased indicating the end of the batch phase. At that point, a glycerol solution containing 0.013 g kg^{-1} EDTA, 233.33 g kg^{-1} glycerol, 10 g kg^{-1} of trace metal solution (with same composition as the one used to prepare batch medium), and 12.3 g kg^{-1} $MgSO4 \cdot 7H_2O$ (1M aqueous solution), was fed into the bioreactor using a Masterflex peristaltic pump (Cole Parmer, United States) at a value of 36.2 ±1.1 g h^{-1}.

At a fermentation age of 22 h the temperature was lowered to 25°C and cells were induced with 10 mL of aqueous solution containing 0.06 g of IPTG. At 25 h dodecane was added to the medium (153 g dodecane in F03; 190 g dodecane in F04). Large volumes of fermentation broth were drawn from the reactor to allow for the evaluation of different cell and

oil concentration under the same range of volumetric power input. In F03 461g of broth was removed at a fermentation age of 65h (start of period 2), and 717 g was removed at a fermentation age of 95h (start of period 3). In F04 822g was removed at a fermentation age of 63h (start of period 2) (Table 2).

3.4. Analyses

1.5 mL vials containing 1mL of broth were weighed and set in a centrifuge (Heraeus, Biofuge Pico) at 13000 rpm for 10 min. In samples containing a layer of oil, a cotton tip was used to remove the oil and clean the vial walls. Afterwards, supernatant was discarded. The vials containing the cell pellet were dried in an oven (Heraeus instruments) at 70 °C for 48 h and weighed to determine the cell concentration in the reactor (as cell dry weight).

DOT was measured by a dissolved oxygen sensor (Applikon, The Netherlands; Mettler Toledo, The Netherlands). The probe was calibrated with nitrogen (0% DOT) and air (100% DOT) before oil addition in F01, F03, and F04, and in the presence of hexadecane in F02. The CO_2 and O_2 concentrations in the bioreactor off-gas and in pressurized air were analyzed by a Rosemount NGA-2000 gas analyzer (Fisher Rosemount, Germany). pH and temperature were measured by sensors (Applikon, The Netherlands). Feed rate was continuously monitored with a balance (Mettler Toledo, The Netherlands). DOT, concentrations of CO_2 and O_2 in the off gas and in pressurized air, pH, temperature and feed weight were continuously recorded with a MFCS/Win 2.1 software (Sartorius Stedim Biotech S.A., France).

$k_L a$ was determined by the stationary method using DOT and off-gas O_2 concentration data (Eq. 8). Based on the DO-probe calibration method indicated above, $C_{w,eq\_g/w}$ was used as solubility value in F01, F03, and F04 (Eq. 12), and $C_{w,eq\_g/o/w}$ was used in F02 (Eq. 13).

3.5. Kinetic model for estimation of cell concentration and oxygen consumption rate

Cell growth in the fed-batch phase was predicted using the kinetic growth model for *E. coli* K12 described in [14]:

$$R_X = dM_X(t)/dt = \mu(t)\cdot M_X(t) = F_S - m_S \cdot M_X(t)\cdot Y_{X/S} \qquad (15)$$

In a similar way, the oxygen consumption rate was estimated using q_{O2}^{max} = 15.6 mmolO_2·g^{-1}·h^{-1} , m_{O_2}=0.03 molO_2·/C-molX^{-1}·h^{-1} and μ^{max}=0.71 h^{-1} based on [37] and [38].

$$R_{O2}(t) = q_{O2}^{\max} \cdot \mu(t) \cdot M_X(t) + m_{O_2} \cdot M_X(t) \quad (16)$$

3.6. Estimation of droplet and bubble surface

Oil and gas specific areas (a_i) were determined from their respective volumetric fractions (ϕ_i) and the particle diameter (d_i), assuming a monodisperse droplet population.

$$a_i = \frac{6}{d_i} \cdot \left(\frac{\phi_i}{1-\phi_i} \right) \quad (17)$$

The gas volumetric fraction (also known as gas hold-up) was estimated, as suggested by [39], from the volumetric power input (P/V) and the superficial gas velocity (v_{GS}):

$$\phi_g = 0.13 \cdot (P/V)^{1/3} \cdot v_{GS}^{2/3} \quad (18)$$

With the power input for an aerated stirred vessel estimated as [40]:

$$P = N_p \cdot \rho_w \cdot N^3 \cdot D_{imp}^{5} \cdot \left(1 - 9.9 \cdot \Phi_{in} \cdot \frac{N^{0.25}}{D_{imp}^{2}} \right) \quad (19)$$

Droplet diameter estimations in literature are typically based in equilibrium between rates of droplet coalescence and break up [41]. In a high cell density fermentation, it could be expected that the equilibrium is shifted towards the small size droplets due to the presence of SACs. For this reason, the oil droplet size was approximated to the minimum stable droplet diameter as already described in [14]. Also bubble correlations based in oil/water systems predict larger bubbles sizes than those reported by other authors working with multiphase fermentation broths [31, 42]. Therefore, the specific volumetric gas area was estimated from the experimental $k_L a$ of the base case without oil F01 (Eq. 8, Eq. 20) and reported values of k_w (Table 1). The bubble diameter was derived afterwards from (Eq. 17).

$$a = \frac{k_L a}{k_w} \quad (20)$$

3.7. Mass transfer model for dissolved oxygen tension (DOT) profile and $k_L a$

Based on the model by [29], the overall oxygen transfer rate from gas bubbles to aqueous phase (OTR) was assumed to be the sum of oxygen transferred via the oil phase ($OTR_{g/o/w}$), and via the bubble surface non-covered by oil ($OTR_{g/w}$).

$$OTR = k_{o/w} \cdot (\alpha \cdot a_{o/w}) \cdot \left(C_{w,eq} - C_w\right) \cdot V_w + k_{g/w} \cdot (1-\beta) \cdot a_g \cdot \left(C_{w,eq\_g/w} - C_w\right) \cdot V_w \quad (21)$$

The overall g/o/w mass transfer coefficient ($k_{o/w}$) is estimated from the individual mass transfer coefficients of oil and water (Eq. 3) (Table 1). To account for the effect of the dispersed oil droplets as oxygen vectors, the available oil volumetric area ($a_{o/w}$) is multiplied by by an enhancement factor (α) (Eq. 6). In the absence of oil α =0, while in the case that oxygen would be transferred across a thin oil layer covering the total bubble area $\alpha = a_g / a_{o/w}$.

The second right-hand term of Eq. 21 represents the oxygen transferred via g/w across the bubble surface that is not covered by oil. The overall g/w mass transfer coefficient ($k_{g/w}$) is equivalent to the individual mass transfer coefficients in water k_w (Table 1). A coverage factor (β) accounts for the ratio of gas area covered by oil beads ($a_{g/o}$) and the total gas area available (Eq. 4).

The mass transfer coefficients, and equilibrium solubilities required for Eq. 21 were taken from literature data for hexadecane, dodecane and sesquiterpenes (Table 1). The oxygen concentration in water (C_w) was calculated from the DOT experimental data (Eq. 11).

Assuming a pseudo steady state ($OTR \sim R_{O2}$), the DOT profile in the fermentation can be derived from Eq. 11, Eq. 16 and Eq. 21:

$$C_w = \frac{k_{o/w} \cdot (\alpha \cdot a_o) \cdot C_{w,eq} + k_{g/w} \cdot (1-\beta) \cdot a_g \cdot C_{w,eq} - R_{O2}(t)/V_w}{k_{o/w} \cdot (\alpha \cdot a_o) + k_{g/w} \cdot (1-\beta) \cdot a_g} \quad (22)$$

Finally, $k_L a$ was estimated from Eq. 22, Eq. 8, and Eq. 16.

4. Results

The stationary method (Eq. 8) was used to determine $k_L a$ values in fermentations of *E. coli* K12 without oil (F01) and in the presence of 7.5±0.2 %v/v hexadecane (F02) (Table 3). The maximum solubility of oxygen in water was estimated as 0.23 mol-O2 m^{-3}-water in F01 (Eq. 12) and as 0.36 mol-O2/m^3-water in F02 (Eq. 13) (Table 1). In agreement, F02 presented a higher DOT (%) than the base case F01 (Figure 2) and $k_L a$ was also significantly higher (p - value t-test <0.05), resulting in a ca. 12% improvement. Note that an incorrect $C_{w,eq}$ estimate would erroneously suggest improvements up to 72% (Table 3).

Experiment F01 allowed to estimate the bubble diameter as 0.15 mm (Eq. 17, Eq. 20) from the experimental $k_L a$ (Table 3) and a reported k_w of 0.108 m·h^{-1} (Table 1). This diameter was used as reference for all the calculations in this work, including those corresponding to fermentations in the presence of oil.

Table 3 $k_L a$ values for different assumptions on oxygen solubility. Experimental values were determined by the static method in fed-batch fermentations of wild type E. coli K12 without oil (F01) and in the presence of 7.5±0.2% v/v hexadecane (F02). The parameters used to model $k_L a$ values were: α=0, β=0, and d_b =1.5 mm in F01; α=0.3, β=0.5, and d_b =1.5 mm in F02. For F02, $k_L a$ calculations with varying $C_{w,eq}$ estimates (Eq. 17 - Eq. 18) have been included for comparison.

		$C_{w,eq}$ (mol-$O_2 \cdot m^{-3}$-water)	$k_L a$ experimental (s^{-1})	$k_L a$ model (s^{-1})
F01	$C_{w,eq\_g/w}$	0.23	$8.9\times10^2 \pm 0.3\times10^2$	$9.1\times10^2 \pm 0.3\times10^2$
	$C_{w,eq\_g/o/w}$	0.36	$10.0\times10^2 \pm 0.4\times10^2$	$9.9\times10^2 \pm 0.4\times10^2$
F02	$C_{w,eq\_g/w}$	0.23	$15.3\times10^2 \pm 0.5\times10^2$	$15.1\times10^2 \pm 0.2\times10^2$
	$C_{w,eq\_averaged}$	0.25(*)	$14.6\times10^2 \pm 0.5\times10^2$	$14.3\times10^2 \pm 0.2\times10^2$

(*) Estimation based on 10% v/v oil

DOT (Eq. 22) and $k_L a$ (Eq. 8) profiles of F01 and F02 were modeled combining cell growth kinetics (Eq. 15 and Eq. 16) and oxygen transfer parameters (Eq. 21). In the base case without oil (F01), the oil enhancement factor (α) accounting for the role of dispersed droplets in oxygen transfer, and bubble coverage factor (β) accounting for the fraction of bubble surface covered by oil, were kept to zero. Although the model described the experimental DOT profile of F01 with a R^2=0.72 (Figure 2A), the estimated $k_L a$ of 9.1×10^2 s^{-1} $\pm0.3\times10^2$ s^{-1} was statistically the same as the experimental one (p-value t-test >0.15) (Table 3). The low correlation value (R^2<0.75) is rather a consequence of the little variation in DOT along time than a meaningful deviation from the experimental data.

In fermentation F02 a field of model DOT curves for different values of α and β was generated (Figure 2B**).** The impact of the degree of bubble surface coverage by oil (β) in the DOT was relevant at low values of oil enhancement factor (α) (curve α=0.2, β=1 versus α=0.2, β=0.5), but was negligible at high α values (curve α=0.6, β=1 versus α=0.6, β=0.5). By comparing the experimental DOT to model curves, a mixed transfer route in which bubbles are only partially covered by oil (β=0.5), an oil enhancement factor α= a_g / a_o (approximately 0.3) was identified as most probable scenario. This mixed route where both dispersed oil droplets, and oil covering part of the available bubble surface play a role in the oxygen transfer described the experimental data with an R^2 of 0,74 (Figure 2B). Similarly, as in F01, the estimated $k_L a$ (9.9×10^2 s^{-1} $\pm0.4\times10^2$ s^{-1}) was statistically the same as the experimental one (p-value t - test >0.20). Both experimental and model $k_L a$ slightly decreased along the fermentation for the studied period. Such decrease has formerly been linked to a reduction in volumetric power input [30] which happens in this case due to the dilution of the medium during the fed-batch period. In this fermentation, however, the change in experimental $k_L a$ with volumetric power input was steeper than model curves at different α values (Figure 3A), and steeper than reported values in literature for hexadecane-water system [18].

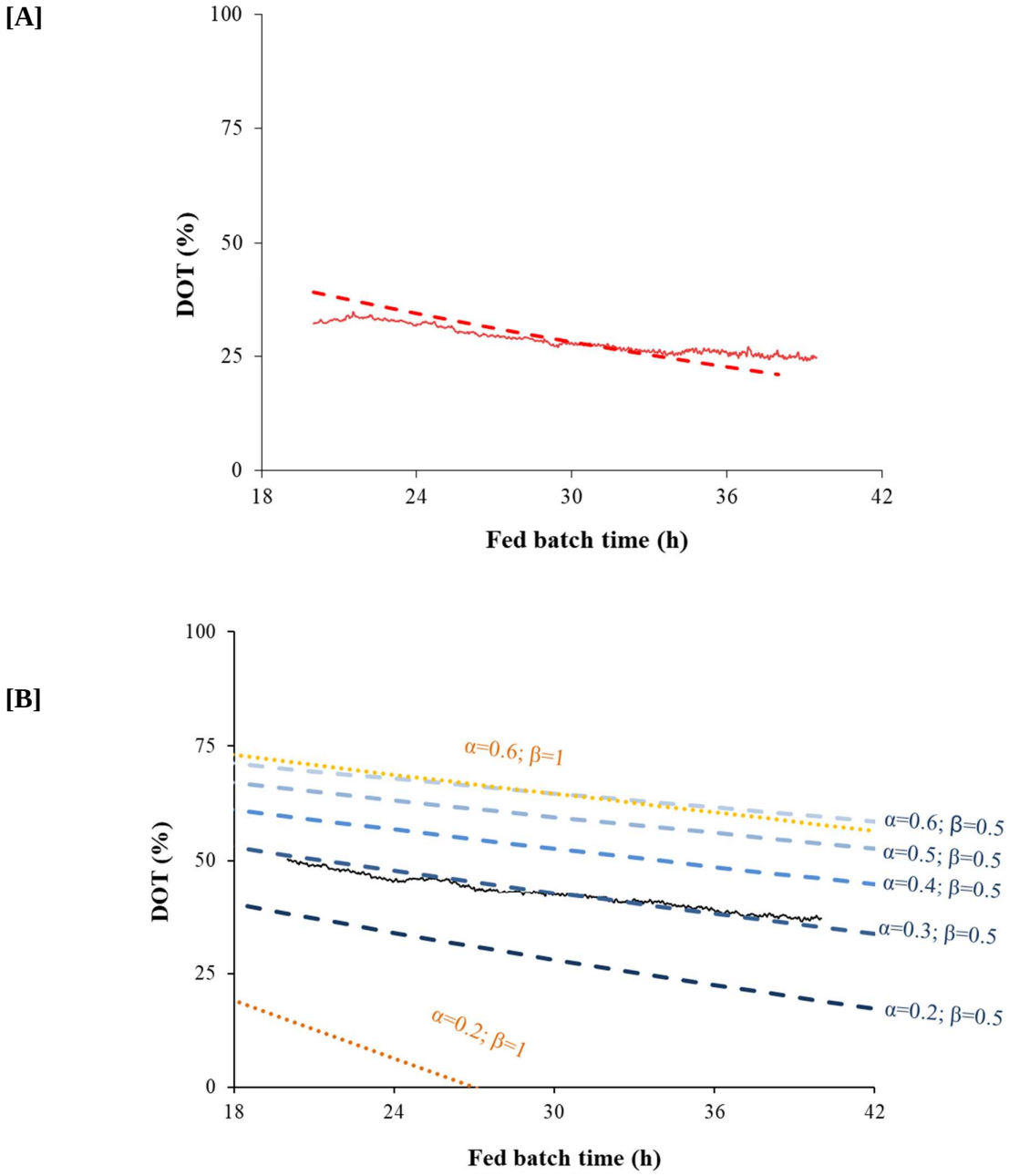

Figure 2. [A] Comparison of experimental DOT profile in F01 without oil to a modelled DOT profile (α= 0; β=0; R^2=0.72). [B] Comparison of experimental DOT profile in F02 containing 7.5% v/v of hexadecane to model trends based on different oil enhancement (α) and bubble coverage (β) values (R^2=0.74).

[A]

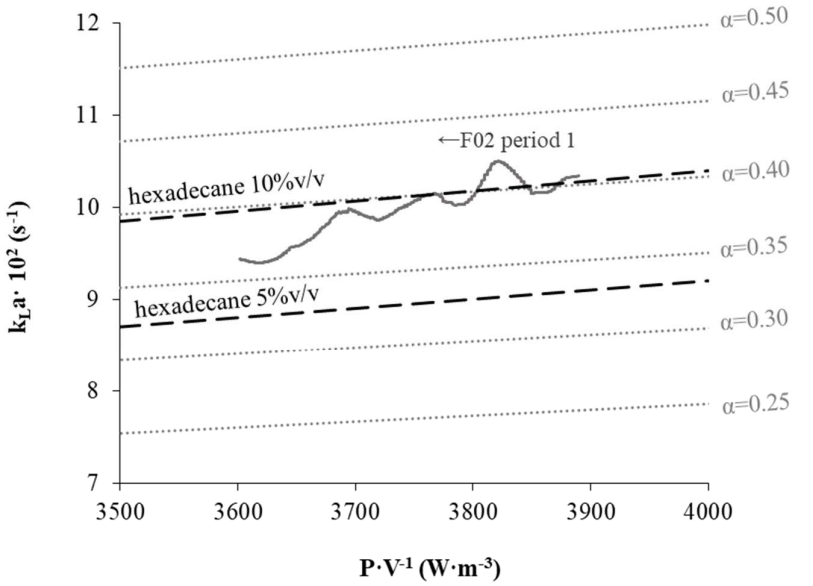
α=0.50
α=0.45
α=0.40
α=0.35
α=0.30
α=0.25
←F02 period 1
hexadecane 10%v/v
hexadecane 5%v/v
$k_La \cdot 10^2$ (s^{-1})
$P \cdot V^{-1}$ ($W \cdot m^{-3}$)

[B]

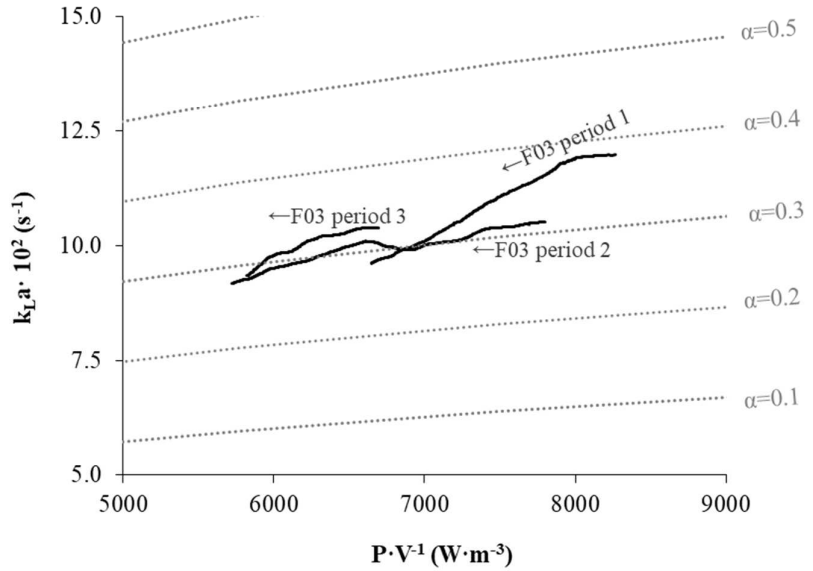
α=0.5
α=0.4
α=0.3
α=0.2
α=0.1
←F03 period 1
←F03 period 3
←F03 period 2
$k_La \cdot 10^2$ (s^{-1})
$P \cdot V^{-1}$ ($W \cdot m^{-3}$)

[C]

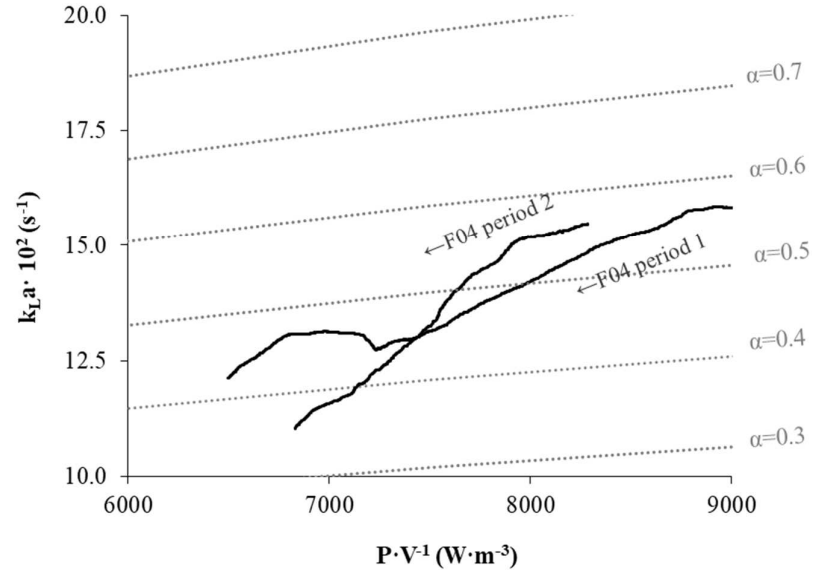
α=0.7
α=0.6
α=0.5
α=0.4
α=0.3
←F04 period 2
←F04 period 1
$k_La \cdot 10^2$ (s^{-1})
$P \cdot V^{-1}$ ($W \cdot m^{-3}$)

Figure 3. Experimental $k_L a$ values corresponding to different volumetric power input. Dotted lines represent modelled results at a bubble coverage of β=0.5 and varying values of oil enhancement (α). [A] Fermentation with *E. coli* K12 containing: 7.5% v/v hexadecane (F02); power input decreased due to increase in volume during the fed batch period. Arrows indicate direction of change. Dashed lines correspond to literature values for dispersion of hexadecane in water at 10%v/v and 5%v/v oil concentration [18]**. [B] Fermentation with sesquiterpene-producing *E. coli* containing 4% to 6% v/v dodecane (F03). [C] Fermentation with sesquiterpene-producing *E. coli* containing 6% to 9% v/v dodecane (F04).**

The variability of $k_L a$ with volumetric power input was higher in F03 and F04 where longer fermentation times were studied. During the first period of fermentation F03 (Figure **3**B), the estimated α value decreased from 0.4 to 0.3 for a decrease in volumetric power input from 8500 $W \cdot m^{-3}$ to 6500 $W \cdot m^{-3}$. However, when the volumetric power input was increased again to about 8000 $W \cdot m^{-3}$ (start of period 2) the estimated α remained almost constant at at level of 0.3 while decreasing the volumetric power input until 6000 $W \cdot m^{-3}$. This behaviour took place again during the last period of the fermentation. In the case of fermentation F04, a decrease in α from 0.55 to about 0.35 was observed in period 1 while decreasing the power input from 9000 $W \cdot m^{-3}$ to 6500 $W \cdot m^{-3}$ (Figure 3C). However, in period 2, towards the end of the fermentation, below ca. 7250 $W \cdot m^{-3}$, there was a more pronounced decrease than during period 1.

Data reported in literature measured by the $k_L a$ dynamic method [15, 18] suggest a decrease of $k_L a$ with increasing cell concentration, and an enhancement of $k_L a$ when increasing oil concentration. However, in this study $k_L a \cdot (P \cdot V^{1})^{-1}$ was not significantly correlated to cell concentration (Pearson coefficients of F01 to F04 were +0.63, -0.63, +0.66, and +0.06, respectively); neither to oil fraction (Figure 4). Consequently, the observed decrease in α value could not be attributed to these variables.

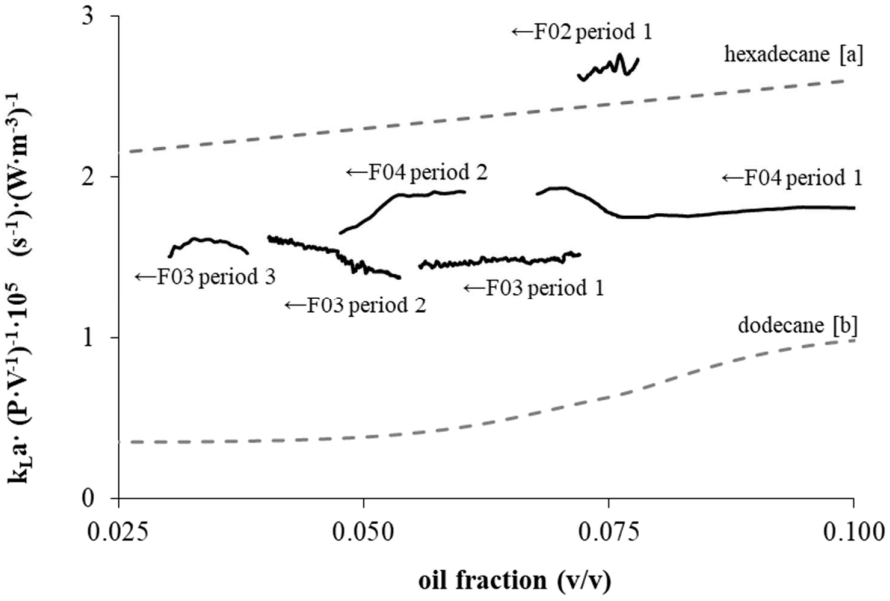

Figure 4. Experimental and literature k_La values corresponding to varying oil fractions. Continuous lines correspond to experimental data (Table 2). Dashed data correspond to literature values for (a) hexadecane in water [18] **at 4000 ($W \cdot m^{-3}$) and (b) dodecane in suspension of quiescent cells** [15] **at 963 ($W \cdot m^{-3}$). For comparison purposes, k_La values have been normalized to account for the effect of power input. Oil fraction in F02 to F04 changed due to dilution of medium during the fed batch period. Arrows indicate direction of change. While increasing values of k_La with oil fraction have been reported in literature (Pearson coefficient >0.95), experimental $k_La \cdot (P \cdot V^{1})^{-1}$ in this work was not significantly correlated to oil concentration (Pearson coefficients of F02 to F04 were +0.82, -0.64, -0.07).**

5. Discussion

In multiphase fermentations many transfer routes of oxygen are possible and determine the estimated oxygen solubility $C_{w,eq}$. Whether the presence of oil results in a significant enhancement in oxygen transfer largely depends on the dominant transport route. In order to properly estimate such enhancement from an experimental DOT profile, one must know whether DOT probe calibration was performed in presence or absence of oil (Eq. 11). The lack of experimental details regarding DOT probe calibration and assumed transfer route (and hence $C_{w,eq}$ value) may explain the contradictory $k_L a$ results reported in literature so far [16, 21]. In our experimental set-up, the presence of oil in F02 lead to an increase in $k_L a$ of ca. 12% compared to a similar fermentation without oil (F01).

Furthermore, $k_L a$ and DOT profiles were described by a model based on a combined g/w and g/o/w oxygen transfer route in which bubbles partially covered by oil and dispersed oil droplets would contribute to the transfer of oxygen. This model implies that any enhancement in oxygen transfer could be limited by the availability of oil area. In the specific case of sesquiterpene fermentations, a contact angle $\theta = 56°$ and droplet sizes between 0.050 mm to 0.200 mm could be expected [10]. Addition of solvents like dodecane might lower g/o contact angles ($\theta = 34°$), improving oxygen transfer by increasing the degree of bubble coverage (β). However, this effect would be cancelled by the presence of SACs in the fermentation broth, since those can lower the o/w interfacial tension to about 20 mN m^{-1} [43, 44] potentially increasing g/o contact angles (Eq. 2). On the other hand, the stabilization of o/w interface by SACs would reduce droplet-droplet coalescence and droplet-bubble interactions, and thus the degree of mixing within the dispersed oil phase and the renewal of the g/o surface, resulting in a lower oil enhancement factor (α) [4, 5, 14, 30]. In this work, all fermentations displayed decreasing α values along the fermentation age, which was not correlated to neither an increase in cell concentration nor a decrease in oil fraction or power input due to fed-batch operation.

6. Concluding remarks

This study highlights how sesquiterpene products and/or organic solvents used for product extraction can affect oxygen transfer in a fermentation by enhancing $k_L a$. Proper quantification of this enhancement, however, is subjected to the dominant oxygen transfer

route. Experimental $k_L a$ measurements by the stationary method supported by a mechanistic mathematical model indicate that in this work a combined g/w and g/o/w oxygen transfer route takes place. In this combined route, both air bubbles partially covered by oil and dispersed oil droplets contribute to the transfer of oxygen from the gas phase. Such contribution, however, decreases with fermentation age likely due to organic phase stabilization in the presence of SACs.

This work has thus provided, for the first time, evidence of the impact of organic phase emulsification in the transfer of oxygen in multiphase fermentations. Considering that sesquiterpene fermentations are known to lead to organic phase emulsification [5], oxygen transfer enhancement strategies such as the use of solvents as oxygen vectors are not expected to be effective [11]. On the other hand, any improvements made in reducing organic phase emulsification at microorganism, feedstock and process technology levels, will result in enhanced oxygen transfer while also improving organic phase recovery.

Acknowledgements

This work was carried out within the BE-Basic R&D Program, which was granted a FES subsidy from the Dutch Ministry of Economic affairs.

Conflict of interest

The authors declare no financial or commercial conflict of interest.

Nomenclature

Roman

a	volumetric transfer area
a_g	volumetric gas area
$a_{g/o}$	volumetric gas surface covered by oil beads
$a_{g/w}$	volumetric gas surface in contact with water
$A_{g/o}$	Interfacial area oil-gas
$A_{o/w}$	Interfacial area oil-water
$A_{g/w}$	Interfacial area gas-water
C_g	Oxygen concentration in gas
C_w	Oxygen concentration in water
$C_{w,eq}$	Oxygen solubility in water
$C_{o,eq\_g/o}$	oxygen solubility from gas-oil equilibrium
$C_{w,eq\_g/w}$	oxygen solubility from gas-water equilibrium
$C_{w,eq\_g/o/w}$	oxygen solubility from gas-oil-water equilibrium
d_i	particle diameter
D_{imp}	impellor diameter
F_s	Feed flow
F_G	Gas flow
k_L	liquid mass transfer coefficient
$k_L a$	volumetric mass transfer coefficient
k_o	mass transfer coefficient oil phase
k_w	mass transfer coefficient water phase
$k_{o/w}$	mass transfer coefficient across oil and water
$m_{o/w}$	oil-water partition coefficient
$m_{g/w}$	gas-water partition coefficient
$m_{g/o}$	gas-oil partition coefficient

m_s maintenance coefficient for substrate

m_{O_2} maintenance coefficient for oxygen

M_X Cell mass in the reactor

N agitation speed

N_p power number

OTR Oxygen transfer rate

$OTR_{g/o/w}$ Oxygen transfer rate from gas to water via the oil phase

$OTR_{g/w}$ Oxygen transfer rate from gas to water via the bubble surface non-covered by oil

P power input

q_{O2}^{max} maximum specific oxygen consumption rate

R_{O2} Oxygen consumption rate

R_X Cell growth rate

SACs surface active components

v_{GS} superficial gas velocity

V System volume

V_w Water volume

$y_{O_2}^{out}$ concentration of oxygen dissolved in the gas out-flow stream

$Y_{X/S}$ Yield of cells on substrate

Greek

α enhancement factor

β degree of coverage

ϕ_g volumetric fraction of gas

Φ_{IN} gas in-flow

Φ_o mass fraction of oil in o/w mixture

μ specific cell growth rate

μ^{max} maximum specific growth rate

ρ_w water density

σ Interfacial tension

θ oil-gas contact angle

References

1. Schirmer, A., Rude, M.A., Li, X., Popova, E., et al., *Microbial biosynthesis of alkanes.* Science, 2010. **329**(5991): p. 559-62.

2. Tsuruta, H., Paddon, C.J., Eng, D., Lenihan, J.R., et al., *High-level production of amorpha-4,11-diene, a precursor of the antimalarial agent artemisinin, in Escherichia coli.* PLoS One, 2009. **4**(2): p. e4489.

3. Westfall, P.J., Pitera, D.J., Lenihan, J.R., Eng, D., et al., *Production of amorphadiene in yeast, and its conversion to dihydroartemisinic acid, precursor to the antimalarial agent artemisinin.* Proc Natl Acad Sci U S A, 2012. **109**(3): p. e111-8.

4. Heeres, A.S., Schroën, K., Heijnen, J.J., Wielen, L.A.M.v.d., et al., *Fermentation broth components influence droplet coalescence and hinder advanced biofuel recovery during fermentation.* Biotechnology Journal, 2015. **10**(8): p. 1206-1215.

5. Tabur, P. and Dorin, G.*Method for purifying bio-organic compounds from fermentation broth containing surfactants by temperature-induced phase inversion.* 2012. WO2012024186

6. Lindahl, A.L., Olsson, M.E., Mercke, P., Tollbom, O., et al., *Production of the artemisinin precursor amorpha-4,11-diene by engineered Saccharomyces cerevisiae.* Biotechnol Lett, 2006. **28**(8): p. 571-80.

7. Newman, J.D., Marshall, J., Chang, M., Nowroozi, F., et al., *High-level production of amorpha-4,11-diene in a two-phase partitioning bioreactor of metabolically engineered Escherichia coli.* Biotechnol Bioeng, 2006. **95**(4): p. 684-91.

8. Scalcinati, G., Knuf, C., Partow, S., Chen, Y., et al., *Dynamic control of gene expression in Saccharomyces cerevisiae engineered for the production of plant sesquitepene alpha-santalene in a fed-batch mode.* Metab Eng, 2012. **14**(2): p. 91-103.

9. Tippmann, S., Scalcinati, G., Siewers, V., and Nielsen, J., *Production of farnesene and santalene by Saccharomyces cerevisiae using fed-batch cultivations with RQ-controlled feed.* Biotechnol Bioeng, 2016. **113**(1): p. 72-81.

10. Pedraza-de la Cuesta, S., Knopper, L., van der Wielen, L.A.M., and Cuellar, M.C., *Techno-economic assessment of the use of solvents in the scale-up of microbial sesquiterpene production for fuels and fine chemicals.* Biofuels, Bioprod. Bioref., 2019. **13**: p. 140-152.

11. Janssen, A.C.J.M., Kierkels, J.G.T., and Lentzen, G.F.*Two-phase fermentation process for the production of an organic compound* ISOBIONICS B.V. 2015. WO2015002528

12. Garcia-Ochoa, F. and Gomez, E., *Bioreactor scale-up and oxygen transfer rate in microbial processes: an overview.* Biotechnol Adv, 2009. **27**(2): p. 153-76.

13. Meadows, A.L., Hawkins, K.M., Tsegaye, Y., Antipov, E., et al., *Rewriting yeast central carbon metabolism for industrial isoprenoid production.* Nature, 2016. **537**(7622): p. 694-697.

14. Pedraza-de la Cuesta, S., Keijzers, L., van der Wielen, L.A.M., and Cuellar, M.C., *Integration of Gas Enhanced Oil Recovery in Multiphase Fermentations for the Microbial Production of Fuels and Chemicals.* Biotechnol J, 2018. **13**(4): p. e1700478.

15. Cascaval, D., Galaction, A.-I., Folescu, E., and Turnea, M., *Comparative study on the effects of n-dodecane addition on oxygen transfer in stirred bioreactors for simulated, bacterial and yeasts broths.* Biochemical Engineering Journal, 2006. **31**(1): p. 56-66.

16. Clarke, K.G. and Correia, L.D.C., *Oxygen transfer in hydrocarbon–aqueous dispersions and its applicability to alkane bioprocesses: A review.* Biochemical Engineering Journal, 2008. **39**(3): p. 405-429.

17. Garcia-Ochoa, F., Gomez, E., Santos, V.E., and Merchuk, J.C., *Oxygen uptake rate in microbial processes: An overview.* Biochemical Engineering Journal, 2010. **49**(3): p. 289-307.

18. Hassan, I.T.M. and Robinson, C.W., *Oxygen transfer in mechanically agitated aqueous systems containing dispersed hydrocarbon.* Biotechnology and Bioengineering, 1977. **19**(5): p. 661-682.

19. Ho, C.S., Ju, L.K., and Baddour, R.F., *Enhancing penicillin fermentations by increased oxygen solubility through the addition of n-hexadecane.* Biotechnology and Bioengineering, 1990. **36**(11): p. 1110-1118.

20. Rols, J.L. and Goma, G., *Enhanced oxygen transfer rates in fermentation using soybean oil-in-water dispersions.* Biotechnology Letters, 1991. **13**(1): p. 7-12.

21. Dumont, E. and Delmas, H., *Mass transfer enhancement of gas absorption in oil-in-water systems: a review.* Chemical Engineering and Processing: Process Intensification, 2003. **42**(6): p. 419-438.

22. Abraham, M.H., Chadha, H.S., Whiting, G.S., and Mitchell, R.C., *Hydrogen Bonding. 32. An Analysis of Water-Octanol and Water-Alkane Partitioning and the ⊿log P Parameter of Seiler.* Journal of Pharmaceutical Sciences, 1994. **83**(8): p. 1085-1100.

23. Sander, R., *Compilation of Henry's law constants (version 4.0) for water as solvent.* Atmos. Chem. Phys., 2015. **15**(8): p. 4399-4981.

24. Ju, L.-K. and Ho, C.S., *Oxygen diffusion coefficient and solubility in n-hexadecane.* Biotechnology and Bioengineering, 1989. **34**(9): p. 1221-1224.

25. Makranczy, J., Megyery-Balog, K., Rusz, L., and Patyi, L., *Solubility of gases in normal alkanes.* Hungarian Journal of Industrial Chemistry, 1976. **4**(2): p. 269-280.

26. Ramesh, H., Mayr, T., Hobisch, M., Borisov, S., et al., *Measurement of oxygen transfer from air into organic solvents.* J Chem Technol Biotechnol, 2016. **91**(3): p. 832-836.

27. Palmerín-Carreño, D.M., Castillo-Araiza, C.O., Rutiaga-Quiñones, O.M., Verde-Calvo, J.R., et al., *Kinetic, oxygen mass transfer and hydrodynamic studies in a three-phase stirred tank bioreactor for the bioconversion of (+)-valencene on Yarrowia lipolytica 2.2ab*. Biochemical Engineering Journal, 2016. **113**: p. 37-46.

28. Rowlinson, J.S. and Widom, B., *Three-phase equilibrium, Molecular Theory of capillarity*. 2002, Dover: Dover Publications.

29. Rols, J.L., Condoret, J.S., Fonade, C., and Goma, G., *Modeling of oxygen transfer in water through emulsified organic liquids.* Chemical Engineering Science, 1991. **46**(7): p. 1869-1873.

30. Pinho, H.J.O. and Alves, S.S., *Semi-Empirical Modeling of Gas–Liquid Mass Transfer in Gas–Liquid–Liquid Systems in Stirred Tanks.* Chemical Engineering Communications, 2016. **203**(1): p. 94-102.

31. Rols, J.L., Condoret, J.S., Fonade, C., and Goma, G., *Mechanism of enhanced oxygen transfer in fermentation using emulsified oxygen-vectors.* Biotechnol Bioeng, 1990. **35**(4): p. 427-35.

32. Brilman, D.W.F., Goldschmidt, M.J.V., Versteeg, G.F., and van Swaaij, W.P.M., *Heterogeneous mass transfer models for gas absorption in multiphase systems.* Chemical Engineering Science, 2000. **55**(15): p. 2793-2812.

33. Chawla, H., Khanna, R., Nigam, K.D.P., and Adesina, A.A., *A homogeneous model for mass transfer enhancement in gas-liquid-liquid systems.* Chemical Engineering Communications, 2008. **195**(6): p. 622-643.

34. Zhang, G.D., Cai, W.F., Xu, C.J., and Zhou, M., *A general enhancement factor model of the physical absorption of gases in multiphase systems.* Chemical Engineering Science, 2006. **61**(2): p. 558-568.

35. Petersen, E.E. and Margaritis, A., *Hydrodynamic and mass transfer characteristics of three-phase gaslift bioreactor systems.* Crit Rev Biotechnol, 2001. **21**(4): p. 233-94.

36. Keitel, G. and Onken, U., *The effect of solutes on bubble size in air-water dispersions.* Chemical Engineering Communications, 1982. **17**(1-6): p. 85-98.

37. Xu, B., Jahic, M., and Enfors, S.O., *Modeling of overflow metabolism in batch and fed-batch cultures of Escherichia coli.* Biotechnol Prog, 1999. **15**(1): p. 81-90.

38. Cuellar, M.C., Zijlmans, T.W., Straathof, A.J.J., Heijnen, J.J., et al., *Model-based evaluation of cell retention by crossflow ultrafiltration during fed-batch fermentations with Escherichia coli.* Biochemical Engineering Journal, 2009. **44**(2): p. 280-288.

39. van der Lans, R., *Gas Transfer*, in *Bioprocess Engineering Part 3 Design and scale up of bioreactors*, J.J. Heijnen, H.J. Noorman, and R.G.J.M. van der Lans, Editors. 2015, ECUST Shanghai. p. 149-189.

40. Cui, Y.Q., van der Lans, R.G.J.M., and Luyben, K.C.A.M., *Local power uptake in gas-liquid systems with single and multiple rushton turbines.* Chemical Engineering Science, 1996. **51**(11): p. 2631-2636.

41. Coulaloglou, C.A., *Dispersed phase interactions in an agitated flow vessel*, in *Ph. D.* 1975, Illinois Institute of Technology.

42. Junker, B.H., Hatton, T.A., and Wang, D.I.C., *Oxygen transfer enhancement in aqueous/perfluorocarbon fermentation systems: I. experimental observations.* Biotechnology and Bioengineering, 1990. **35**(6): p. 578-585.

43. Rodrigues, L.R., Banat, I.M., Mei, H.C., Teixeira, J.A., et al., *Interference in adhesion of bacteria and yeasts isolated from explanted voice prostheses to silicone rubber by rhamnolipid biosurfactants.* Journal of Applied Microbiology, 2006. **100**(3): p. 470-480.

44. Good, R.J. and Girifalco, L.A., *A theory for estimation of surface and interfacial energies. III. Estimation of surface energies of solids from contact angle data*. The Journal of Physical Chemistry, 1960. **64**(5): p. 561-565.

Chapter 5. Integration of Gas Enhanced Oil Recovery in multiphase fermentations for the microbial production of fuels and chemicals

Abstract

In multiphase fermentations where the product forms a second liquid phase or where solvents are added for product extraction, turbulent conditions disperse the oil phase as droplets. Surface-active components (SACs) present in the fermentation broth can stabilize the product droplets thus forming an emulsion. Breaking this emulsion increases process complexity and consequently the production cost. In previous works, it has been proposed to promote demulsification of oil/supernatant emulsions in an off-line batch bubble column operating at low gas flow rate. The aim of this study is to test the performance of this recovery method integrated to a fermentation, allowing for continuous removal of the oil phase.

A 500 mL bubble column was successfully integrated with a 2 L reactor during 24 h without affecting cell growth or cell viability. However, higher levels of surfactants and emulsion stability were measured in the integrated system compared to a base case, reducing its capacity for oil recovery. This was related to release of SACs due to cellular stress when circulating through the recovery column. Therefore, it is concluded that the gas bubble-induced oil recovery method allows for oil separation and cell recycling without compromising fermentation performance; however, tuning of the column parameters considering increased levels of SACs due to cellular stress is required for improving oil recovery.

This chapter has been published as:

Pedraza-de la Cuesta, S., Keijzers, L., van der Wielen, L.A.M., Cuellar, M.C., Integration of Gas Enhanced Oil Recovery in Multiphase Fermentations for the Microbial Production of Fuels and Chemicals. Biotechnol J, 2018.;13(4):e1700478.

1. Introduction

Recent advances in strain development have enabled the production of extracellular hydrocarbons such as alkanes and sesquiterpenes in microbial fermentations [1]. The immiscible product, with a lower density than the aqueous medium, forms an oil phase that readily separates from the fermentation broth (Figure 1A). This opens the opportunity of integrating a low-cost recovery operation such as settling or hydrocyclone into the fermentation allowing for cell recycling and process cost reduction. In reality, however, turbulent mixing conditions in the reactor and the presence of surface-active components (SACs) in the fermentation broth (e.g., salts, glycolipids, proteins, cells and cells debris) disperse the product phase forming an emulsion of small stable oil droplets (Figure 1B). Reported recovery methods at large scale require using costly surfactants and changes of temperature [2], which might compromise the purity specifications [3], increase costs, and prevent cellular recycling by affecting cell viability [4]. Although the need for a low-cost demulsification process might be more relevant in the case of applications with tight economic margins such as biofuels, the problem of recovery of microbial emulsions is not new. Solvents are widely used for product extraction in fermentations and bioconversions to enhance product recovery, avoid toxicity problems, or reduce product evaporation [5, 6]. The dispersion of solvent containing product leads to similar emulsification problems as encountered in microbial fermentations of extracellular hydrophobic hydrocarbons [7]. Technologies such as gravity settling [8], and membranes [9] have been described for organic phase recovery during the bioconversion.

Figure 1. Representation of production (left) and recovery subprocesses (right) taking place in different scenarios of multiphasic fermentations: [A] Ideal scenario if no surface active components (SACs) are present and a continuous oil layer is formed after the fermentation; [B] Scenario in which emulsification takes places preventing direct oil phase recovery after fermentation; [C] Illustration of an integration of a GEOR column using gas bubbles at mild mixing conditions to aid demulsification, while allowing for cell recycle; [D] Mild mixing conditions required for droplet separation could lead to cellular stress and release of SACs reducing recovery efficiency.

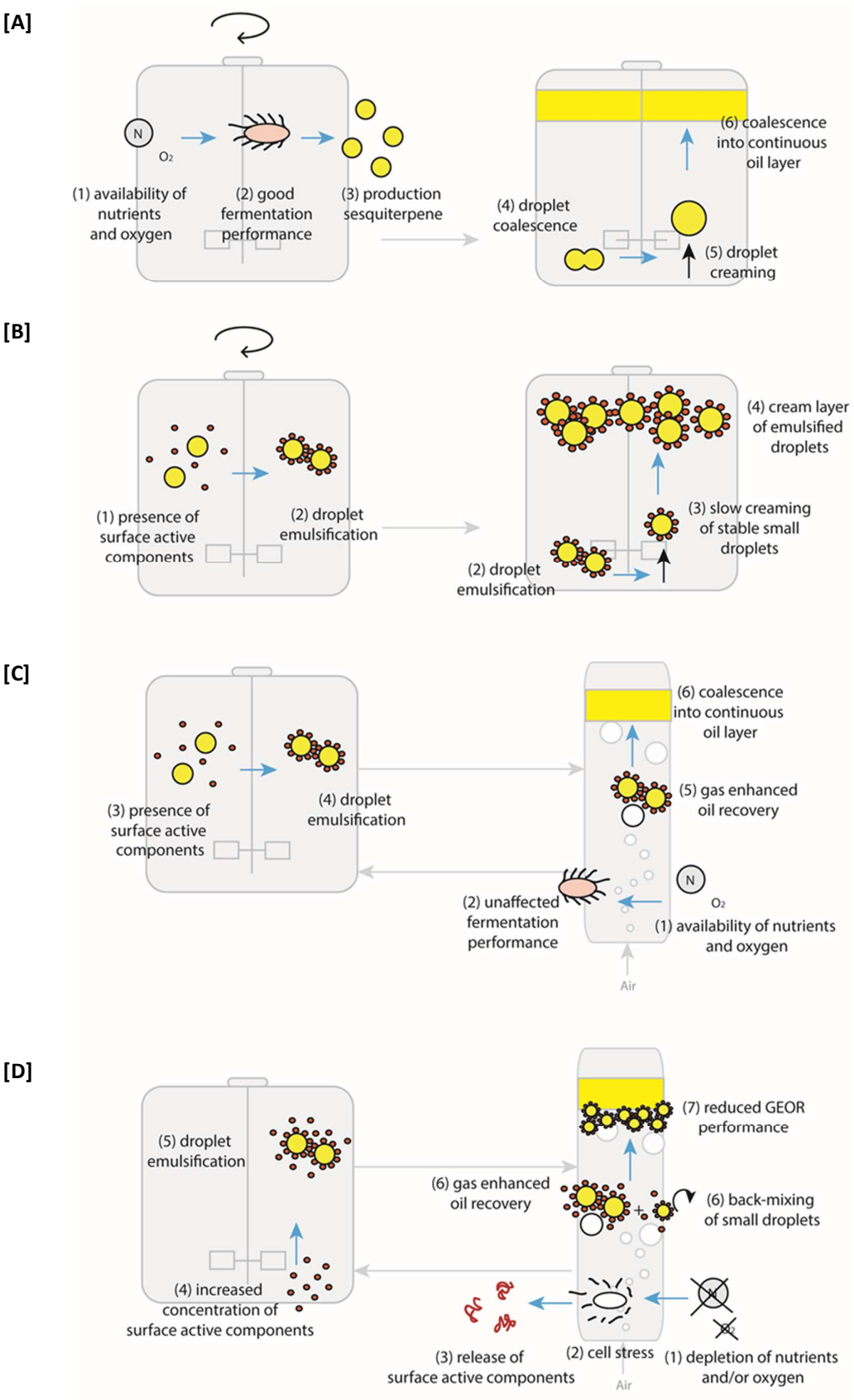
[A]
N
O2
(1) availability of nutrients and oxygen
(2) good fermentation performance
(3) production sesquiterpene
(4) droplet coalescence
(5) droplet creaming
(6) coalescence into continuous oil layer
[B]
(1) presence of surface active components
(2) droplet emulsification
(2) droplet emulsification
(3) slow creaming of stable small droplets
(4) cream layer of emulsified droplets
[C]
(3) presence of surface active components
(4) droplet emulsification
(2) unaffected fermentation performance
N
O2
(1) availability of nutrients and oxygen
Air
(5) gas enhanced oil recovery
(6) coalescence into continuous oil layer
[D]
(5) droplet emulsification
(4) increased concentration of surface active components
(6) gas enhanced oil recovery
(3) release of surface active components
(2) cell stress
(1) depletion of nutrients and/or oxygen
Air
(6) back-mixing of small droplets
(7) reduced GEOR performance

Recently a gas enhanced oil recovery technology (here abbreviated as GEOR) has been proposed as an alternative to recover emulsified fermentation products [10]. This technology consists of promoting the coalescence of oil droplets forming a continuous oil layer by passing gas bubbles through an emulsion. By adjusting bubble size, number of bubbles, and aspect ratio, GEOR was proven to be effective in diverse emulsions of hexadecane in an aqueous mixture of water and the yeast *Saccharomyces cerevisiae*. It remains unknown how the technology would perform in an actual fermentation broth where SACs can affect the stability of the emulsion.

This work concerns the implementation of GEOR in the recovery of oil from microbial emulsions by presenting an integrated bioreactor-GEOR system. In this integrated configuration, the fermentation broth containing a dispersion of oil droplets is circulated through a GEOR column. In the column, the oil/water separation takes place with the aid of gas bubbles, and the oil depleted broth is transferred back into the reactor (Figure 1C). The main advantage of GEOR lies in reducing the number of separation steps, while avoiding the use of costly chemicals. In addition, GEOR might offer several advantages when continuously integrated into a fermentation, such as: (i) cell recycle, (ii) prevention of further stabilisation of the emulsion over time, and (iii) avoiding oxygen transfer problems [11] in case of excessive accumulation of oil in the bioreactor. On the other hand, GEOR is typically performed at low gas flow rates and mild mixing conditions. This poses some operational and design challenges, namely related to possible oxygen and nutrient limitation occurring in the recovery compartment (Figure 1D).

The aim of this work is to study the feasibility of integrating a GEOR column to a bioreactor, with especial focus on fermentation performance, emulsion behaviour, and oil recovery.

2. Theoretical Background

The integrated process presented in this work consists of a well-mixed fermentation compartment operating in fed-batch mode, connected to an external bubble column which typically operates at milder mixing conditions to promote oil recovery [10] (Figure 2B). The main subprocesses taking place in the separation column are: (i) circulation of the broth through the column, (ii) mixing of the bulk liquid due to bubbles, (iii) creaming of the oil droplets due

to difference of density, and (iv) coalescence of separated oil droplets into a clear oil layer on the top part of the column aided by the gas bubbles. Although the exact mechanism(s) whereby the separated oil droplets coalesce into a clear oil layer are not yet understood, the degree of oil recovery in the column can be estimated by performing a regime analysis as the one presented in [12].

Separation of oil droplets from the continuous phase takes place when the time required for a droplet to rise (addressed in this work as creaming characteristic time, τ_{cream}) is shorter than the time required to mix the liquid in the column (τ_{mix}):

$$\tau_{cream} < \tau_{mix} \tag{1}$$

In addition, the residence time of the bulk liquid in the column (τ_{res}) should be larger than the creaming time in order to allow droplets to stay in the column:

$$\tau_{cream} < \tau_{res} \tag{2}$$

The characteristic time for mixing in columns with aspect ratio higher than three depends on the column aspect ratio and the superficial gas velocity at which the column operates (v_{GS}) [13].

$$\tau_{mix}^{column} = 1.496 \cdot \left(\frac{{D_{column}}^2}{g \cdot v_{GS}} \right)^{\frac{1}{3}} \cdot \left(\frac{H_{column}}{D_{column}} \right)^2 \tag{3}$$

The residence time of the fermentation broth in the column (τ_{res}) depends on the bulk liquid flow (F_L) and the volume of liquid in the column (V_{col}):

$$\tau_{res} = V_{column} / F_L \tag{4}$$

Finally, the characteristic time for creaming (Eq. 5) depends of the column height (H), and the and the droplet velocity (v_d), which at the same time depends on the density difference between the oil (ρ_{oil}) and the continuous phase (ρ_L), the droplet size diameter (d_d), gravitational acceleration (g) and the drag coefficient (C_D) (Eq. 6).

$$\tau_{cream} = H / v_d \tag{5}$$

$$v_d = \sqrt{\frac{4 \cdot g \cdot (\rho_L - \rho_{oil}) \cdot d_d}{3 \cdot C_D \cdot \rho_L}} \quad (6)$$

As previously described in [12], the estimated sizes the oil droplets dispersed in the fermentation compartment due to the turbulent conditions range between d_{min} (Eq. 7) and d_{max} (Eq. 8) depending on the o/w interfacial tension (σ_{oil}), the continuous phase density (ρ_L) and viscosity (η_w), and the volumetric power input (e_v), which depends on the stirring rate (N), the aeration rate (F_G), the diameter of the impeller ($D_{impeller}$), and the bioreactor working volume (V_R) (Eq. 9).

$$d_{\min} = \left(\frac{\sigma_{oil}^{1.38} \cdot (10^{-28})^{0.46} \cdot \rho_L^{0.05}}{0.072 \cdot \eta_w \cdot e_v^{0.89}} \right)^{\frac{1}{3.11}} \quad (7)$$

$$d_{\max} = \left(\frac{\sigma_{oil}^{3}}{\rho_L \cdot e_v^{2}} \right)^{\frac{1}{5}} \quad (8)$$

$$e_v^{reactor} = (5.5 \cdot \rho_L \cdot N^3 \cdot D_{impeller}^5) \left(1 - \frac{9.9 \cdot F_G \cdot N^{0.25}}{D_{impeller}^2} \right) \frac{1}{V_R} \quad (9)$$

Considering Equations 1-9 it is possible to find an operational window where column geometry, column aeration rate, and bulk liquid flow allow for droplet separation. However, when designing the recovery compartment, not only hydrodynamics are important but also cellular responses and their effect on productivity and recovery. Although mild mixing conditions are required in the column to promote oil creaming [10] this regime could lead to cellular stress caused by oxygen or nutrients limitation (Figure 1). The possible consequences are diverse, such as release of surface active components (SACs) that include proteins [14], polysaccharides [15], carboxylic acids [16], to the increase of cell membrane hydrophobicity, loss of productivity and viability [14]. These cellular responses could have an effect in the oil emulsification; either by reducing droplet coalescence [17], or by stabilising the o/w interface [18], [19]. In addition, the accumulation of oil in the column could increase bubble coalescence and the medium apparent viscosity contributing to oxygen limitation [11].

2.1. Aim and approach

The aim of this work is to study the effect of broth circulation through a GEOR column on fermentation performance and oil recovery. Model fermentations with wild-type *E. coli* were performed, and hexadecane was eventually added to mimic microbial oil production and/or solvent extraction. Hexadecane was chosen due to its biocompatibility (log *P* of 8.8) [20], its similarity in number of carbons compared to commercial microbial oils like sesquiterpenes (C15), and the availability of GEOR data with this organic phase [10]. This approach allows to fix the oil concentration regardless of fermentation performance. Consequently, fermentation performance and degree of oil recovery can be decoupled.

Four sets of experiments with duplicates were performed (Figure 2A): A base case consisting of a fed-batch fermentation in a reactor vessel (B1, B2); a fed-batch fermentation in a reactor vessel circulating part of the broth through a GEOR column for 24 hours (C1, C2); addition of 10% w/w of hexadecane to a base case fermentation and recovering the oil by circulating the dispersion through the GEOR column for 1 hour (B3, B4); and addition of 10% w/w of hexadecane to a fermentation similar to C1 and C2, and recovering the oil by circulating the dispersion through the GEOR column for 1 hour (C3, C4).

In order to study how the circulation of broth through the column affects the fermentation performance, cell growth, cell viability, and level of SACs in the integrated system (C1 to C4) were compared to the base case (B1 to B4). Proteins have been shown to play an important role in stabilization of hexadecane microbial emulsions [10, 21], and consequently, they have been chosen as reference component for measuring levels of SACs. In order to discard any possible source of cellular stress other than the circulation though the GEOR column, feed rate, aeration and stirrer speed were chosen such to avoid oxygen limitation in the main vessel.

As it was shown in Figure 1D, the cellular stress responses to the circulation of broth through the recovery column can have an effect in the emulsion stability. Consequently, the extent of oil recovery can be reduced. The impact of eventual cell stress responses in separation performance was evaluated by comparing the oil hold-up in the GEOR column of the base case (B3, B4) and circulation case (C3, C4).

[A]

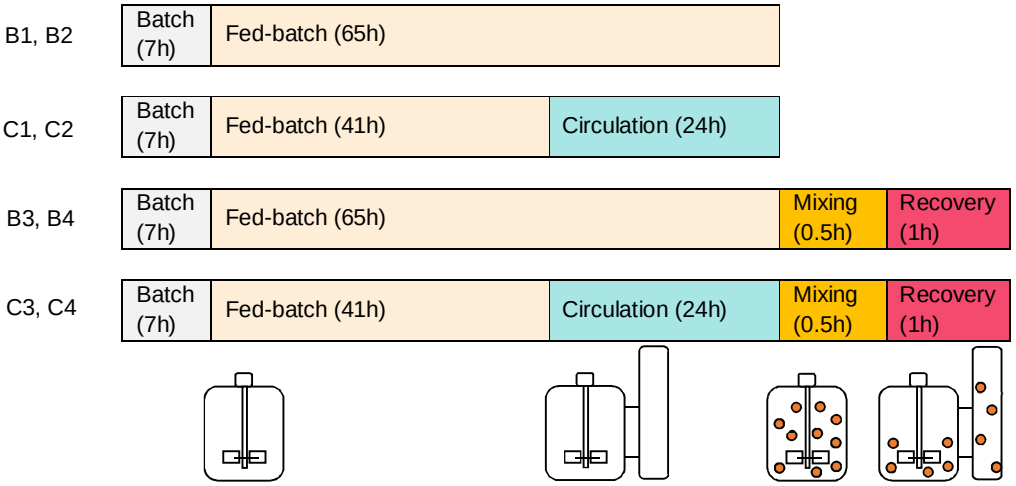

[B]

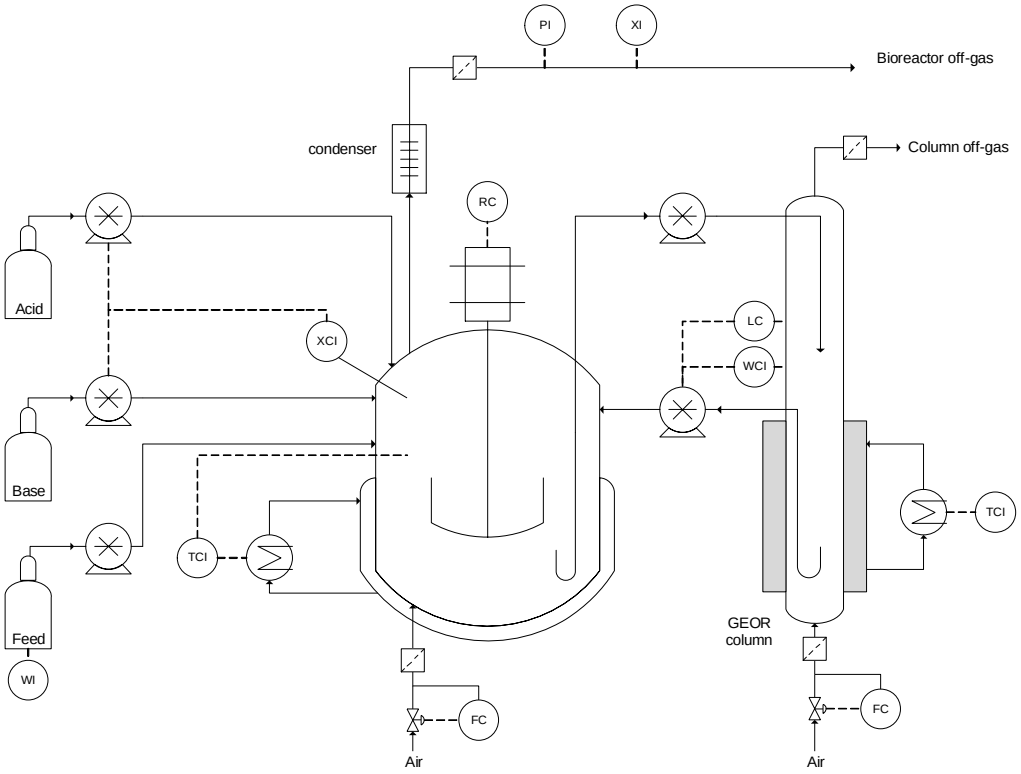

Figure 2. [A] Overview fermentation stages in the different experiments. [B] Schematic representation of the integrated system. P-pressure; X-composition; R-agitation speed; T-temperature; W-weight; F-mass flow; L-level; I-indicator; C-controller.

3. Materials and methods

3.1. Experimental set up

The experimental set up consisted of a 2 L jacketed reactor (Applikon, The Netherlands), working in fed batch mode under glucose limitation connected by a Masterflex peristaltic pump (Cole Parmer, United States) and Masterflex Tygon Fuel & Lubricant tubing L/S 17 to a 500 mL glass-column as indicated in Figure 2.

The custom-made column of 37 mm inner diameter (40 mm outer diameter) and 600 mm height was aerated at 0.1 cm s^{-1} through a stainless-steel bottom plate with a single nozzle of 0.3 mm diameter and an off-gas outlet located at the top. The nozzle and aeration rate conditions in the column were selected based on the results reported by [8] to allow the formation of phase gradient in the column.

In order to avoid excessive circulation of bubbles from the bioreactor vessel to the recovery column, the extreme of the outlet port was designed as a u-tube. The cell broth was circulated back to the fermentation vessel by a second Masterflex peristaltic pump (Cole Parmer, United States) activated either by a level sensor (C1 and C2) or by a weight sensor (C3 and C4). The temperature in the column was maintained at 35 °C by an external heating coil, connected to a cryostat (Lauda, United States), and tubes connecting the two compartments were insulated to avoid heat loss.

3.2. Strain, pre-culture medium, and fermentation medium.

The strain used in this work is a *Escherichia coli* K12 (MG1655) obtained from The Netherlands Culture Collection of Bacteria (Utrecht, The Netherlands). 0.5 mL of stock culture stored at -80°C in Luria-Bertani (LB) medium containing 15% v/v glycerol, were inoculated in 100 mL of sterile synthetic medium (SM) [22] supplemented with 15 g L^{-1} $C_6H_{12}O_6 \cdot H_2O$, and 0.0045 g L^{-1} Thiamine·HCl. Precultures were incubated overnight (approximately 14 h) in 300 mL shake flasks at 35°C and 200 rpm in a rotary shaker (Sartorius Stedim Biotech S.A., France), and inoculated in 900 mL of sterile fermentation medium following the composition as reported in [23] using 5 g L^{-1} $C_6H_{12}O_6 \cdot H_2O$ as carbon source and 0.1 mL EROL DF 7911 K (PMC Ouvrie, France) as antifoaming agent.

3.3. Fed-batch fermentation

Fermentations were performed at an aeration rate of 1.5 nL min^{-1} controlled by a mass flow controller (Brooks, United states), and stirred with a 6-blade Rushton impeller of 45 mm diameter at speed of 1000 rpm. For fermentations B3, B4, C3 and C4 stirring speed was increased to 1200 rpm during the fed-batch phase in order to ensure a dissolved oxygen tension (DOT) above 20%; the temperature was set to 35°C and the pH was maintained at 6.5 by adding acid (2M H_2SO_4) and base (NH_4OH 25%v/v). Fermentation settings were controlled by a ADI - 1030 controller (Applikon, The Netherlands). Foam was controlled by manual addition of an aqueous solution of 10% v/v antifoam Erol-DF7911K (PMC Ouvrie, France) up to a maximum of 30 g.

After approximately 7.2 h of fermentation, glucose was consumed and the DOT increased indicating the end of the batch phase. At that point, a glucose solution containing 700 g L^{-1} $C_6H_{12}O_6 \cdot H_2O$, 20 g L^{-1} $MgSO_4 \cdot 7H_2O$, 0.045 g L^{-1} Thiamine·HCl, and the same trace metal concentration as in the batch medium, was fed into the bioreactor using a Masterflex peristaltic pump (Cole Parmer, United States). In fermentations B1, B2, C1, C2, different feed mass flow rates between 5 and 10 g h^{-1} were chosen to test the validity of the model at different conditions. Experiments B3, B4, C3, C4 were performed at a constant feed rate of 7 g-solution h^{-1}. These feeding conditions were maintained throughout the experiments including circulation and recovery periods.

3.3.1. Circulation period (C1, C2, C3 and C4)

After 48 h from the beginning of the fermentation the broth was circulated in fermentations C1- C4 through the recovery column for a period of 24 h at a mass flow of 3.16 g s^{-1} with a Masterflex pump and Tygon 17' tubings (Masterflex), keeping a column working volume of 350 mL, and providing a liquid residence time one order of magnitude higher than the expected creaming time.

3.3.2. Recovery period (B3, B4, C3 and C4)

After 72 hours of fermentation 10.0±0.3 %w/w of hexadecane (Sigma-Aldrich) colored with oil red-O dye (Sigma-Aldrich) was added to the reactor in fermentations B3, B4, C3 and C4. In fermentations C3, and C4, all the broth was transferred back to the reactor vessel prior to the addition of oil. After mixing the oil for 30 min, the dispersion was circulated through the GEOR column for one hour, and pictures of the top of the column (equivalent to a picture area of 20x40

mm) were taken to evaluate the degree of oil recovery. The conditions in the reactor vessel and column, including feed rate, were the same as in the circulation period.

3.4. On-line analyses

DOT was measured by a dissolved oxygen sensor (Applikon, The Netherlands; Mettler Toledo, The Netherlands). The CO_2 and O_2 concentrations in the bioreactor off-gas and in pressurized air were analyzed by a Rosemount NGA-2000 gas analyzer (Fisher Rosemount, Germany). pH was measured by a pH sensor (Applikon, The Netherlands). Temperature was measured with a temperature sensor (Applikon, The Netherlands). Feed rate was continuously monitored with a balance (Mettler Toledo, The Netherlands). DOT, concentrations of CO_2 and O_2 in the off gas and in pressurized air, pH, temperature and feed weight were continuously recorded with a MFCS/Win 2.1 software (Sartorius Stedim Biotech S.A., France).

3.5. Off-line analyses

3.5.1. Optical density and cell dry weight

Optical density of samples was measured in a spectrophotometer (Biochrom) at 600 nm. 1.5 mL microcentrifuge tubes containing 1mL of broth were set in a centrifuge (Heraeus, Biofuge Pico) at 13000 rpm for 10 min. After discarding the supernatant, the tubes containing the cell pellet were dried in an oven (Heraeus instruments) at 70 °C for 48 h.

3.5.2. HPLC, TOC and protein analysis

Supernatant was separated from the cells in a centrifuge (Heraeus instruments, Stratos) at 17000 rpm for 20 minutes at 4 °C and filtered with a disk filter (Whatman) of 0.45 µm in fermentations B1, B2, C1, and C2 and a disk filter (Whatman) of 0.22 µm in fermentations B3, B4, C3, and C4.

Extracellular amount of residual glucose, ethanol, glycerol and acetate were determined in supernatant by high-performance liquid chromatography (HPLC) as described in [24].

The total amount of organic carbon (TOC) in broth and supernatant was analyzed at the end of the fermentation (except in B3 and C3) with a Total Carbon (TC) analyzer (Shimadzu). Extracellular protein concentration in the supernatant was determined using a Bradford Protein Assay Kit (Thermo Scientific). Protein concentrations for circulation and non-circulation experiments were statistically compared by a two-tailed t-test assuming homoscedasticity.

3.5.3. Cell viability

The concentration of colony forming units (CFU) in the sample was obtained by plating cells on sterile LB medium plates. Samples were diluted with sterile SM medium to ca. 10 CFU, 100 CFU and 1000 CFU per plate. The plates were incubated for 24 hours in an incubator (Heraeus instruments) at 30 °C after which the colonies were counted. Results for circulation and non-circulation experiments were statistically compared by a two-tailed t-test assuming homoscedasticity.

3.5.4. Oil recovery: Experimental and theoretical values

Pictures of the top of the column were processed in Adobe Photoshop CS6, selecting and area of 20x20 mm (10 mm radius from the centre of the column) and cropping the rest of the picture. The selected area was processed with the software ImageJ 1.47, characterizing number of droplets (N_i), droplet size distribution (d_i) and droplet area (A_i). The total area of droplets ($A_{oil,droplets}$) was compared to the total area of the picture (A_{20x20}) to estimate the oil hold-up, ε_{oil}:

$$\varepsilon_{oil} = \frac{A_{oil,droplets}}{A_{20x20}} \tag{10}$$

Under the assumption that this hold-up remained constant in the top of the column, the percentage of recovery was then estimated by comparing the volume of oil in the top of the column with the total volume of oil added in the experiment ($V_{oil,TOTAL}$):

$$\text{Recovery } (\%) = \frac{\varepsilon_{oil} \cdot A_{20x40} \cdot \pi \cdot D_{col}}{4 \cdot V_{oil,TOTAL}} \cdot 100 \tag{11}$$

With A_{20x40} the picture area of the top of the column and D_{col} the column diameter. In addition, a theoretical oil droplet size distribution was calculated assuming a normal distribution between theoretical d_{min} and d_{max} (Equations 7 and 8, 0.04 and 1.55 mm respectively) with a standard deviation equal to three times half of the range. For such droplet size distribution, the volume of oil accumulated in the column ($V_{oil,theoretical}$) when the droplets of sizes between d_i and d_{max} cream to the top section of the column is:

$$V_{oil,theoretical} = \sum_{i}^{i=\max} \frac{d_i^3}{6} \cdot \pi \cdot N_i \quad (12)$$

Where N_i is the number of droplets of diameter d_i. The theoretical recovery percentage then becomes:

$$\text{Recovery}_{theoretical}(\%) = \frac{V_{oil,theoretical}}{V_{oil,TOTAL}} \cdot 100 \quad (13)$$

Note that when $d_i = d_{\min}$ the theoretical recovery would be 100%, while if $d_i = d_{\max}$, the theoretical recovery would be near 0%. Theoretical recovery values were estimated for a varying threshold of minimum droplet size being able to cream in the column (Figure 5C).

3.6. Fermentation model and Carbon balance

A model was developed to predict the cell and CO_2 fermentation profiles in the fed-batch phase. The mass balances of cells, substrate (glucose), and CO_2 in the reactor at constant feed rate are:

$$dM_X(t)/dt = \mu(t) \cdot M_X(t) \quad (14)$$

$$dM_S(t)/dt = F_S + q_S(t) \cdot M_X(t) = 0 \quad (15)$$

$$dM_C(t)/dt = q_C(t) \cdot M_X(t) \quad (16)$$

For the substrate balance (Eq. 15) a pseudo-steady state was assumed (*$dM_S/dt \sim 0$)* as glucose accumulation in the reactor during the carbon-limited fed-batch phase was negligible. The specific rates of glucose consumption and CO_2 production are given by their respective Herbert-Pirt relations:

$$q_S(t) = -\frac{1}{Y_{X/S}} \cdot \mu(t) - m_S \quad (17)$$

$$q_C(t) = \frac{Y_{C/S}}{Y_{X/S}} \cdot \mu(t) + m_{CO_2} \quad (18)$$

Combining Equations 14,15, and 17, and Equations 16 and 18, the resulting cell-growth rate and CO_2 production rates are:

$$R_X = dM_X(t)/dt = \mu(t)\cdot M_X(t) = F_S - m_S \cdot M_X(t)\cdot Y_{X/S} \quad (19)$$

$$R_C = dM_C(t)/dt = \frac{Y_{C/S}}{Y_{X/S}}\cdot \mu(t)\cdot M_X(t) + m_{CO_2}\cdot M_X(t) \quad (20)$$

The total cell mass profile (Equation 21) was obtained integrating Equation 19. M_{X0} and t_0 represent the mass of cells and the fermentation time at beginning of the fed-batch phase.

$$M_X(t) = \left(M_{X0} - \frac{F_S}{m_S}\right)e^{(-m_S\cdot Y_{X/S}\cdot(t-t_0))} + \frac{F_S}{m_S} \quad (21)$$

The profile of cumulative CO_2 produced during the fed-batch phase was obtained integrating Equation 20 using the rectangle rule.

$$M_C(t) = \sum_i \frac{R_C(t_{i-1}) + R_C(t_i)}{2}(t_i - t_{i-1}) \quad (22)$$

Based on reported models for *E. coli* [16, 25], the kinetic parameters used in this model were $Y_{X/S}$=0.69 Cmol-X·Cmol-S^{-1}, m_S=0.024 Cmol-S·Cmol-$X^{-1}\cdot h^{-1}$ $Y_{C/S}$=0.26 Cmol-C·Cmol-S^{-1}, and m_C=0.02 Cmol-C·Cmol-$X^{-1}\cdot h^{-1}$.

The carbon balance was calculated considering the carbon fed into the system ($N^{in}_{S,feed}$), the amount of cells produced during the fed-batch phase ($N_{X,ferm} - N_{X,ferm}(t_0)$), the total amount of CO_2 produced during the fed-batch phase (N_C), and the by-products as total organic carbon in the supernatant ($N_{TOC,sn}$):

$$N_{C,acc} = N^{in}_{S,feed} + N_{X,ferm}(t_0) - N_{X,ferm} - N_C - N_{TOC,sn} \quad (23)$$

$$C-gap(\%) = \frac{N_{C,acc}}{N^{in}_{S,feed}}\cdot 100 \quad (24)$$

4. Results

All experimental profiles of total cell mass (M_x) and the total CO_2 produced (N_{CO2}) followed the trends predicted by the model based on reported kinetic parameters for non-producing E. coli under aerobic conditions [16, 25] and the experimental feed rates, with an R^2>0.96 (Figure 3) and R^2>0.96 (results not shown), respectively. Furthermore, the carbon balances closed with less than 5% gap. Profiles of cell mass, dissolved oxygen, CO_2, residual glucose and typical anaerobic by-products such as ethanol or acetate (results not shown) suggest that there was no of oxygen limitation in the vessel. These results indicate that all fermentations were comparable in terms of fermentation performance, independent on whether broth had been circulated through the recovery column (experiments C1-C4) or not (experiments B1-B4). On the other hand, protein levels in the fermentations with both circulation and oil addition (C3 and C4) at the end of the fermentation were, in average, three times higher than in fermentations with oil addition but no circulation (B3 and B4, $p=0.01<0.05$, Figure 4A). However, there was no statistically significant difference in viability data ($p=0.86>0.05$) when comparing fermentations with and without circulation through the recovery column (Figure 4B).

Oil hold-up in the top of the column and the percentage of oil recovered indicated a higher degree of coalescence in fermentations without prior circulation to the recovery column (experiments B3 and B4, Figure 5A). However, coalescence into a continuous oil layer could be seen in experiment B4 only. Foam content was considerably higher in fermentations with prior circulation (C3 and C4). This is in agreement with the increased supernatant protein content as seen in Figure 4A and it could indicate a stabilization of gas bubbles by the excess

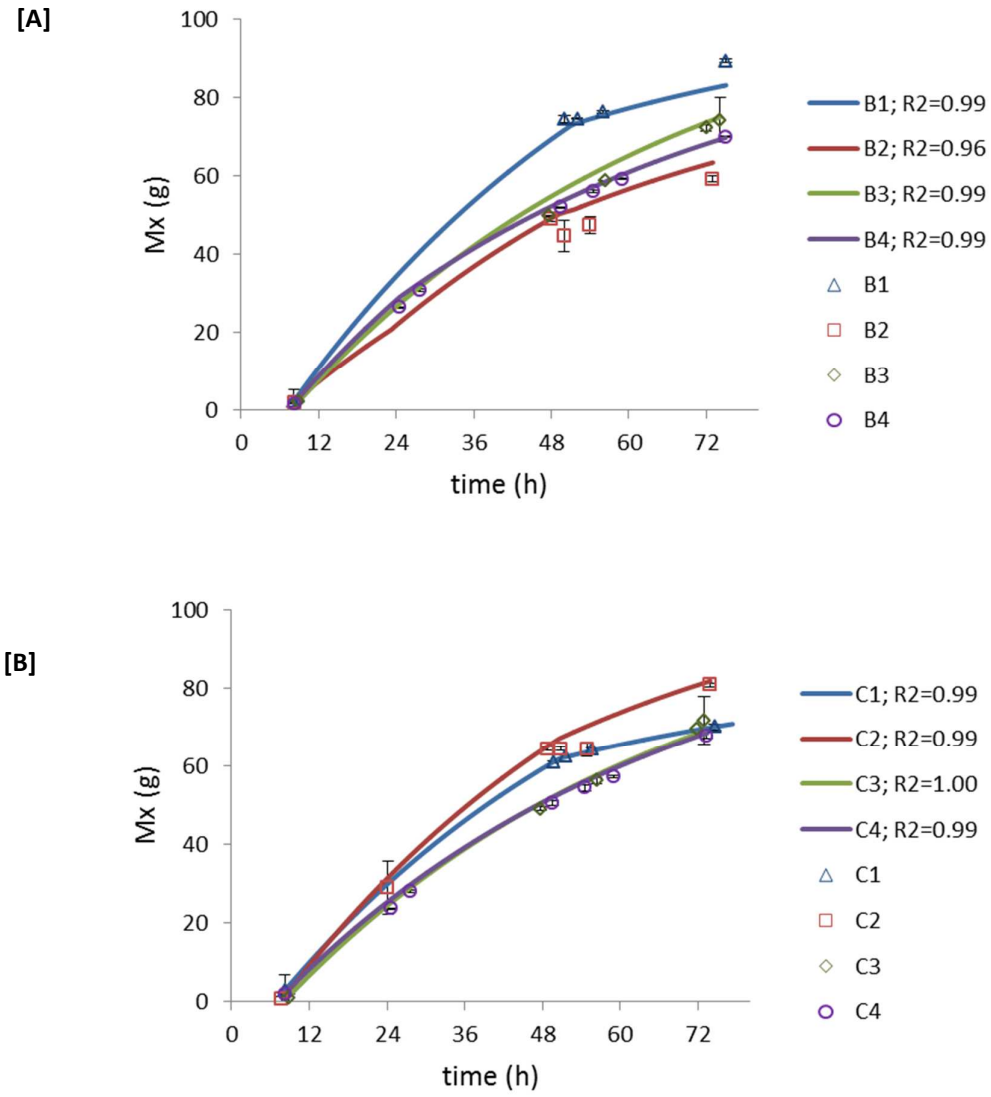

Figure 3. Total mass of cells in the reactor for base case fermentations [A] and circulation case fermentations [B]. Solid lines represent data obtained from the kinetic model. Markers represent experimental data obtained from cell dry weight measurements.

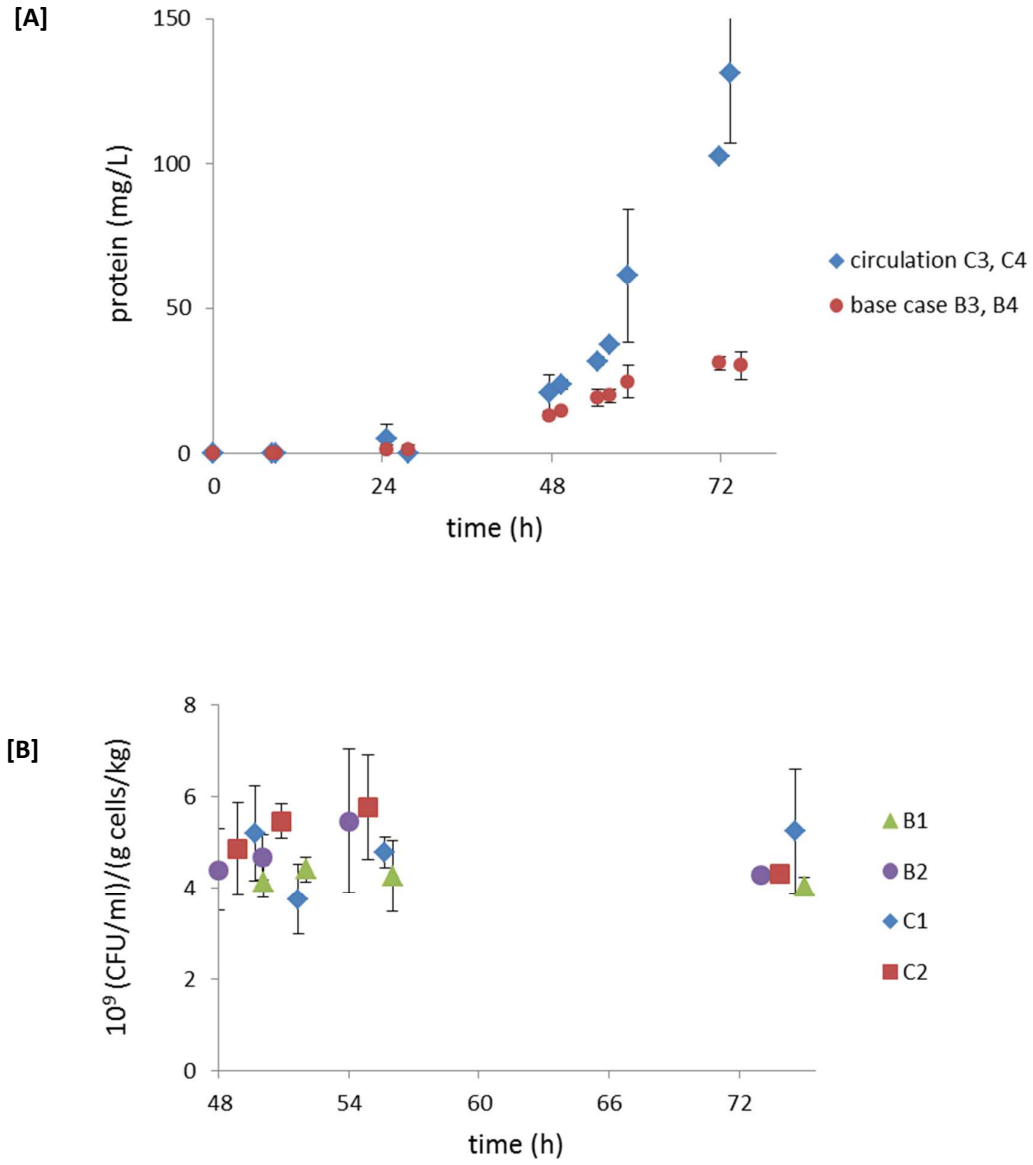

Figure 4. Comparison of base case (B1 to B4) and circulation case (C1 to C4) based on extracellular protein concentration [A] and cellular viability [B]. Error bars represent the standard deviation of the average.

of SACs generated during the fermentation. The resolution of the images did not allow to find significant differences in averaged droplet size between experiments (results not shown). However, oil hold-up was significantly higher ($p=0.015<0.05$) in experiments B3 and B4, at the studied conditions in the GEOR column.

By comparing characteristic times of the main subprocesses (Eq. 1 and Eq. 2) three different regimes were identified (Figure 5B, from left to right): (i) circulation of small droplets back to the reactor when the residence time in the recovery column (τ_{res}) is smaller or in the same order of magnitude than the creaming time (τ_{cream}); (ii) medium-sized droplets back-mixed in the column when τ_{res} is an order of magnitude larger than τ_{cream} but the mixing time in the recovery column (τ_{mix}) and τ_{cream} are in the same order of magnitude; (iii) large droplets creaming to the top of the column when τ_{mix} is an order of magnitude larger than τ_{cream}. Considering the theoretical droplet size distribution calculated at the bioreactor conditions (see Section 3.5.4), the theoretical recovery as a function of the minimum droplet size able to cream was estimated (see Figure 5C). When comparing the theoretical analysis (Figures 5B and 5C) to the experimental results (Figure 5A) it can be observed that: a) in all four experiments (B3, B4, C3 and C4) there was creaming, indicating that there were oil droplets of sizes corresponding to regime (iii) in Figure 5B; and b) the percentage of oil recovered in the experiments corresponds to the theoretical recovery for such droplet sizes (Figure 5C). In addition, the minimum droplet size measured in experiments B3, B4, C3 and C4 (0.30 ±0.04 mm) agreed with the theoretical estimation based on comparison of characteristic times.

Figure 5. Experimental and theoretical results for oil recovery. [A] Experimental results. Bars indicate the significant difference ($p=0.015<0.05$) in oil hold up and percentage of oil recovered between base case (B3, B4) and circulation experiments (C3, C4). Above the bars, pictures of the top of the recovery column for each experiment are shown. [B] Comparison of characteristic times as a function of droplet size leading to three regimes in the column (from left to right): (i) circulation of small droplets back to the reactor ($\tau_{res}<\tau_{cream}$), (ii) back-mixing of medium-sized droplets in the column ($\tau_{cream}\sim\tau_{mix}$), (iii) large droplets creaming to the top ($\tau_{cream}<<\tau_{mix}$). [C] Theoretical recovery as a function of minimum droplet size able to cream ($\tau_{cream}<<\tau_{mix}$). Red arrows indicate experimental values.

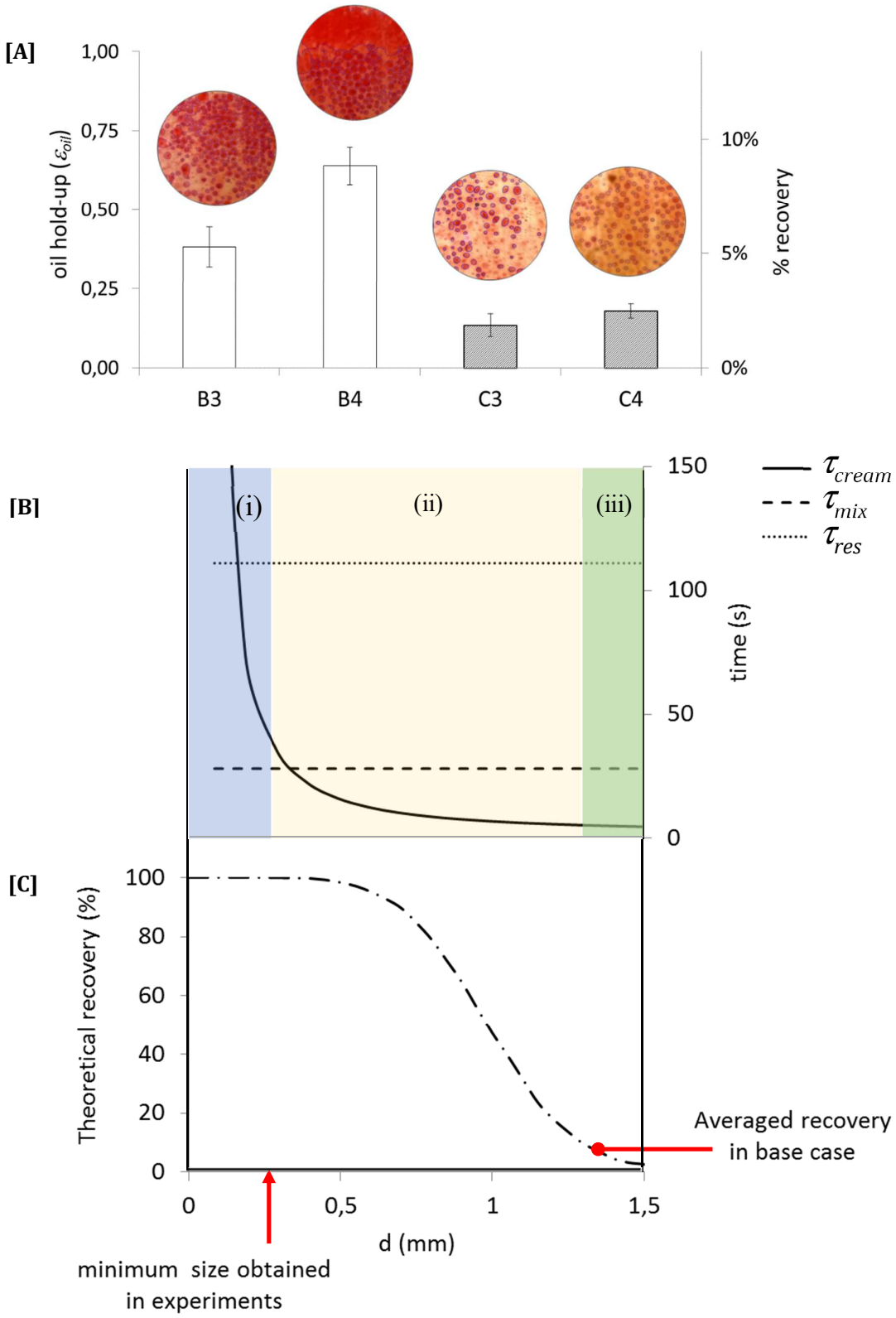
[A]
1,00
0,75
0,50
0,25
0,00
oil hold-up (ε_{oil})
10%
5%
0%
% recovery
B3
B4
C3
C4
[B]
(i)
(ii)
(iii)
150
100
50
0
time (s)
τ_{cream}
τ_{mix}
τ_{res}
[C]
100
80
60
40
20
0
Theoretical recovery (%)
0
0,5
1
1,5
d (mm)
Averaged recovery
in base case
minimum size obtained
in experiments

5. Discussion

The feasibility of integrating GEOR into a fed-batch fermentation was assessed through kinetic modelling of four integration experiments (B3, B4, C3 and C4) which presented same fermentation performance as four fermentations run without oil recovery (B1, B2, C1 and C2). Duplicates, modelling, and experimental design allowed to systematically study and compare the system with and without circulation through the recovery column, and with and without oil addition. Although circulation through the GEOR column for 24h at mild mixing and aeration conditions did not affect cell growth or cell viability, it increased the level of SACs in the medium and hindered oil droplet coalescence. The concentration of extracellular proteins in the circulation experiments was up to three times higher than that of the base case, and most probably have contributed to the emulsion stabilization, as pointed out by [21, 26]. However, further research is needed to determine if other possible SACs like glycolipids from the membrane exopolysaccharides, or cells with increased hydrophobicity due to stress could have also played a role [14, 15]. In any case, it can be stated that from a fermentation perspective it would be desirable to decrease the residence time as much as possible in the circulation loop to reduce the time during which cells are exposed to stress conditions.

The results shown in Figure 5 suggest that stabilization of the oil phase in the form of small droplets decreased the capacity for oil recovery of the GEOR column since small droplets were recirculated back into the vessel or remained back mixed in the column. Estimations based on characteristic times as described in section 2 indicated that the liquid residence time in the column (111 seconds) was high enough to retain almost the 100% of the oil fed to the system (Figure 5C). Therefore, according to the estimations, it could be possible to reduce the liquid residence time without significantly reducing the degree of oil recovery. On the other hand, the difference between mixing and creaming time in the column allowed to recover only about 10% v/v of the oil droplets in the top section of the column, while the rest remained back mixed in lower sections (Figure 5). A tuning of the settings in the column is thus required to increase the degree of oil recovery in the GEOR while keeping fermentation performance unaffected. In other words, targeting settings that would lead to a broadening of regime (iii) in Figure 5B. It can be seen that this can be achieved by lowering τ_{cream} and/or increasing τ_{res} and τ_{mix}. In particular, a decrease in aspect ratio would reduce the creaming time (Eq. 5) increasing the operational window at which oil can be recovered. Clearly, the limit for τ_{res} lies in the stress tolerance and will be microorganism dependent. Although the O_2 transfer in the column could be improved by increasing gas-liquid contact area (e.g., increasing the aeration rate, or reducing

the bubble size), these measures might have a negative impact on τ_{mix}. Hence, integration concepts where τ_{res} is minimised are still preferable, for example through novel bioreactor concepts. Furthermore, droplet coalescence and creaming could be promoted by increasing the oil fraction and selecting solvents with lower density (e.g., dodecane). Finally, further studies on the mechanism of oil recovery will allow for more robust design, achieving a compromise between fermentation and recovery requirements in terms of bubble size, number of bubbles, column geometry, residence time, and oil fraction. These studies require improving the acquisition of droplet size data, for example by implementing an in-situ optical probe [27].

From an operational perspective, an in-line GEOR column compared to an off-line separation at the end of the fermentation is more advantageous in cases where long fermentations runs are required (e.g., low productivity, or continuous fermentations). In these cases, prevention of emulsion stabilisation over time [28], or excessive accumulation of oil phase in the bioreactor [11] becomes more relevant. On the other hand, in continuous fermentations the concentration of SACs in the broth is expected to be lower since the medium is continuously refreshed, and therefore the current recovery capacity of the GEOR column could be enough to achieve a formation of a continuous oil phase.

In summary, this study is a step forward in the implementation of GEOR as a feasible *in situ* product removal technology in multiphase fermentations without affecting fermentation performance in terms of cell growth and cell viability. Further studies with specific microbial systems should be performed to assess the possible effects on product formation. Tuning of GEOR operational parameters is required to improve oil recovery, either by reducing cellular stress conditions or by allowing oil coalescence in an environment with higher concentration SACs. This works consolidates the opportunity for reduction in cost and environmental impact of multiphase fermentations allowing for cell recycle, reducing energy requirements and avoiding the use of chemicals such as surfactants that might compromise product quality.

Acknowledgements

This work was carried out within the BE-Basic R&D Program, which was granted a FES subsidy from the Dutch Ministry of Economic affairs.

Conflict of interest

The authors declare no financial or commercial conflict of interest.

References

1. Rude, M.A., Schirmer, A. *New microbial fuels: a biotech perspective.* Curr. Opin. Microbiol., 2009, 12(3):p. 274-81

2. Tabur, P. and Dorin, G. *Method for purifying bio-organic compounds from fermentation broth containing surfactants by temperature-induced phase inversion*. 2012. WO2012024186

3. McPhee, D.J., *Deriving Renewable Squalane from Sugarcane.* Cosmetics & Toiletries, 2014. **129**(6): p. 20-26.

4. Van Hamme, J.D., Singh, A., Ward, O.P. *Physiological aspects: Part 1 in a series of papers devoted to surfactants in microbiology and biotechnology*. Biotechnology Advances, 2006. 24(6): p. 604-620.

5. Dafoe, J.T. and Daugulis, A.J., In situ product removal in fermentation systems: improved process performance and rational extractant selection. Biotechnology Letters, 2014. 36(3): p. 443-460.

6. Newman, J.D., Marshall, J., Chang, M., Nowroozi, F., et al., *High-level production of amorpha-4,11-diene in a two-phase partitioning bioreactor of metabolically engineered Escherichia coli.* Biotechnology and Bioengineering, 2006. **95**(4): p. 684-691.

7. Brandenbusch, C., Glonke, S., Collins, J., Bühler, B., et al., *Stable Emulsions in Biphasic Whole-Cell Biocatalysis: The Mechanism of scCO2-Assisted Phase Separation.* Chemie Ingenieur Technik, 2013. **85**(9): p. 1420-1420.

8. Dolman, B.M., Kaisermann, C., Martin, P.J., Winterburn, J.B. *Integrated sophorolipid production and gravity separation*. Process Biochem., 2017, 54: P. 162-171

9. Kim, J., Iannotti, E., Bajpai, R. *Extractive recovery of products from fermentation broths.* Biotechnology and Bioprocess Engineering, 1999, 4(1):p. 1-11

10. Heeres, A.S., Heijnen, J.J., van der Wielen, L.A.M., and Cuellar, M.C., *Gas bubble induced oil recovery from emulsions stabilised by yeast components.* Chemical Engineering Science, 2016. **145**: p. 31-44.

11. Clarke, K.G. and Correia, L.D.C., Oxygen transfer in hydrocarbon–aqueous dispersions and its applicability to alkane bioprocesses: A review. Biochemical Engineering Journal, 2008. 39(3): p. 405-429.

12. Heeres, A.S., PhD Thesis, Delft University of Technology, December, 2016.

13. Groen, D.J., PhD Thesis, Delft University of Technology, October, 1994.

14. Hewitt, C.J., Nebe-Von Caron, G., Axelsson, B., McFarlane, C.M., et al., *Studies related to the scale-up of high-cell-density E. coli fed-batch fermentations using multiparameter flow cytometry: Effect of a changing microenvironment with respect to glucose and dissolved oxygen concentration.* Biotechnology and Bioengineering, 2000. **70**(4): p. 381-390.

15. Neu, T.R., *Significance of bacterial surface-active compounds in interaction of bacteria with interfaces.* Microbiological Reviews, 1996. **60**(1): p. 151-166.

16. Xu, B., Jahic, M., and Enfors, S.O., *Modeling of overflow metabolism in batch and fed-batch cultures of Escherichia coli.* Biotechnol Prog, 1999. **15**(1): p. 81-90.

17. Keitel, G. and Onken, U., *The effect of solutes on bubble size in air-water dispersions.* Chemical Engineering Communications, 1982. **17**(1-6): p. 85-98.

18. Heeres, A.S., Picone, C.S.F., van der Wielen, L.A.M., Cunha, R.L., et al., *Microbial advanced biofuels production: overcoming emulsification challenges for large-scale operation*. Trends Biotechnol. , 2014. **32**(4): p. 221-229.

19. Dorobantu, L.S., Yeung, A.K.C., Foght, J.M., and Gray, M.R., *Stabilization of oil-water emulsions by hydrophobic bacteria*. App. Environ. Microb., 2004. **70**(10): p. 6333-6336.

20. Laane, C., Boeren, S., Vos, K., Veeger, C. *Rules for optimization of biocatalysis in organic solvents. Biotechnology and Bioengineering*, 1987, 30(1): p. 81-7

21. Heeres, A.S., Schroen, K., Heijnen, J.J., van der Wielen, L.A.M., et al., *Fermentation broth components influence droplet coalescence and hinder advanced biofuel recovery during fermentation.* Biotechnology Journal, 2015. **10**(8): p. 1206-15.

22. Verduyn, C., Postma, E., Scheffers, W.A., and Van Dijken, J.P., *Effect of benzoic acid on metabolic fluxes in yeasts: A continuous-culture study on the regulation of respiration and alcoholic fermentation*. Yeast, 1992. **8**(7): p. 501-517.

23. Korz, D.J., Rinas, U., Hellmuth, K., Sanders, E.A., et al., *Simple fed-batch technique for high cell density cultivation of Escherichia coli.* J Biotechnol, 1995. **39**(1): p. 59-65.

24. Cruz, A.L., Verbon, A.J., Geurink, L.J., Verheijen, P.J., et al., *Use of sequential-batch fermentations to characterize the impact of mild hypothermic temperatures on the anaerobic stoichiometry and kinetics of Saccharomyces cerevisiae.* Biotechnol Bioeng, 2012. **109**(7): p. 1735-44.

25. Cuellar, M.C., Zijlmans, T.W., Straathof, A.J.J., Heijnen, J.J., et al., *Model-based evaluation of cell retention by crossflow ultrafiltration during fed-batch fermentations with Escherichia coli.* Biochemical Engineering Journal, 2009. **44**(2): p. 280-288.

26. Damodaran, S., *Protein Stabilization of Emulsions and Foams.* Journal of Food Science, 2005. **70**(3): p. R54-R66.

27. Panckow, R.P., Reinecke, L., Cuellar, M.C., and Maaß, S., *Photo-Optical In-Situ Measurement of Drop Size Distributions: Applications in Research and Industry*. Oil Gas Sci. Technol. – Rev. IFP Energies nouvelles, 2017. **72**(3): p. 14.

28. Kang, Z., Yeung, A., Foght, J.M., and Gray, M.R., *Mechanical properties of hexadecane-water interfaces with adsorbed hydrophobic bacteria*. Colloids and Surfaces B: Biointerfaces, 2008. **62**(2): p. 273-279.

Chapter 6. Conclusions, recommendations and outlook

The challenges of microbial sesquiterpene production process addressed in this thesis are the emulsification of the product in the reactor, the loss of product in the off-gas due to evaporation, and the modification of the gas-liquid oxygen transfer mechanisms in a multiphase system. These issues derive from a complex network of mechanisms, where the modification of one parameter has an effect in several aspects of the process (Figure 1).

For example, when production pathway is coupled to growth metabolism, cellular growth can lead to sesquiterpene production. This increases the concentration of oil phase, which in turn enhances the rate of droplet-droplet coalescence. Consequently, there is a larger averaged droplet size and droplet creaming is enhanced. On the other hand, higher cell concentrations imply higher concentration of SACs in the medium (e.g. extracellular proteins, exopolysaccharides, cell, cell debris), which can stabilize droplet and bubble surface preventing droplet growth by coalescence. In addition, the viscosity of the fermentation broth rises with the concentration of cells. This reduces the degree of mixing in the system, affecting coalescence, creaming and oxygen transfer mechanisms.

Although the insolubility of sesquiterpenes in the aqueous medium can be advantageous for product recovery, the complexity of a multiphase system should not be underestimated when scaling-up the production process. In this work, the different mechanisms, their interconnections, and their impact on the process scale-up have been studied, and the main conclusions are summarized in the following sections.

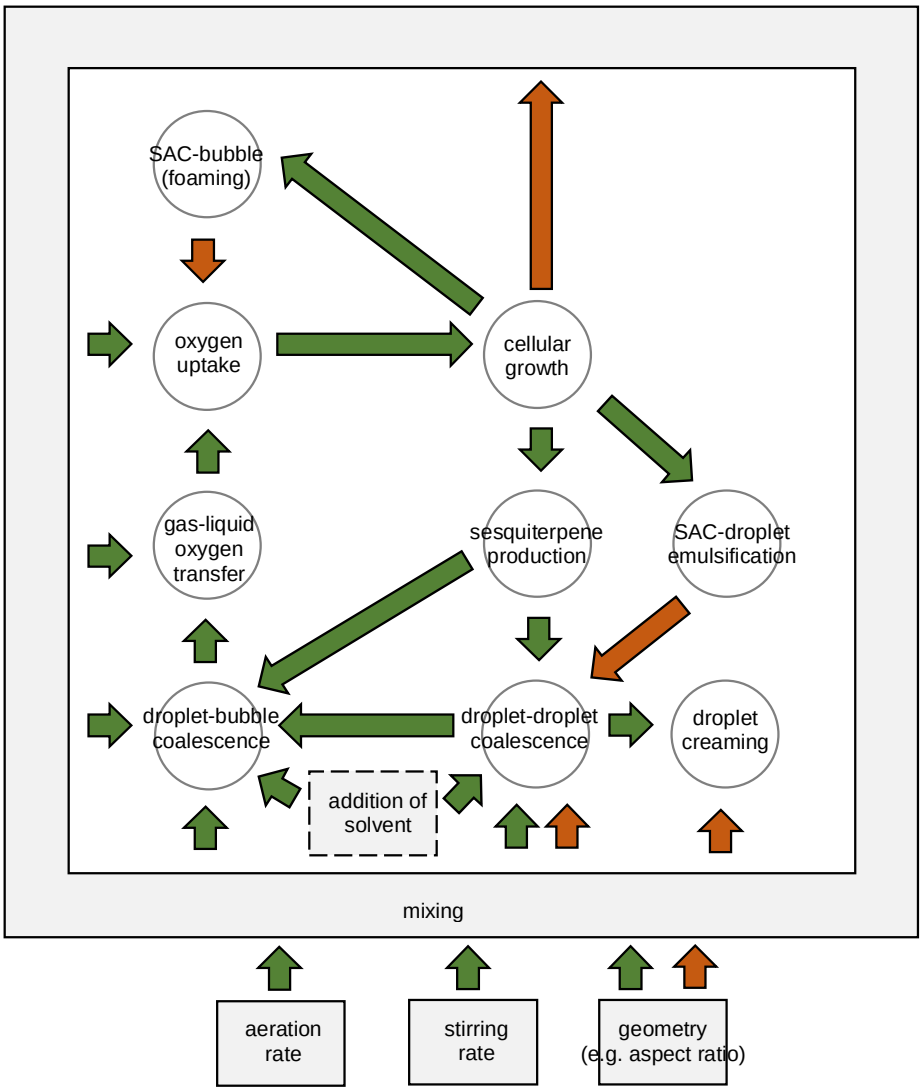

Figure 1. Network of interaction between mechanisms (circles) and operating conditions (squares) in a sesquiterpene fermentation. Mechanisms related to product evaporation were not included to simplify the scheme.

1. Regime analysis as a tool to identify scale-up bottlenecks

Regime analysis resulted a useful technique to identify bottleneck mechanisms for product recovery at different scales. In chapter 2, the characteristic times of droplet coalescence, SACs adsorption, droplet creaming and mixing mechanisms were compared at different scales and process conditions. In the case of droplet creaming, it was concluded that the ratio of creaming time to mixing time increases with the reactor volume. Therefore, although creaming is not necessarily a problem at small volume and low aspect ratios, it becomes a rate-limiting mechanism at larger scales. Other mechanisms, like SACs adsorption and coalescence, are in principle independent on process scale. However, they depend on parameters that not necessarily have to be the same at different scales. For example, higher cell concentrations might be required at large scale, potentially increasing the concentration of SACs, and reducing the characteristic time of adsorption onto a droplet. In addition, at laboratory scale solvents are typically added to the broth for product extraction [1, 2]. This increases the oil concentration and the coalescence rate. However, references to the use of solvents in large-scale sesquiterpene fermentations are scarce [3]. This means that coalescence rate will differ at larger scales when solvent is not implemented.

The main conclusion of chapter 2 is that mixing in the reactor at fermentation conditions enhances droplet coalescence upon droplet stabilization by SACs. However, the resulting mixing regime hinders droplet creaming. This implies that product recovery by gravity settling is not possible at the conditions of aeration and agitation required for fermentation. Hence, two compartments operating at different mixing conditions are required for integrating fermentation and gravity settling. This can be done in one piece of equipment (as it is being further developed within the Deft Integrated Recovery Column project), but also as an external loop, as studied in chapter 5.

2. Consequences of using solvents in microbial production of sesquiterpene

Sesquiterpenes are slightly volatile molecules with vapour pressures in the range of 3 to 8 Pa at 25°C (values predicted by EPISuite™ ChemSpider database). Product evaporation complicates the evaluation of the productivity of microbial strains in laboratory scale. This is especially a problem in shake flasks, where recovery methods like off-gas condensers are not readily available and product titres are low. A common solution at laboratory scale is adding

10-20 % v/v of a solvent to the fermentation broth to capture the produced sesquiterpene [1, 2]. In chapter 3 it was concluded that volatility of sesquiterpenes could lead to 5-10% of product loss at scales of 1000 m^3. Experimental results presented in chapter 3 suggest that sesquiterpene evaporation takes places via a parallel transfer route across air/water and air/oil interfaces. The prevalent route depends on the type of bubble coverage by the oil phase, the concentration of oil, the concentration of SACs and the interfacial properties of the gas, water and oil phase. When a solvent is added, the overall concentration of sesquiterpene in the oil phase is reduced and so the sesquiterpene equilibrium concentration in the gas phase. As a result, the evaporation rate is reduced (e.g. 50% of evaporation rate reduction when adding 10% v/v of dodecane to the medium).

As previously mentioned, addition of solvent also promotes coalescence of the dispersed oil phase. Laboratory scale protocols report the addition of 2 volumes of solvent (e.g. Methyl-tertbutyl-ether) per volume of fermentation broth to achieve phase inversion. Once that the emulsion of oil droplets in water is inverted to an emulsion of water droplets in oil, water is separated from the continuous oil phase by centrifugation. At large scale, phase inversion is rather achieved by adding a commercial demulsifier (e.g. Triton-X114) and changing its solubility in oil by modifying the temperature of the mixture [4]. In principle, phase inversion by solvent addition could be also an alternative at large scale, however this requires additional product/solvent separation steps (e.g. distillation). Chapter 3 presents a techno-economic evaluation of using solvents in the fermentation broth and in DSP at production scales of 25 MT $year^{-1}$ and 25000 MT $year^{-1}$. Due to the several simplifications made (e.g. assumption of solvent/broth ratio based on laboratory protocols), absolute values should be taken with care. However, trends and comparison among cases are expected to be correct. This evaluation concluded that a solvent-based process at scale typical of flavours and fragrances (25 MT $year^{-1}$) has larger costs that the current state of the art using commercial demulsifiers like Triton-X114 (82.4 \$ kg^{-1} versus 49.0 \$ kg^{-1}). However, when increasing the scale, the impact of the CAPEX in the overall cost is reduced in comparison to, for example, expenditure in raw materials. As a result, a solvent-based process at scale typical of bulk chemicals and fuels (25000 MT $year^{-1}$) presents cost (3.7-5.6 \$ kg^{-1}) similar to the current state of the art based on commercial demulsifiers (3.2 \$ kg^{-1}). Furthermore, if solvents compatible with the final product formulation are selected (e.g. diesel in the process of farnesene for jet fuel production), unit production cost can be lowered (37.7 \$ kg^{-1} at scale of 25 MT $year^{-1}$; 0.7 \$ kg^{-1} at 25000 MT $year^{-1}$), while decreasing environmental impact. Further cost reduction in a solvent-

based sesquiterpene process would require improving the CPI demulsification efficiency, by reducing the required amount of solvent and reducing the loss of solvent and product in the aqueous streams of the centrifuges.

Finally, the presence of an oil phase (solvent and/or product) in the broth can also affect the mechanisms of oxygen transfer from the gas bubbles to the aqueous medium. In chapter 4, it was concluded that a g/o/w transfer parallel to g/w transfer was the scenario that better described experimental oxygen concentration profiles and $k_L a$ values in *E. coli* fermentations containing up to 10% v/v of oil. In this mixed route, part of the bubble surface in direct contact with the aqueous phase, and part is covered by an oil layer. Oil droplets can be enriched in oxygen, either by direct contact with the gas bubble and a subsequent detachment from its surface, or by entering in the stagnant aqueous layer rich in oxygen that surrounds the bubble. In this way, the dispersed oil droplets become a source of oxygen increasing the available transfer area. In addition, solubility of oxygen in hydrocarbons is higher than in water, and consequently, their presence can rise the oxygen concentration in the medium. Results presented in chapter 4 confirmed indeed an enhancement in concentration of dissolved oxygen and $k_L a$ upon addition of hexadecane to the fermentation medium. This enhancement, however, is subjected to the dominant oxygen transfer route which in turn is affected by the presence of SACs in the medium. Results in chapter 4 highlight that emulsification is a problem that affects not only product recovery but also oxygen transfer. This is especially relevant at large scale, where oxygen limitation is typically a design constraint [5].

3. Continuous oil removal by integration of production and oil recovery

The outcome of the regime analysis presented in chapter 2 was the requirement of two-separation compartment reactor for an integrated production and recovery of sesquiterpenes at large scale. In line with this conclusion, chapter 5 presents the integration of a Gas Enhanced Oil Recovery (GEOR) column to a fed-batch reactor. The GEOR column consists of a bubble column where low aeration conditions allow for droplet creaming. Once those droplets reach the top, they form an emulsion layer. Although the mechanisms are still not clear, it has been observed that bubbles circulating through this emulsion layer can lead to the coalescence of the emulsion into a clear oil layer.

The main advantage of the integration of a GEOR column compared to an off-line separation equipment (e.g. settler, centrifuge), is that oil can be removed from the system while keeping the microbial cells alive, so they can immediately be recirculated to the fermentation compartment. From experimental results based on fermentations with *E. coli* and 10% v/v of hexadecane, together with a cellular growth model based on kinetic parameters, it was concluded that circulation of fermentation broth through a GEOR column does not affect cellular growth neither cell viability. However, it results in a higher concentration of SACs compared to a base case fermentation in one vessel. This increased level of SACs does have a repercussion in the emulsion stability and the degree of oil recovery. Although the integrated GEOR column does separate oil droplets dispersed in the reactor vessel, it needs further optimization to promote coalescence of these droplets into a clear oil layer. After performing a regime analysis of this system, it was shown that creaming, and thus recovery, could be further promoted by reducing the column aspect ratio. The decrease in aspect ratio requires rather an increase in diameter, and consequently an increase in the volume of the recovery section. At laboratory scale, the set-up flexibility is limited by the volume of the reactor vessel (2-L jacketed reactor). Therefore, it is required to work at larger fermentation scales in order to test the GEOR column at its maximum recovery capacity.

4. Overcoming experimental challenges

While addressing some of the challenges of microbial sesquiterpene production process, this project faced its own difficulties. These were mainly related to the lack of a producing strain with high productivity for experimental testing, the scarcity of data regarding physical properties of sesquiterpenes, the impact of the oil phase in typical fermentation analytics (e.g., cell dry weight, extracellular protein concentration, dissolved oxygen concentration), and the need to develop new analytical protocols to characterize emulsion stability and oil phase recovery. The latter was indeed, one of the key issues along the project. Not only there are several ways to define emulsion stability (e.g., against chemicals, pressure, temperature), but also there is a dynamic component in the degree of stability that makes difficult to compare samples not simultaneously processed. In addition, the properties of the obtained emulsion highly change along a fermentation. The lack of a method with a wide sensitivity range, leads to a binary result (completely demulsified/completely emulsified) rather than to an indication about the degree of stability. Even if methods could be slightly modified to measure each type

of emulsion, the experimenter should know in advance what the stability of the emulsion is, leading to a paradox situation. So far, as shown in chapter 5, the link of emulsion stability to SACs concentration, droplet diameter, and degree of recovery in a bubble column, has given the most satisfactory results. In that chapter, an estimation of the averaged droplet size was made from pictures of the recovery column. It would be interesting to perform a direct quantification of the recovery, by removing the oil phase from the inline column implementing a decanter, such as the one described by [6].

The chosen approach to overcome the experimental difficulties was mimicking sesquiterpene fermentations with non-producing *E. coli K12* strain and hexadecane as oil phase. This allowed to decouple oil concentration from cell productivity, and to support experimental data with modelling based on well-known fermentation kinetic parameters of *E. coli K12*. In first place a black box kinetic model described the profiles of cellular growth and CO_2 production. In this way, cell mass in the reactor could be estimated from off-gas data supporting cell dry weight measurements that can be affected by the presence of oil. In addition, by implementing this model in a flow-sheet software, the impact of fermentation and recovery strategies in the productivity and process costs could be evaluated.

Furthermore, a regime analysis was developed to determine the dominating mechanisms at different process conditions. Droplet creaming, mixing in the reactor, droplet coalescence, and adsorption of surface active components (SACs) onto the droplet surface, were described as function of their characteristic times. These were dependent on process conditions such as volumetric power input, droplet size, oil concentration, and SACs concentration. To complement the regime analysis with experimental data, droplet sizes in oil-water mimic mixtures were measured. An optical probe successfully tested in Heeres, Schroën [7], was used for in situ image acquisition of oil in water dispersions in chapter 3 of this thesis. However, in oil-fermentation broth mixtures with high concentration of cells, the smaller droplet size and the optical density of the medium did not allow to obtain reliable data. In consequence, models based on coalescence and breakage rates [8] were used in this thesis to estimate droplet sizes at different conditions. The implementation of an optical probe with higher resolution would be desirable for determination of droplet size distribution in systems with high concentration of SACs and low droplet diameters [9]. Regarding the concentration of SACs in the medium, from the several components that can interact with droplet surface [7], this thesis used extracellular proteins (Chapter 5) and mannoproteins (Chapter 2) as an indication. Further research on glycolipids and microbial cells could be interesting to increase the portfolio of

SACs markers. Especially in fermentations performed with *E. coli*, the use of cell cytometry could aid to establish a link between membrane integrity and emulsification [10].

In addition, transfer models were developed to support and predict oxygen transfer and sesquiterpene evaporation data in a multiphase system. These models rely on physical properties such as vapour pressure, partition coefficients, interfacial tension, averaged particle size (e.g., bubbles and droplets), and viscosity. Most of these properties are not available (e.g. volatility data and partition coefficients of sesquiterpenes), or are difficult to obtain from a multiphase fermentation with high cell density (e.g. viscosity, interfacial tension).

Finally, different alternatives for microbial production of sesquiterpenes were evaluated from a techno-economic perspective in chapter 3. The developed flow-sheet model relies on several assumptions such as the amount of solvent required for demulsification of the product, and the efficiency of o/w separation using centrifuges. In addition, several physical properties (e.g. vapour pressure) were estimated using predictive models. Although the results obtained using these assumptions were useful for comparison of different process alternatives, experimental data would be desired for obtaining more accurate cost values.

5. Outlook

This thesis was performed within the Delft Reactor Integrated Column project (DIRC). The main goal of DIRC project is to design an integrated reactor for the production and recovery of hydrocarbons such as isoprenoids and alkanes. The knowledge generated in this thesis allows moving a step forward on the design of a process in which a low-cost separation technology integrated into a reactor can recover products dispersed in a second phase from a fermentation broth (Figure 2).

According to the regime analysis performed in chapter 2 fermentation and recovery are separated in different compartments. On the one hand, a reactor compartment with enough mixing and aeration to promote production, while keeping cellular stress low avoiding over production of SACs. On the other hand, a separation compartment with mild aeration conditions, so droplets can cream. The residence time, geometry (e.g. aspect ratio), and aeration rate in the separator should be not be chosen only based on hydrodynamic constrains (e.g. allow droplet creaming and avoid back mixing). Instead, cellular stress mechanisms leading to an increase of SAC concentration (e.g. overproduction of proteins, and increase in cell membrane

hydrophobicity) should be also considered so that the operational conditions do not promote product emulsification. In case this cannot be avoided, the design of the column parameters should consider the cellular response and its impact in the level of SACs.

Parameters which play a key role in the coalescence of dispersed product, like oil fraction, do not necessarily depend on the strain productivity. Solvents can be added to the system contributing to enlarge the averaged droplet size, by promoting coalescence. As shown

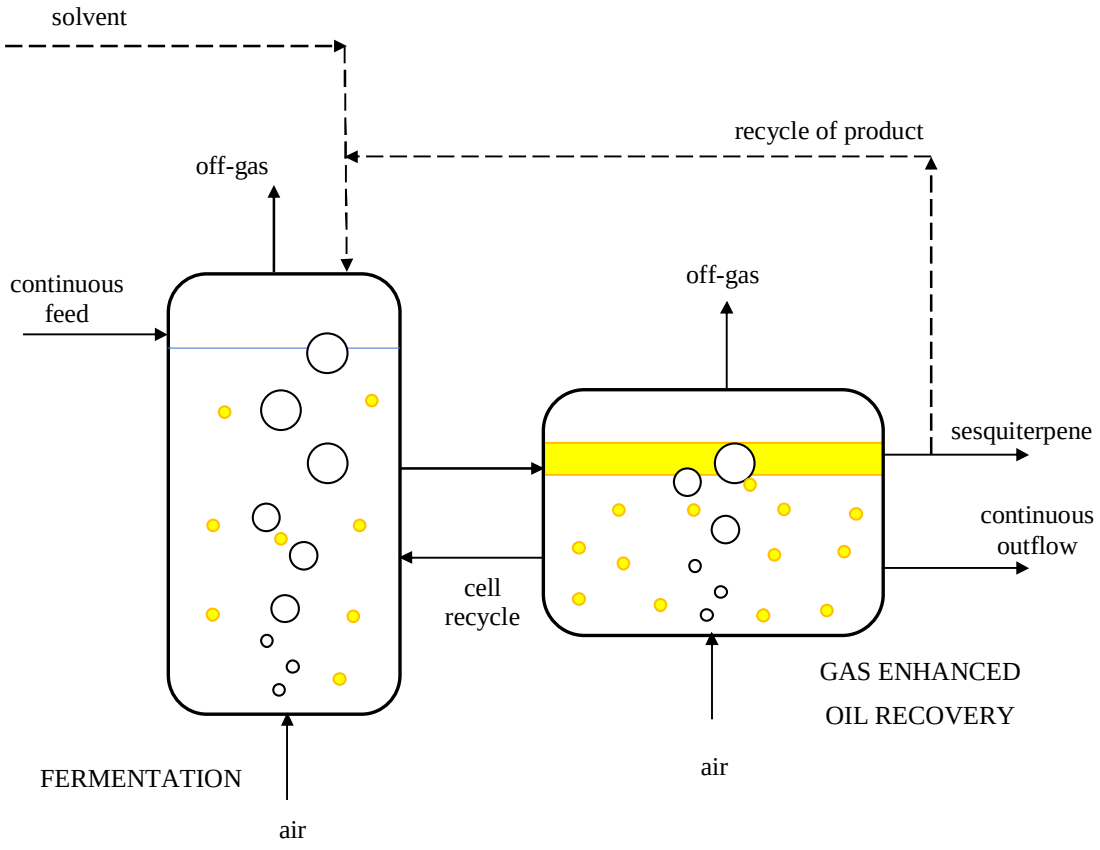

Figure 2. Schematic representation of an integrated process for continuous production and recovery of microbial sesquiterpene. In this system, the reactor would be a bubble column mixed by the power input provided by the gas bubbles. Solvents can be added to the system promoting oil coalescence and enhancing oxygen transfer. Alternatively, product could be recycled for the same purposes. Part of the fermentation broth is transferred to the gas enhanced recovery compartment where oil is separated from the aqueous phase. Broth with lower oil content is transferred back into the reactor, and the clear oil layer is removed from the top.

in chapter 3, this could lower as well the loss of product in the off gas, without incurring in higher unit production costs or increasing the environmental impact. This is especially relevant in the case of using solvents compatible with the final product formulation (e.g. diesel as solvent for the jet fuel precursor farnesene), or in the case of recycling the product itself. The implementation of in-situ optical probes could help to monitor the droplet size distribution along the fermentation. Consequently, the amount of solvent added to the system could be controlled to optimize the recovery in the separation compartment.

On a more critical look, the technology still need to be proven with a producing strain to discard any impact in the production metabolism of the strain. In addition, although results presented in chapter 5 concluded that a gas enhanced oil recovery compartment integrated to a fermentation can successfully recover oil from an emulsion, it is still required further improvement of the column settings to increase the degree of oil recovery. This requires scaling up the equipment, to have more flexibility in terms of volume and aspect ratio. In addition, it needs to include other surfactants different than proteins in the study, considering for example the effects of antifoam, and of components present in industrial feedstocks.

References

1. Scalcinati, G., Knuf, C., Partow, S., Chen, Y., et al., *Dynamic control of gene expression in Saccharomyces cerevisiae engineered for the production of plant sesquitepene alpha-santalene in a fed-batch mode.* Metab Eng, 2012. **14**(2): p. 91-103.

2. Schalk, M.*Method for producting beta-santalene.* Firmenich SA 2011. US 0281257 A1

3. Janssen, A.C.J.M., Kierkels, J.G.T., and Lentzen, G.F.*Two-phase fermentation process for the production of an organic compound* ISOBIONICS B.V. 2015. WO2015002528

4. Tabur, P. and Dorin, G.*Method for purifying bio-organic compounds from fermentation broth containing surfactants by temperature-induced phase inversion.* 2012. WO2012024186

5. Garcia-Ochoa, F. and Gomez, E., *Bioreactor scale-up and oxygen transfer rate in microbial processes: An overview.* Biotech. Adv., 2009. **27**(2): p. 153-176.

6. Dolman, B.M., Kaisermann, C., Martin, P.J., and Winterburn, J.B., *Integrated sophorolipid production and gravity separation*. Process Biochemistry, 2017. **54**: p. 162-171.

7. Heeres, A.S., Schroën, K., Heijnen, J.J., Wielen, L.A.M.v.d., et al., *Fermentation broth components influence droplet coalescence and hinder advanced biofuel recovery during fermentation.* Biotechnology Journal, 2015. **10**(8): p. 1206-1215.

8. Coulaloglou, C.A. and Tavlarides, L.L., *Description of interaction processes in agitated liquid-liquid dispersions.* Chemical Engineering Science, 1977. **32**(11): p. 1289-1297.

9. Panckow, R.P., Reinecke, L., Cuellar, M.C., and Maaß, S., *Photo-Optical In-Situ Measurement of Drop Size Distributions: Applications in Research and Industry*. Oil Gas Sci. Technol. – Rev. IFP Energies nouvelles, 2017. **72**(3): p. 14.

10. Hewitt, C.J., Boon, L.A., McFarlane, C.M., and Nienow, A.W., *The use of flow cytometry to study the impact of fluid mechanical stress on Escherichia coli W3110 during continuous cultivation in an agitated bioreactor.* Biotechnology and Bioengineering, 1998. **59**(5): p. 612-620.

List of publications[1]

Journal articles

- Pedraza-de la Cuesta Cuesta, S., Knopper, L. , van der Wielen, L. A. and Cuellar, M. C. (2019), Techno-economic assessment of the use of solvents in the scale-up of microbial sesquiterpene production for fuels and fine chemicals. Biofuels, Bioprod. Bioref., 2019. 13: 140-152.
- Pedraza-de la Cuesta, S., Keijzers, L., van der Wielen, L.A.M., Cuellar, M.C., Integration of Gas Enhanced Oil Recovery in Multiphase Fermentations for the Microbial Production of Fuels and Chemicals. Biotechnol J, 2018.;13(4):e1700478.

Oral presentations

- Pedraza-de la Cuesta, S., Keijzers, L., van der Wielen, L.A.M., Cuellar, M.C., Integration of oil recovery and fermentation of sesquiterpenes. 38th SBFC, Baltimore, 2016.
- Pedraza-de la Cuesta, S., Keijzers, L., van der Wielen, L.A.M., Cuellar, M.C., Integration of fermentation and recovery of sesquiterpenes, European Symposium of Biochemical Engineering Sciences (ESBES), 2016.
- Pedraza-de la Cuesta, S., Keijzers, L., Knopper, L., van Houten, C., van der Wielen, L.A.M., Cuellar, M.C., Integration of fermentation and recovery of sesquiterpenes, European Symposium of Biochemical Engineering Sciences (ESBES), Malcolm Lilly Award, 2016.

[1] Since summer 2018, Dr. Cuellar, Profs Heijnen and van der Wielen are (indirect and minority) shareholders in DAB BV, following the TU Delft regulations for staff inventors of intellectual property.

Curriculum vitae

Susana Pedraza de la Cuesta was born on the 30th of November of 1984 in Madrid, Spain. She completed her high school studies at the Instituto Rosalia de Castro in Santiago de Compostela (Spain) in 2002. Between September 2002 and June 2009 she completed her bachelor and master program in Chemical Engineering at the University of Santiago de Compostela (Spain) and a master program in Biotechnology Engineering at the same university. After a period of working in the powder coating industry in TIGER-coatings GmbH. (Austria), she took part in a collaboration project between University of A Coruña (Spain) and the cheese factory Queizuar S.L. for the scale-up of bioethanol production process from cheese whey.

She decided to focus her career on Bioprocess Engineering, and in February 2011 she started a Professional Doctorate program in BioProcess Engineering at Delft University of Technology (the Netherlands). Under the supervision of Dr. M.C. Cuellar Soares and Prof. dr. ir. L.A.M. van der Wielen she worked on the conceptual design of an integrated reactor and separator for the microbial production of diesel-like biofuels applying regime analysis methodology. In May 2013 she started as PhD candidate at the Bioprocess Engineering group, in the Department of Biotechnology of Delft University of Technology with Prof. dr. ir. L.A.M. van der Wielen as promotor and Dr. M.C. Cuellar Soares as co-promotor. The subject of her research, presented in this thesis, was the integration of multiphase fermentation and oil recovery for the microbial production of fuels and fine chemicals.

In September 2017 she joined the Global Centre of Excellence Processing in Danone Nutricia Research (the Netherlands), where she is currently working in simulation and scale-up of enzymatic conversions and membrane separations.

Acknowledgements

A difficult question, acknowledgements, and an easy question.

The most difficult question I was asked in my PhD was “why do you want to make PhD?”. Not because I didn’t know the answer, but because I feared mine was not good enough for others to find it appropriated. And so, every time a person asked, I replied an arbitrary selection of words that fitted in. It was not until one evening while drinking beers with a friend, that I gave a sincere answer. He liked it and encouraged me to tell it, so I decided it would become part of my acknowledgements.

My favourite store in Santiago had a lava lamp next to the window. I loved to pass by and stand there watching those droplets going up and down. It was like staring at fire, I could never get tired of looking at it. I decided I would save money to buy one. After a lot of time saving money, I came across a set of crayons with more than 50 colours for about the same price as the lamp. My heart was divided. I could not make a choice. Years later, when I had enough money to buy both the lamp and the set of colours, I bought a programmable calculator instead.

At some point of my life I stopped climbing to my favourite tree and sitting there to spend the evenings. Instead, I tried *climbing the ladder of success* and ended up sitting in the lecture room A at the Kluyver Laboratorium in Delft. At the second part of the fermentation course there was this guy talking about bubble sizes, superficial gas velocities and mixing patterns. At first, I thought it was impossible someone could ever get interested in calculating those boring parameters. But then something happened. The lecturer left behind the blackboard and started playing with a bubble-column filled with soap and water. He was completely lost looking into that column. And I knew that look. Any former lava lamp-addict can ever forget that look. And so, I felt a great admiration for that guy. After all, could someone ever dream of a better job than drawing with numbers how bubbles dance with water?

Next time someone asks me the difficult question, I will reply with a simple answer:
-*Why did you wanted to do a PhD?*
-*Because when I grow up I want to be like Rob van der Lans.*

It was another question (apparently asking things is a popular hobby in Delft) that led me to meet the person who would become my promotor, Luuk van der Wielen. “So…where do you see your career in the coming years?”. And me being me, I replied “I have no idea. I like

everything". And Luuk, being Luuk he answered something like "This is not bad, our best engineers are the ones flexible enough to engage in different projects (…)". I think I stopped listening, because that sounded too cool to keep paying attention to reality. It took me several hours to realise that that man had broken into my mental barrier against compliments. I got very pissed that day. But also defeated warriors admire their opponents. Luuk, thanks for all the fun. I feel immensely lucky to have shared all those hours learning from you, especially during the supervision of Design Project course. I really take all the advices with me.

Not all the characters in this story came in the form of a question. It was the graduate school who brought Gandalf the Grey into my life in the form of a PhD mentor. I don't think we have discussed many problems (if any) of my PhD during these years. On the other hand, my knowledge about plagiarism and scientific integrity has considerably increased since I met you. Peter, thanks for making me feel like a hobbit.

Every Thursday Mr. Alex used to bring muffins from the market, congregating the best-worst elements of the Kluyver Laboratorium fauna around a table. Relevant information brought from the outside world was shared (Camilo and the royal weddings…), also bad jokes (I think Rob Kerste was quite good at this, but I must say the level always reached the lowest whenever Maria was around). Besides the bad jokes and the sugar rush, the best part of the muffins sessions was that professors, lab technicians, students, postdoc and PhDers, left behind who they were, to become just people chatting and laughing around a table. Thanks Dutch culture for being so flat.

During these years I collected many nice memories: making cat memes with all the DIRC team, Carlos entering the office saying "Buenos dias a la vida!", HEMA-breakfast (HEMAyuno) with Alex and David, Marcelo singing all by himself, Chema making me laugh at one of his stupid jokes, Silvia taking pictures by the sea, Joana apologizing for saying "I'm sorry", Rita getting excited about Disney stuff, a sarcastic remark by Debby, Victor realizing too late that his joke lacked any political correctness, sharing office with Camilo, Erik telling stories about Wacken, Shima's eyes when she smiles, Arjan the old at his nerdiest, Arjan the young bringing cake, getting lost in a hug every time I see David... I have not even started listing and I'm already lost…

… *"bajo el ala aleve del leve abanico"* I get lost so easily, that sometimes I wonder if I spend more time lost than present. This is especially difficult in meetings. And in particular in the meetings with a group of students. And specifically, with my group of students. It is impossible

to get that alliteration from Ruben Dario out of my head. *Loes, Lore, Lisanne, Lisette…*I thought it would become easier with *Caroline,* but then *Carla* arrived, and it started all over again. I could write endless words about how thankful I am for all I have learnt from you. But I hope you understand how much appreciation I try to express by saying that your names sound like poetry to me.

Somewhere in my head there is a long version of this acknowledgements section. A version in which I thank Karel for letting me use his reactor so I could finish my experiments in time before the moving; where I thank Song and Dirk for all the help and patience with my set-up (that became at some point like a Christmas tree full of tubings and aluminium paper), especially those hectic days before the moving. In that long section, I would also thank Max and Stef for all their support with the image analyses and the gas chromatography analyses, but especially because of being super nice to me every time that I passed by with a question. I'm not sure if it is ok to include pictures in the acknowledgements, but my long version would have a full colour page with a foto of Kawieta inside a pink heart. That version should have like almost a page thanking Rob Kerste for all I learnt from him about fermentations. And another one thanking Adrie for all his good advices and his patience supervising together the course of Bioprocess Integration. It would thank all the DABbers especially Kirsten, Arjan, Fabienne and Marina, because I enjoyed so much working with them. It would explain how Arturo and Jay have taken care of me so many times, preparing dinner for me, helping me taking samples during the weekend, or by preventing that I spend too many weekends at home hiding from people. It would thank non-BPEers like mi "Marsita", Mariana, or Paulina for being the best excuse for a coffee break. It would explain how thankful I am to Ioanna and Paschalis for always being there. David would probably get several pages full of uncomfortable emotional stuff. And I would find some excuse to include Jelle as well. I would thank Anouk Sugito for being my favorite Scheherazade, and explain how important is to learn the language of the country you live in. And I would save some lines to thank DEWIS (Delft Women in Science) association and especially the intervision group guided by Rosemarijn Koenen. I would thank Armando Toledo, Daan Admiraal, Ron Ephrat, Emmy Storms, and Margreet Markerink, and explain how musicians made me a better scientist. And I would thank Krashna Musika, VU Orkest, and my dear crazy "Griekse Beek" and explain how amateur musicians made me a better person. I would even have some lines for my plants, and next to them I would thank Yvonne for teaching me something so basic as "how to breathe". Somewhere in my head there is a long version, but it had to become short because otherwise I cannot tell you the easy question.

The easy question “Why did you do a PhD?” has an easy answer: “Maria”. The most valuable information is often hidden behind obvious facts. The ones that no one bothers to write down in materials and methods because everyone assumes everyone knows. I could simplify this paragraph by saying “Thank you Maria for all your support”, but I thought that it would be a good idea to state the obvious things, so I make sure they don’t get lost. Thank you Maria for taking the challenge of accepting me as your student. Thank you for teaching me that dialogue is the best weapon. Thank you for telling me that just talking about music can be also a good topic to start a conversation with someone in a conference. Thanks for wearing colorful dresses to conferences full of grey blazers. Thanks for coming to my concerts. Thanks for your support when things outside PhD were getting a bit messy. I still use your colouring mandalas book from time to time. Thanks for letting me make the posters as I wanted, and the presentations as I wanted. Thanks for all the feedback on my posters. Thanks for all the feedback to improve the story-telling in my presentations. Thanks for the infinite feedback documents full of comments in my papers. Thanks for your time, and thanks for caring. Thank you for accepting me as I am, with the good and the bad things, and at the same time having the capacity of teaching me how to grow and become better. I think only very skillful coaches are able to do both. I don’t think I knew the meaning of self-esteem before I met you. Thank you for that. I came quite broken to Delft. Expending all these years next to you was an invaluable healing process. 5 years are maybe too long to be considered a discontinuity, but I think it is fair to say that you have meant a before and after in my life.

My dear Maarten. And you? Where do I thank you for your “Don’t think, minimize the thinking”? Let the needle fall on the vinyl while gently closing this book. A tango of Piazzola…Balada para un loco! Whatever it comes after writing this thesis, I want it to start by dancing together with you.